The Effect of Surface Modification of PLGA Drug Carriers on Vascular Wall Adhesion and Plasma Protein Corona for Improved Vascular Targeting

by

Genesis Lopez

A dissertation submitted in partial fulfillment
of the requirements for the degree of
Doctor of Philosophy
(Chemical Engineering)
in the University of Michigan
2022

Doctoral Committee:

Professor Omolola Eniola-Adefeso, Chair
Assistant Professor Carlos Aguilar
Professor Joerg Lahann
Associate Professor Greg Thurber

Genesis Lopez

glope@umich.edu

ORCID iD: 0000-0001-9360-6471

Dedication

This dissertation is dedicated to all family and friends that have supported me in this journey. I am grateful for your unconditional love and constant encouragement.

Acknowledgments

First, I want to thank my Advisor, Professor Omolola Eniola-Adefeso, for her mentorship throughout my graduate career and for helping me grow as a researcher. When I started grad school, I had no idea how rewarding this journey would be. I am thankful for your guidance and for motivating me to keep moving forward even in the most challenging moments, especially throughout this pandemic. My experience in your lab has helped me grow into a stronger person and a better scientist. I am excited to see the continued work coming out of your lab, and I am grateful for allowing me to be a part of it.

I would also like to thank my thesis committee members, Professors Joerg Lahann, Greg Thurber, and Carlos Aguilar. Thank you for serving on my thesis committee, and I appreciate the time and feedback you have provided to help me complete my degree. I am thankful for all your insights and discussions that have improved the quality of my work.

Additionally, I want to thank the past and current members of the Eniola lab that have been wonderful to work with and provide a welcoming environment. Thank you to the past members, Professor Catherine Fromen, Margaret Fish, Daniel Sobczynski, and Alex Thompson, for their guidance and feedback when I first joined the lab and for taking the time to answer all my questions as I learned to navigate grad school. Thank you to Billy Kelley, Hanieh Safari, Mario Gutierrez, and Violet Sheffey for your support, and it was a pleasure working with you all. Additionally, I would like to thank Dr. Korie Grayson, Emma Brannon, and Alison Banka for your assistance in wrapping up the work in this thesis and daily encouragement. Thank you to the current members

of the lab, Jonathan Lee, Valentina Guevara, Rue Felder, Logan Piegols, Daniel Kupor, Saja Al-Saloum, and Seun Akanbi. It has been fantastic working with you all, and I have enjoyed our conversations. You have made this experience truly rewarding.

I am thankful for all the great friends I have met during my time in Ann Arbor, with whom I have created incredible memories. I want to give a special thanks to my friends: Phillip Spinosa, Kathy Kosinski, Martin de Beer, and Zixuan Wang, who have supported and encouraged me even from miles away. I am so grateful for your friendship.

I want to give special thanks to my partner, David Carruthers, and his family for their support and love that have helped me continue this journey.

Lastly, I would like to thank my family for their unconditional love and support. I want to give special thanks to my parents, Maria and Jose Lopez, who taught me never to give up and that you can accomplish anything with hard work. I would also like to thank my siblings, Jose, Gerald, and Guadalupe Lopez, for their support and laughs that helped me through. Additionally, I'd like to thank my closest friends, Audria Romero and Alisha Lawrence, who are incredibly supportive and like family. I love you all, and I could not have completed this journey without you.

Table of Contents

List of Tables

List of Figures

List of Abbreviations

CVD	Cardiovascular disease
LDL	Low density lipoprotein
VTC	Vascular targeted carrier
PLGA	Poly (lactic-co-glycolic acid)
PLA	Poly (lactic acid)
PCL	Polycaprolactone
CS	Chitosan
GC	Glycol chitosan
PEI	Polyethylenimine
PVA	Polyvinyl alcohol
PEG	Poly (ethylene glycol)
PEO	Poly (oxyethylene)
SEM	Scanning Electron Microscopy
XPS	X-ray Photoelectron Spectroscopy
HSA	Human serum albumin
BSA	Bovine serum albumin
FB	Flow buffer
sLe^A	Sialyl Lewis A
ICAM	Intercellular Adhesion Molecule 1

aICAM	Anti-ICAM-1
MPS	Mononuclear phagocyte system
WBC	White blood cell
RBC	Red blood cell
HUVEC	Human umbilical vein endothelial cell
IL-1β	Interleukin 1 beta
ACD	Acid-citrate-dextrose
HEP	Heparin
ACF	Anticoagulant-free
EDAC	N-(3-Dimethylaminopropyl)-N-ethyl carbodiimide hydrochloride
MES	2-(N-morpholino) ethane sulfonic acid
PPFC	Parallel plate flow chamber
HRG	Histidine-rich glycoprotein
Ig	Immunoglobulin
U	Unloaded
R	Rhodamine loaded

Abstract

Vascular-targeted drug delivery requires the successful localization and adhesion of drug carriers to diseased sites via biomarkers, such as inflammation. Poly (lactic-co-glycolic acid) (PLGA), a negatively charged copolymer, is one of the most appealing biodegradable materials because of its biocompatibility and FDA approval. Unfortunately, the adhesion of targeted PLGA to an inflamed endothelium is reduced in the presence of plasma proteins acquired in human blood. Hydrophobic and strongly charged surfaces typically adsorb more protein than hydrophilic or neutrally charged surfaces. The addition of polyethylene glycol (PEG) chains to particle surfaces is a commonly used approach to mitigate protein adsorption. However, past work also saw a reduction in adhesion for PEGylated PLGA in human plasma conditions creating a need for alternative coatings.

In this dissertation, we explored coating PLGA with chitosan (CS), glycol chitosan (GC), human serum albumin (HSA), and CS plus HSA to evaluate their effect on vascular targeting. PLGA microparticles (MPs) were mainly used since they have shown enhanced binding over nanoparticles (NPs). Sialyl Lewis A (sLe^A) and anti-ICAM antibodies were conjugated onto particles to target E-selectin and ICAM-1 expressed by inflamed endothelial cells (ECs), serving as a model system for vascular adhesion. Adhesion of targeted particles to inflamed ECs was evaluated *in vitro* using a parallel plate flow chamber assay. The binding of particles in red blood cells (RBC) in plasma was normalized to their binding RBC-in-flow buffer depicted as adhesion

efficiency. Additionally, the adhesion of PLGA NPs modified with optimized coatings, HSA and HSA-CS, was evaluated to determine the impact of size.

The adhesion efficiency of bare PLGA was consistently below 20%, while coated PLGA produced different levels of adhesion in plasma. The adhesion efficiency of targeted CSPLGA MPs showed no improvement over PLGA MPs. Conversely, sLe^A GCPLGA MPs maintained an adhesion efficiency of 80% independent of shear rate. Additionally, sLe^A HSA-PLGA and HSA-CSPLGA MPs showed significant improvement in adhesion in plasma conditions. sLe^A HSA-CSPLGA had a max adhesion efficiency of 80%, which was dependent on ligand density and shear rate. Lastly, we discovered that sLe^A HSA-PLGA NPs also saw an adhesion efficiency of 40%. Interestingly, sLe^A HSA-CSPLGA NPs did not show improved adhesion, which suggests that changes in size affect adhesion of coated PLGA .

To better understand the impact of different coatings, we characterized association to ECs and protein corona composition. GCPLGA MPs had increased association to ECs and changes in protein corona composition, mainly a decrease in large molecular weight proteins, potentially driving its enhanced adhesion. HSA-PLGA MPs did not associate with ECs in plasma, while HSA-CSPLGA showed an increase in EC association likely due to the higher amount HSA. Protein corona characterization of HSA coated MPs showed increases in 75 and 150 kDa proteins, which could correlate to histidine-rich glycoprotein (HRG) and immunoglobulin G. The enhanced adhesion of HSA coated MPs is likely driven by multiple interactions with HSA-specific receptors and HRG receptor found on ECs. Interestingly, the use of different anticoagulants led to differences in protein adsorption and impacted particle adhesion efficiencies. This work suggests that coating PLGA with favorable proteins enhances adhesion over non-fouling coatings. Overall, we found that surface modification via HSA, HSA plus CS, and GC onto PLGA MPs positively

influenced particle binding and emphasized the importance of understanding protein-particle interactions.

Chapter 1 : Introduction

1.1 Background and Significance

Although cardiovascular disease (CVD) has been declining, it continues to be the leading cause of death in the US, especially for vulnerable groups at increased risk.[1] Atherosclerosis is the most common cause, typically resulting in a stroke or heart attack.[2] It is characterized by the progressive formation and rupture of plaques in the arterial wall associated with inflammation and endothelial dysfunction.[3] The plaques consist of lipids, macrophages, foam cells, smooth muscle cells, and several other components that accumulate over time, leading to calcification and thrombus formation.[4] Accumulated lipids are oxidized, which leads to tissue damage, the release of pro-inflammatory chemokines, and increased leukocyte and platelet adhesion. Current treatments focus on stabilizing these plaques by prescribing statins that decrease low-density lipoprotein (LDL) plasma concentrations, as well as lifestyle changes that reduce inflammation. Higher statin doses can further lower the LDL concentration in blood, but side effects, such as hepatotoxicity and myopathy, can develop.[5] The variability and progression of these plaques among patients make ubiquitous treatments ineffective, demanding the use of imaging agents that can characterize their location and progression for an early, informed diagnosis. Additionally, the delivery of drugs that can potentially reduce the size of plaques, repair the endothelial layer, or further lower LDL plasma concentration are essential in treating atherosclerosis.

Vascular targeted carriers (VTCs) can localize imaging agents and therapeutics to diseased sites that are difficult to reach by targeting the vasculature after intravenous administration.[2] The

benefits of VTCs include increasing drug concentration at target sites and reducing systemic side effects. Potential applications for VTCs are in the treatment of vascular diseases, such as CVD or cancer, which typically have medications that result in adverse side effects or require invasive surgery. The endothelial cells lining the lumen of the blood vessel wall are ideal targets in vascular diseases since they display unique biomarkers, such as increased endothelial cell permeability and overexpression of cell adhesion molecules during inflammation.[4,6,7] The targeting scheme can be classified as passive or active each having its advantages. Passive targeting mainly relies on the enhanced permeability effect, where VTCs are thought to preferentially accumulate and penetrate the endothelium due to increased permeability at inflammation or tumor sites.[8] Alternatively, active targeting can be achieved by attaching specific molecules to VTCs that have an affinity to cellular markers present at diseased areas.[9] Regardless of the targeting approach, a successful VTC must navigate complex blood flow dynamics, effectively marginate, and localize at diseased tissues to deliver its payload, which is critical to keep in mind during their design.

Several types of VTCs have been studied for various applications, and some examples include drug-conjugates, liposomes, dendrimers, or solid polymer particles.[10] Most drug carriers demonstrate significant advantages in delivering drugs over their free drug counterparts by improving the stability of drugs, extending circulation time, and increasing interactions with target cells.[11] Several drug carrier systems have successfully been translated into the clinic, but many injection formulations still suffer from low clinical success rates, specifically micron and nano-sized particle systems.[12] Liposomes were first discovered in the 1960s and have successfully translated into the clinic.[13] They are composed of lipids or synthetic amphiphilic molecules that self-assemble into vesicles with a bilayer. Hydrophobic drugs can be loaded within the bilayer, and hydrophilic drugs are encapsulated in the core.[14] Later in the 1970s, polymer-drug conjugates

were introduced as drug delivery systems, where a drug and polymer are covalently attached.[13] Polymer-drug conjugates have also made it into the clinic, typically using polyethylene glycol (PEG) as the polymer to promote extended circulation.[15] Polymeric particle systems are of great interest due to improved drug stability, effective controlled release, and the ability to encapsulate various drug molecules.[16] Each type of drug carrier has its advantages and disadvantages, depending on the application. The work in this thesis will focus on biodegradable polymeric particles. There is a need to further study how to make drug carriers more efficient by paying close attention to design parameters, such as the materials utilized.

Negatively charged, biodegradable polymers, such as polylactic acid (PLA) or polylactic-co-glycolic acid (PLGA), have been widely studied since their byproducts are non-toxic and can be easily cleared by the body.[17] Additionally, PLGA has been approved by both the FDA and EMA facilitating the translation of any future formulations into the clinic that shows promise. Recently, preclinical studies using PLGA and other polymeric materials as potential delivery vehicles for statins have shown encouraging results increasing interest in further research.[18] Past work in our lab directly investigated the ability of PLGA particles to act as a VTC and target an inflamed endothelial cell monolayer *in vitro*. First, PLGA particles were decorated with sialyl Lewis A (sLe^A), a ligand specific for the E-selectin receptor expressed by endothelial cells during inflammation. The binding of sLe^A PLGA particles to inflamed endothelial cells was evaluated after being added to buffer, or blood conditions, where its binding in blood was significantly reduced compared to buffer conditions.[19] Blood is a complex fluid, which consists of red blood cells localizing within the core, white blood cells interacting with the endothelium, and the cell-free layer consisting of plasma proteins and platelets. By exposing PLGA to individual blood components, it was found that the presence of plasma proteins was driving the reduced adhesion

of PLGA particles. When drug carriers enter the bloodstream, the adsorption of plasma proteins onto the surface occurs quickly and forms a corona that can affect their biological fate, as well as block the targeting ligand on the particle surface from interacting with its respective receptor on the endothelium. The plasma contains several types of proteins, including coagulants involved in blood clotting, proteins that maintain osmotic pressure, ions keeping blood pH, immunoglobulins helping fight infection, and other nutrients.[20] The characterization of the protein corona can assist us in identifying key proteins that may influence biological interactions, such as adhesion to the endothelium.

Further work in our lab and throughout literature showed immunoglobulins as having an abundant and unique presence on the PLGA surface.[19,21] Studies involving the depletion and re-addition of individual immunoglobulins identified that the presence of IgA and IgM in the plasma was responsible for the reduced adhesion of PLGA.[22] The unfavorable adsorption of plasma proteins onto the PLGA surface is a major obstacle that needs to be addressed for successful vascular targeting. There are two approaches that can be employed to improve the adhesion of PLGA by either reducing plasma protein adsorption or manipulating the corona to incorporate favorable proteins, which can be achieved via surface modification. The research presented in this thesis aims to understand the effect of surface modification of PLGA particles on adhesion to the vascular wall and plasma protein corona. Specifically, PLGA was coated with albumin, chitosan, and glycol chitosan to alter the surface hydrophobicity and charge, which have been shown to impact protein adsorption. The rest of this chapter will discuss how drug carrier properties impact plasma protein adsorption, as well as surface modification techniques implemented in PLGA drug delivery systems.

1.2 Vascular targeted carrier properties and impact on plasma protein adsorption

There are many barriers that a VTC must overcome to effectively reach the diseased tissue and deliver its cargo for therapeutic effect. A VTC will need to navigate the blood flow, evade the mononuclear phagocyte system (MPS), and accumulate at the inflamed blood vessel wall.[23] The ability of a VTC to overcome these barriers is greatly influenced by the adsorption of plasma proteins onto its surface, also known as opsonization, affecting circulation time and clearance from the body by phagocytic cells that are part of the MPS. As a VTC comes in contact with plasma, abundant proteins, such as albumin, initially adsorb onto the surface and are replaced by higher affinity proteins over time, this dynamic exchange of proteins is described as the Vroman effect.[24] The proteins that adsorb onto the surface can be classified as opsonin or dysopsonin, which increase or decrease the uptake of VTCs by macrophages and other phagocytic cells, respectively.[25] There are several opsonins involved in clearing pathogens from the body, which include complement proteins and immunoglobulins. Some examples of dysopsonins include albumin, clusterin, and histidine-rich glycoprotein. The types and amount of proteins present in the corona are dependent on the physicochemical properties of VTCs, for example size or shape. Since PLGA is a relatively hydrophobic material and has a strong negative charge, these properties could be driving the increase of unfavorable proteins on the surface leading to the reduction in particle binding as described above. It is important to understand how surface hydrophobicity and charge influence protein adsorption and identify key surface characteristics that reduce protein adsorption or promote the adsorption of favorable proteins (dysopsonins).

1.2.1 Surface hydrophobicity

Several studies have probed the impact of surface hydrophobicity on protein adsorption and biological interactions. In general, a higher surface hydrophobicity typically leads to an

increase in the amount of protein adsorbed resulting in quicker clearance.[26] A study using latex particles with a variety of functional groups found that decreases in surface hydrophobicity lead to a decrease in the amount of protein adsorbed, specifically in the amount of fibrinogen, apolipoproteins, and immunoglobulin G.[27] More importantly, the adsorption of plasma proteins on particles utilizing biodegradable polymers with differing surface hydrophobicity has been examined since they are of great interest. One study incubated PLA, PLGA and particles incorporating a hydrophilic, poly(oxyethylene) (PEO) polymer in citrated human plasma and characterized the adsorption of proteins, as well as compared the method of fabrication.[28] PLA particles are more hydrophobic and had an increase in the amount of albumin adsorbed compared to PLGA. Additionally, the study compared fabrication methods, spray-drying and double emulsion technique that uses polyvinyl alcohol (PVA) as the surfactant. They saw significant differences in protein patterns, specifically an increase in apolipoprotein adsorption on PLGA fabricated via spray-drying method possibly due to the absence of PVA in the fabrication process. PLA and PLGA particles with the hydrophilic polymer drastically reduced the total amount of protein. Polycaprolactone (PCL) is another biodegradable polymer commonly used in drug delivery systems, which is more hydrophobic than both PLA and PLGA. A direct comparison between PLGA and PCL nanoparticles found that serum proteins had a higher binding affinity to PCL compared to PLGA.[29] Interestingly, apolipoproteins were determined to preferentially bind to PCL, most likely due to lipid binding domains that interact with hydrophobic materials.[29] Overall, hydrophobic surfaces tend to promote the adsorption of certain proteins, for example albumin, complement and immunoglobulins.[30]

1.2.2 Surface chemistry and charge

Throughout the literature, the effect of drug carrier surface chemistry and charge on plasma protein adsorption has been explored to understand its effects on the immune response.[31] Lundqvist et al. evaluated the effect of surface chemistry on the protein corona using 100 and 50 nm polystyrene nanoparticles with methoxyl, carboxyl, or amine functional groups.[32] The authors found that 100 nm carboxyl modified PS saw an increase in immunoglobulin adsorption compared to 50 nm amine and carboxyl PS. The 50 nm amine modified PS had the highest number of apolipoproteins over other particles tested. The methoxyl PS nanoparticles showed a significant amount of complement proteins compared to amine or carboxyl PS. All PS nanoparticles had some level of acute-phase and coagulation proteins present on the surface. Another study modified the surface of poly(lactide-co-glycolic)-lipid poly (ethylene glycol) nanoparticles with methoxyl, carboxyl, and amine groups to examine changes on protein adsorption to control complement activation and immune responses.[33] After exposure to human serum, all PLGA-PEG particles induced complement activation but still relatively low compared to activation with zymosan. Methoxyl modified particles experienced the lowest complement activation because of the adsorption of complement deactivating proteins (factor H). The authors also fabricated hybrid particles to study the effect of charge on complement activation. It was determined that hybrid particles with neutral charges had the lowest level of complement activation, while a positive charge resulted in increased complement activation. The amine/methoxyl hybrid particles showed the highest amount of C3b β chain, a component of the complement cascade, resulting in an increase in complement activation. A study by Deng et al. showed that negatively, charged gold nanoparticles induced the unfolding of fibrinogen, which lead to activation of the Mac-1 receptor on THP-1 cells and release of proinflammatory molecules.[34] Walkey et al altered the surface of gold and silver nanoparticles with a variety of ligands resulting in a range of charge, as well as,

size.[35] Both anionic and cationic particles experienced higher plasma protein adsorption compared to neutral particles. Additionally, cationic gold nanoparticles interacted more with cells than anionic and neutral particles, but it was not seen throughout all surface modifications. The fingerprinting of the plasma protein corona was then used to build a predictive model for cell-particle association dependent on adsorbed proteins. The model demonstrated that cellular association was also dependent on core material other than just surface chemistry. Overall, the surface charge and chemistry have a significant impact of protein adsorption and corona composition, where neutrally charged and methoxyl surfaces showed a decrease in protein adsorption. Additionally, the surface charge and chemistry affected the immune response and cellular association mainly driven by the composition of the protein corona obtained after exposure to plasma or serum.

1.3 Surface modification and biological implications

As previously discussed, PLGA particles are negatively, charged and relatively hydrophobic, which adsorb a significant amount of immunoglobulin affecting their ability to bind to an inflamed endothelium. Surface modification is a potential approach used to alter surface properties of VTCs and affect their interactions with the biological environment. To improve the adhesion of PLGA, we can either modify the surface to reduce protein adsorption or alter the protein corona to incorporate more favorable proteins, such as albumin. Adjusting the surface of PLGA to a more hydrophilic and neutral charge can potentially lead to a decrease in protein adsorption. Additionally, we can explore the effect of changing PLGA's negative charge to a positive charge to increase affinity to the endothelium, as well as influence compositional changes in the protein corona. A recent approach to improve biological interactions of drug carriers is to modify the surface with proteins or other cellular components as a way to camouflage within the

body. Below, I will discuss some examples of surface modification that have been previously utilized that could assist in improving the adhesion of targeted PLGA to the vasculature.

1.3.1 PEGylation – most common

Poly(ethylene glycol) (PEG) is a hydrophilic, biocompatible polymer with high solubility that was first used in 1977 attached to bovine serum albumin and liver catalase proteins and learned of its ability to increase circulation time.[36] The first time a PEGylated therapeutic was approved by the FDA occurred in 1990 and several other formulations were later approved for a variety of diseases. The attachment of PEG to the surface of drug carriers provides many benefits, including decreased protein adsorption, improved drug carrier stability, protection from aggregation and reduced phagocytosis. For these reasons, PEG is the gold standard for designing "stealth" drug carriers. One example is the PEGylation of organic nanotubes which resulted in increased circulation time and changes in biodistribution.[37] PEGylated nanotubes accumulated in the liver, while non-PEGylated nanotubes were found in the lungs. The PEGylation of PLGA nanoparticles also demonstrated prolonged presence in blood compared to bare PLGA.[38] Another study found that the adsorption of human serum albumin was decreased on PLGA after PEGylation.[39] The protein corona of PEGylated PLGA was drastically different compared to PLGA. Overall, there was a decreased in total protein adsorption. The corona of PEGylated PLGA was mainly comprised of albumin and apolipoproteins and there was a reduction in higher molecular weight proteins and immune response proteins.[40]

There are two main methods of PEGylating the surface carriers, either self-assembly of PEG-conjugated molecules or covalent attachment to pre-formed particles using different chemistries.[36] As presented above, the addition of PEG onto the surface of carriers can have many benefits but these are dependent on polymer chain length, functionality, and confirmation. The

most important characteristic to keep in mind is the polymer confirmation, which can be in a brush or mushroom position. The mushroom confirmation describes PEG chains that are entangled and close to the surface, while the brush confirmation is preferable due to its ability to extend outwards from the surface.[41] Previous work in our lab evaluated the binding of polystyrene particles to endothelial cells. The PEG chain length did not affect particle binding, but there was a reduction in particle binding at higher shear rates when the PEG was in mushroom confirmation. It was suggested that the reduction in particle binding was due to PEG chains interfering with receptor-ligand interactions. Additionally, the adhesion of polystyrene particles is reduced when exposed to porcine blood, which is a harsher environment, and our lab evaluated whether PEGylation could recover particle binding.[42] Interestingly, the adhesion of micron sized particles was improved with PEGylation, whereas it did not help nano sized particle binding. The dependence of size could be due to differences in protein adsorption, where other studies have shown protein adsorption increase as particle size decrease.[42,43] Aside from studying the PEGylation of polystyrene, our lab also investigated the effect of PEGylation on PLGA to improve adhesion in the presence of plasma. Unfortunately, the PEGylation of PLGA did not improve particle binding possibly due to protein adsorption not being completely eliminated or a need for higher PEG brush density that may be difficult since PLGA has limited functional groups.[19] Since PEGylation did not help the adhesion of PLGA, there is a need to find alternative coatings for surface modification that may improve particle binding.

1.3.2 Chitosan

Chitosan (CS) is the deacetylated form of chitin, which is abundantly found on the exoskeleton of crustaceans.[44] CS is a positively charged, polysaccharide that has high solubility in acidic conditions and is degraded by chemical process and enzymatic catalysis.[45] It is also

biocompatible, pH sensitive, antibacterial and mucoadhesive.[44,46] Several types of drug carriers have been coated with chitosan, including liposomes, metal and polymeric particles. The addition of chitosan onto the surface can be achieved during or after particle fabrication via physical adsorption or chemical conjugation.[47] Surface characterization techniques, such as FTIR, XPS, or zetapotential, are typically used to confirm the presence of chitosan coating. Focusing on PLGA, the addition of chitosan onto its surface has been shown to result in a shift in surface charge from negative to positive depending on chitosan concentration and pH.[47,48]

Chitosan-coated PLGA particles have been extensively characterized for a variety of drug and imaging delivery systems. Li et al. probed the utility of PLGA, chitosan, and chitosan-PLGA particles for vascular delivery through evaluation of platelet activation.[49] Both PLGA and CSPLGA particles exhibited inhibitory response toward collagen-induced platelet aggregation, but chitosan particles seemed to have a higher inhibition. The authors proposed the use of PLGA and CSPLGA as potential drug carriers, but pure chitosan particles have shown to absorb proteins that prompt platelet adhesion and thrombosis. Zhang et al. assembled gadolinium-loaded chitosan-PLGA particles targeted with RGDS peptide for imaging thrombus. Particles were exposed to blood clots, i.e. platelets, and the accumulation was imaged with high resolution MRI, where visibility of clots was improved by the chitosan coating.[50] These studies demonstrate the potential of CSPLGA particles to act as a vascular targeted carrier.

1.3.3 Albumin surface coatings

Recent studies have focused on utilizing biological materials to modify the surface of drug carriers to improve biological interactions, such as protein adsorption and improving immunogenicity. Surface modification of drug carriers by coating with cellular membranes, individual plasma proteins, or pre-forming a protein corona to camouflage and evade recognition.

Albumin is the most abundant protein in blood, which is considered to have dysopsonin properties. It has been used as the main material for drug carriers or as a surface coating.[51] The albumin coating can be added by physically adsorbing or covalent attachment. Several types of drug carriers have attached albumin onto their surface for the treatment of cancer and have shown enhanced delivery of anticancer therapeutics.[52,53] Peng et al. incubated polymeric nanoparticles in a solution of bovine serum albumin to coat the surface. The addition of BSA saw a reduction in the adsorption of immunoglobulin G, decreased complement activation, lowered mouse macrophage uptake, and prolonged blood circulation.[54] Cationic albumin has been conjugated to the surface of PLGA particles to improve delivery to the brain, which enhanced uptake by tumor cells.[55–57] Additionally, a study compared the antifouling capabilities of BSA with or without fatty acids.[58] Fatty acid-free BSA coatings resulted in higher surface coverage and may protect from complement activation after exposure to NPs. Albumin has also been used a targeting molecule, since it can interact with a variety of receptors. For example, the endothelial cells express several receptors involved in the recycling of albumin.[59] Azevedo et al. albumin functionalized PEG-PLGA nanoparticles for the oral delivery of insulin. These particles were found to bind human FcRn, which is involved in transporting albumin across the intestinal epithelium.[60] Overall, albumin coatings have demonstrated several benefits, which include biocompatibility, dysopsonin properties, and targeting opportunities that could assist in improving the adhesion PLGA.

1.4 Dissertation Outline

As previously discussed above, there are several obstacles that vascular targeted carriers must overcome to successfully reach the damaged vasculature and deliver therapeutics. The protein corona is one of the main factors influencing the biological fate, including circulation time, phagocytosis, and targeting. Drug carrier design parameters have been shown to influence the

adsorption of plasma proteins, as well as the composition of the protein corona obtained after a VTC enters the blood stream. Biodegradable polymeric particles are of great interest in the development of drug delivery systems. Previous work demonstrated a significant reduction in binding to an inflamed endothelial cell monolayer for PLGA and PLA particles after exposure to plasma proteins. Further studies identified that immunoglobulin A and M were the main culprits leading to the negative adhesion in plasma conditions. Thus, the focus of this thesis is to improve the adhesion of PLGA particles via surface modification.

Chapter 1 provides an overview of on how VTC design parameters influence protein adsorption with a specific focus on surface hydrophobicity and charge. Additionally, potential surface modifications and their implications are discussed that may ameliorate PLGA's negative adhesion.

Chapter 2 details the materials ad methods used to collect the data presented in this thesis. The methods for particle fabrication and characterization are described, as well as the protocols used for evaluating particle adhesion.

Chapter 3 examines the effect of hydrophilic, positively charged coatings on PLGA microparticle adhesion and protein adsorption. We evaluated the adhesion of PLGA coated with chitosan and glycol chitosan.

Chapter 4 explores the impact of surface modification of PLGA with chitosan and albumin on microparticle binding after exposure to plasma proteins. Additionally, we determine how modifying the surface of PLGA and CSPLGA particles with albumin alters protein adsorption. A preliminary in vivo study was carried out to determine the impact of coating with albumin on biodistribution.

Chapter 5 focuses on evaluating the adhesion of PLGA nanoparticles modified with optimized surface coatings found in Chapter 3. The objective of this chapter is to determine whether PLGA particles in the nanosized range can benefit from the same coatings used to successfully improve microparticle adhesion. Specially, the focus is on coating with albumin only and dual coating of albumin and chitosan on PLGA.

Chapter 6 summarize the main conclusions of this thesis and discusses future directions.

Chapter 2 : Materials and Methods

2.1 Introduction

This chapter details the materials and methods used to collect experimental data presented in Chapters 3 through 5. The details for the fabrication of PLGA particles is described below including the various surface coatings studied here. The particle characterization was carried out using various chemical surface techniques to confirm size and presence of coatings. The adhesion of surface modified PLGA particles to an inflamed endothelium was evaluated using a parallel plate flow chamber assay in different physiological conditions. Additionally, the protein adsorption onto the particle surface was characterized using SDS-PAGE to see any changes between surface coatings studied. A preliminary *in vivo* biodistribution study was conducted for a set of particles detailed below. Specific details on materials used are listed within each subsection.

2.2 Particle Fabrication

2.2.1 Standard PLGA microparticles

PLGA microparticles were fabricated using the emulsion solvent evaporation method established in the literature.[61,62] First, the water phase was prepared by dissolving 1.25 g of polyvinyl alcohol (PVA, 30-70 kDa, Millipore Sigma) in 250 mL of deionized water at 150 C and 800 rpm on a stir plate. After two hours, the water phase was allowed to cool, diluted to 250 mL (0.5% w/v PVA), and filtered. Next, the oil phase was prepared by dissolving 100 mg of low molecular weight PLGA (~6.4 kDa, 50:50, 0.15-0.25 dL/g, Lactel Absorbable Polymers) in 18 mL of methylene chloride (Fisher Chemical). To begin particle fabrication, 75 mL of water phase was

centered on an overhead mixer (Caframo) and stirred at high speed (4500 rpm). The oil phase was slowly injected with a glass syringe and mixed for 2 hours to allow the solvent to evaporate. The resulting particle solution was allowed to separate, placed into 2-50 mL centrifuge tubes equally, and diluted with deionized water. Particle solution was centrifuged at 750 rpm for 20 minutes, the supernatant was transferred to clean 50 mL tubes, and pellet disposed of. The supernatant was centrifuged at 980 rpm for 20 minutes. The supernatant was aspirated, pellet resuspended in deionized water, and centrifuged at 1100 rpm for 20 minutes. The pellet was collected, resuspended in 1-2 mL of deionized water, freeze-dried in liquid nitrogen, lyophilized, and stored at -20 C. To fabricate fluorescent particles, rhodamine B was added to the oil phase containing the PLGA polymer during oil phase preparation.

2.2.2 Chitosan, Glycol chitosan, and Polyethylenimine coated PLGA Microparticles

The surface of PLGA microparticles was modified via physical adsorption of coating polymer during the emulsion solvent evaporation method. First, the water phase for each type of surface coating was prepared individually. For chitosan coated PLGA, 1 g of low viscosity chitosan (CS, 5-20 mP.s, TCI America) was dissolved in 0.3M HCl solution at a 0.4% w/v concentration. The solution was stirred at 800 rpm and 150 C for 2 hrs. After cooling, the pH of the chitosan solution was adjusted to 4.5 and filtered before use. For glycol chitosan coated PLGA, 1 g of glycol chitosan (GC, ~2000-2900 degree of polymerization, MP Biomedicals) was dissolved in 250 mL of deionized water at 150 C and 800 rpm. The pH was adjusted to 6.5 and filtered. Lastly, 2.5 g of polyethylenimine (PEI, ~25 kDa branched, Millipore Sigma) were dissolved in 250 mL of deionized water at 150 C and 800 rpm. The pH was adjusted to 6.5 and filtered. Next, the oil phase was prepared by dissolving 100 mg of low molecular weight PLGA in 18 mL of methylene chloride. To begin particle fabrication, 75 mL of desired water phase (CS, GC, or PEI)

was centered on an overhead mixer and stirred at high speed (5000 rpm). The oil phase was slowly injected with a glass syringe and mixed for 2 hours to allow the solvent to evaporate. The resulting particle solution was put through centrifugation steps and washed with deionized water to obtain approximately 2 µm diameter particles. The collected particles were lyophilized and stored at -20 C. Rhodamine B was added to the oil phase containing the PLGA polymer for fluorescent particles.

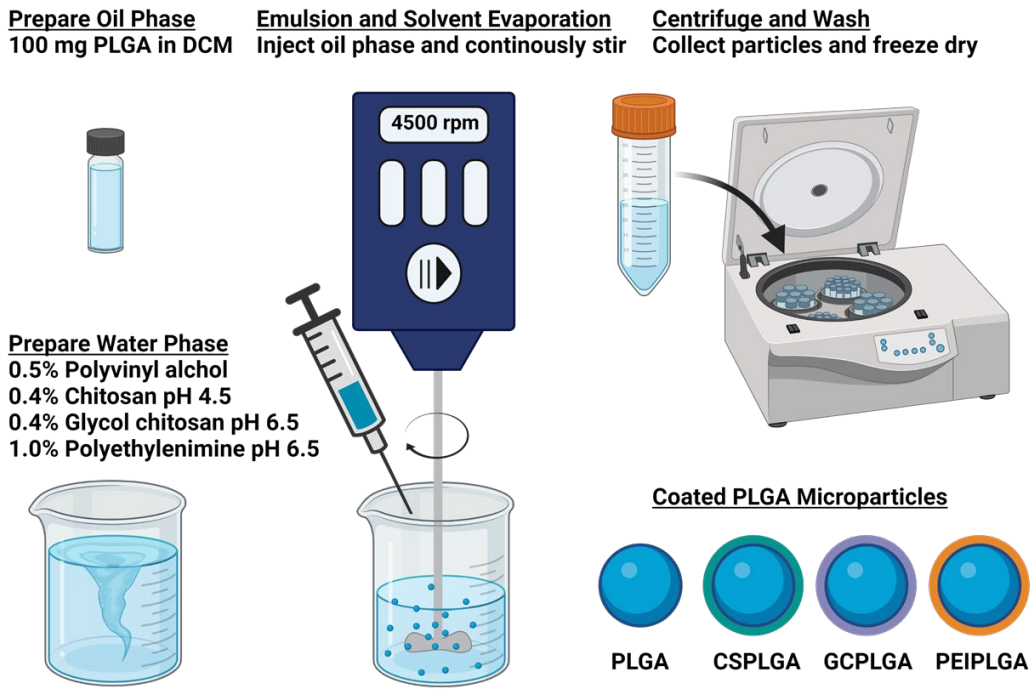

Figure 2.1 Solvent evaporation fabrication method for coated-PLGA microparticles. Created with BioRender.com.

2.2.3 PLGA and CSPLGA nanoparticle fabrication

To begin nanoparticle fabrication, 100 mg of low molecular weight PLGA was dissolved in 2 mL of methylene chloride in a 4 mL glass vial to form oil phase. For the water phase, 10 mL of 0.5% PVA or 0.4% CS solution was added to a 20 mL glass vial. The oil phase was added to the water phase using a glass syringe to form droplets. The mixture was placed over ice and probe sonicated to 2 minutes at 80% amplitude. The emulsion was poured into a 100 mL glass beaker on

a stir plate set to 300 rpm and stirred for 2 hours to allow solvent to evaporate. The resulting particle solution was put through centrifugation steps and washed with deionized water to obtain approximately 300 nm diameter particles. The collected particles were lyophilized and stored at -20 C. Rhodamine B was added to the oil phase containing the PLGA polymer for fluorescent particles.

2.3 Particle Surface Morphology and Chemical Characterization

The size and surface morphology of particles was characterized by scanning electron microscopy (SEM). To prepare samples for SEM, lyophilized particles were resuspended in deionized water and dried on glass slides. Before imaging, the glass slides were mounted on SEM stubs and sputter-coated with gold. SEM images were analyzed using ImageJ to determine mean particle size. The zeta potential was measured using the Malvern Zetasizer Nano ZS, where particles were tested in deionized water. Microparticles and nanoparticles were resuspended at a concentration of $5x10^7$ or $2x10^8$ particles/mL, respectively. Each sample was sonicated before measuring zetapotential. X-ray photoelectron spectroscopy (XPS) was used to chemically characterize the surface of CS, GC, or PEI coated PLGA particles by mounting dried samples onto indium foil.

2.4 Albumin conjugation and staining for MPs and NPs

The attachment of albumin onto PLGA and CSPLGA particles was carried out using carbodiimide chemistry. The carboxyl group is activated during this reaction and allowed to react with an amine group to form an amide bond. Luckily, proteins have an abundance of amine and carboxylic acid groups at the C-terminus, N-terminus, and several amino acid side chains.[63] Here, albumin reacts with the carboxylic groups on PLGA and the amine groups on CSPLGA. First,

human serum albumin (HSA from human plasma, Millipore Sigma, ≥ 95%) was dissolved in filtered deionized water at a concentration of 16 mg/mL. $5x10^6$ microparticles or $2x10^8$ nanoparticles were added to 0.5 mL of albumin solution and placed on a rotator for 20 minutes. Next, N-(3-dimethylaminopropyl)-N′-ethyl carbodiimide hydrochloride (EDAC, Millipore Sigma) was dissolved in a 200 mM MES buffer at pH 7.2 at 100 mg/mL. 0.5 mL of EDAC/MES solution was added to particles incubated with albumin to start the reaction. The final solution was vortexed and placed on a rotator at room temperature for 4 hours for microparticles and 2 hours for nanoparticles. The reaction was quenched with 20 mg of glycine for 20 minutes and centrifuged. Albumin-conjugated particles were kept in pellet form until being reacted with avidin or stained. To measure the amount of albumin on the particle surface, HSA-PLGA and HSA-CSPLGA were stained with anti-human serum albumin APC-conjugated antibody (R&D Systems) and a mouse IgG2A APC-conjugated antibody as the isotype control. The stained particles were run on a flow cytometer (Attune) with APC calibration beads (Bang Laboratories) used to create a curve correlating median fluorescence to the number of fluorescent molecules present, which is then used to calculate the number of albumin sites on conjugated particles.

2.5 Avidin conjugation and targeting ligand attachment

PLGA, HSA-PLGA, CSPLGA, HSA-CSPLGA, GCPLGA, and PEIPLGA particles were conjugated with avidin utilizing carbodiimide chemistry and then reacted with a biotinylated sialyl Lewis A (sLe^A, Glycotech Corporation) or human anti-ICAM-1 antibody (aICAM, R&D Systems) for targeting as previously described.[64] Briefly, particles (range of $5x10^6$-$5x10^7$ for microparticles and $2x10^8$ for nanoparticles) were incubated with NeutrAvidin (ThermoFisher) in 0.5 mL of filtered deionized water for 20 minutes. The concentration of avidin ranged between 1-3 mg/mL depending on particle type. Next, EDAC was dissolved in 200 mM MES at a pH of 4.5 for

uncoated PLGA or pH 7.2 for coated PLGA for microparticles. The MES/EDAC solution was kept at a pH 7.2 for all nanoparticles used. 0.5 mL of EDAC/MES solution was added to the particle/NeutrAvidin mixture. The final solution was rotated and reacted for 4 hours. The reaction was quenched with 20 mg of glycine and rotated for 20 minutes. Avidin conjugated particles were collected by centrifugation and used the following day. The amount of avidin was measured with biotin-FITC. Avidin conjugated particles were incubated with biotinylated sLe^A or human aICAM for 30 minutes in PBS +/+ with 1% BSA pH 7.4 (flow buffer, FB). The targeted particles were then washed and stained with ANTI-CLA-FITC (Miltenyi Biotec) and Rat IgM FITC (isotype, BD Biosciences) for 15 minutes to quantify the sLe^A surface density. For aICAM density determination, goat anti-mouse IgG FITC (Jackson ImmunoResearch Laboratories) and goat IgG FITC (isotype) were used. Control and stained particles were run on a flow cytometer (Attune) to measure fluorescence and compared to FITC calibration beads (Bangs Laboratories) to correlate fluorescence to number to molecules present.

2.6 Zeta Potential of Targeted Nanoparticles

PLGA and CSPLGA nanoparticles were conjugated with albumin, avidin, and biotinylated sLe^A as described above. Conjugated particles were washed with PBS+/+ with 1% bovine serum albumin (BSA) at least twice. Next, particles were resuspended in filtered deionized water for final wash. The pellet was resuspended in filtered deionized water and the zeta potential was measured on Malvern Zetasizer Nano ZS. The size of these samples was also measured.

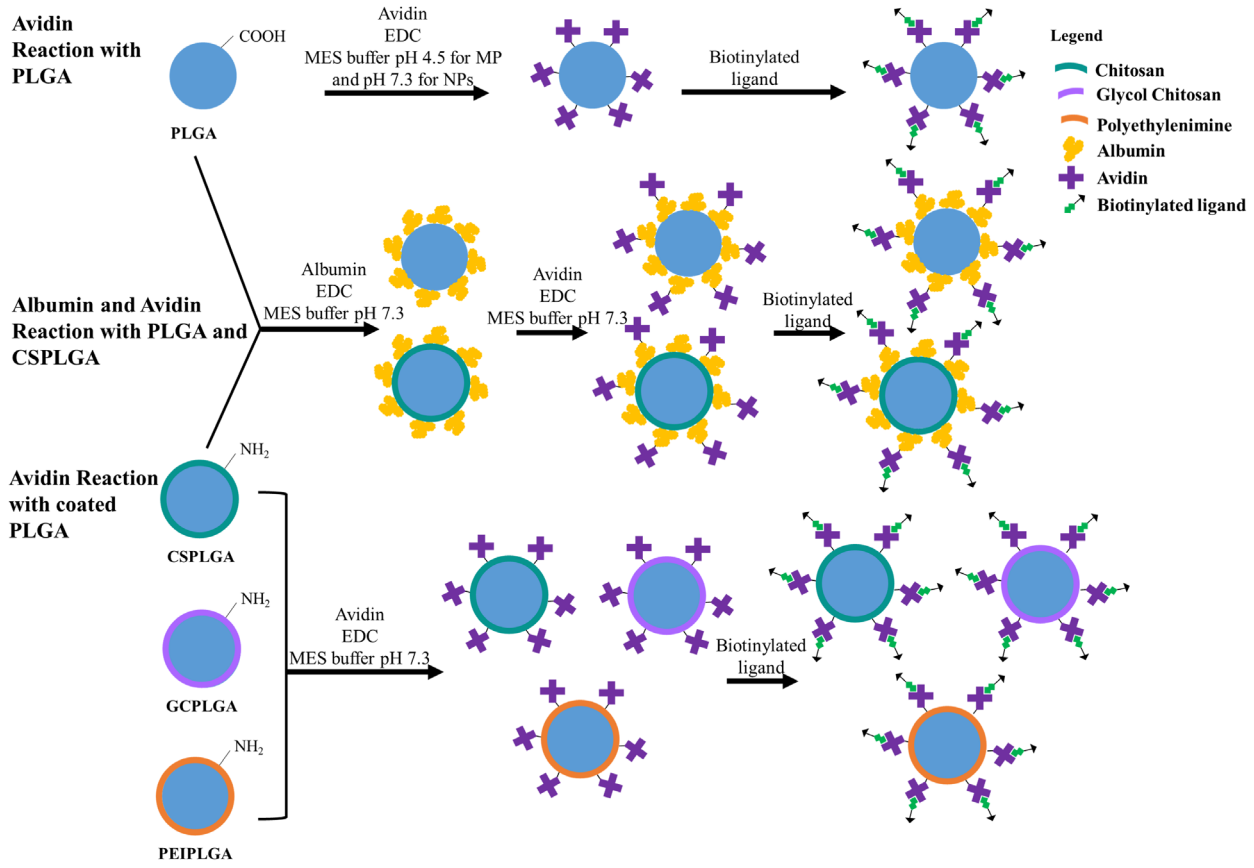

Figure 2.2 Protein and targeting ligand conjugation with PLGA and coated PLGA particles.

2.7 HUVEC Cell Culture

Human umbilical vein endothelial cells (HUVEC) were harvested from umbilical cords donated by the Motts Children's Hospital at the University of Michigan under a Medical School Internal Review Board (IRB-MED) approved human tissue transfer protocol (HUM00026898). This protocol is exempt from informed consent per federal exemption category #4 of the 45 CFR 46.101. (b). HUVEC were isolated using a collagenase perfusion method, pooled, and grown in T75 flasks pretreated with 0.2% gelatin at 37 C and 5% CO_2 until confluent as previously described.[65] The HUVEC flasks were trypsinized and seeded onto 30 mm glass coverslips pretreated with gelatin crosslinked with glutaraldehyde. The seeded HUVEC were incubated for

approximately 48 hours at 37 C and 5% CO_2 until confluent. HUVEC monolayers were activated with 2 mL of 1 ng/mL interleukin-1β (IL-1β) for 4 and 24 hours to induce high E-selectin and intercellular cell adhesion molecule-1 (ICAM-1) expression, respectively.

2.8 Blood Preparation

Venous blood was obtained from healthy donors with written consent following a protocol approved by the University of Michigan Internal Review Board. Anticoagulant, either acid-citrate dextrose (ACD) or heparin (HEP), was added to blood at a ratio of 0.14 anticoagulant to whole blood. To examine the role of plasma, blood was centrifuged at 2250g for 7 minutes to remove white blood cells (WBCs) and isolate red blood cells (RBCs) and plasma for flow adhesion assays. The RBCs were washed with PBS -/-, and plasma was placed in a new tube. Plasma and RBCs were centrifuged one more time at 2250g for 7 minutes to remove any remaining WBCs. For anticoagulant free plasma (ACF), whole blood was centrifuged after being drawn as described above and immediately used in flow assays. All samples were kept at 37 C before usage, except for ACF.

2.9 Parallel Plate Flow Chamber

Flow adhesion experiments were conducted using a parallel plate flow chamber (PPFC) (Glycotech Corporation, 127 μm channel) assay with a rectangular channel gasket. For each experiment, a confluent monolayer of HUVEC activated for 4 or 24 hours, as previously described, was vacuum sealed to the bottom of PPFC. 5×10^5 particles/mL were added to a mixture of RBCs in flow buffer or plasma (ACD, HEP, or ACF) at a hematocrit of 40%. The particle mixture was perfused through the chamber for 5 minutes of laminar flow at a shear rate of 200, 500, or 1000 s^{-1} controlled by a syringe pump. The particle samples in ACD or HEP plasma conditions were

preincubated for 5 minutes before added to the chamber. To measure base particle binding, particles were added to flow buffer (FB) mixed with RBCs and added into the chamber without incubation. For ACF plasma experiments, particles were mixed with ACF plasma/RBCs and immediately added to the chamber at the same flow conditions before any significant clotting. After each experiment, ten fluorescent images of the HUVEC monolayer along the chamber's center were captured and counted using ImageJ. Control adhesion experiments were conducted with untargeted particles (unconjugated and avidin conjugated particles) exposed to inactivated HUVEC in similar flow conditions as described above.

2.10 SDS-PAGE

The adsorption of plasma proteins onto the particle surface was qualitatively characterized using SDS-PAGE. First, sLe^A PLGA, HSA-PLGA, CSPLGA, and HSA-CSPLGA particles were incubated in 78% plasma at a concentration of 3.85 x 10^6 particles/mL for 5 minutes at 37 C to mimic flow experiment conditions detailed above. Following incubation, particles were washed with PBS -/- to remove unbound proteins. Particles were resuspended in 50 µL of 1X lane marker non-reducing buffer (Thermo Scientific Pierce). The particle solution was heated to 95 C for 5 min using a thermocycler to de-nature and release surface-bound proteins. The resulting solution was centrifuged. Next, 25 µL of supernatant from each sample was pipetted into individual wells on 4-20% Tris-Glycine protein gels (Invitrogen Novex WedgeWell). The gel ran for ap-proximately 30 min at 200 V along with a standard molecular weight ladder (Precision Dual Color Protein Standard, Bio-Rad Laboratories) for comparison. The gel is removed from the cast and stained with Coomassie blue (Invitrogen SimplyBlue SafeStain) overnight. Gels were washed in deionized water to de-stained and imaged.

2.11 Biodistribution Study of PLGA and CSPLGA coated with albumin only

First, PLGA and CSPLGA microparticles were fabricated as above with the addition of 1% PLGA polymer conjugated to Cy5.5 in the oil phase. Microparticles were conjugated with albumin using the conditions described above. Particles were reacted in a 50 mL polypropylene tube to scale-up reaction. The particle solution was aliquoted into 1.7 mL centrifuge tubes at the end of reaction and centrifuged. Supernatant was aspirated and the pellets were combined. Particles were washed with flow buffer and the final resuspension was in PBS-/- at a concentration of $2x10^8$ particles/mL. A total of $2x10^7$ particles were injected into C57BL/6J mice via a tail vein catheter. Mice were euthanized via CO_2 asphyxiation at 30 minutes after particle injection as previously discussed.[66] The spleen, kidneys, liver, heart, and lungs were collected, as well as the blood via cardiac puncture. Whole organ scans were obtained using an Odyssey CLx infrared imaging system (LI-COR). The intensity of blood was estimated by scanning 100 uL of blood in a 96-well black sided, clear bottom plate then multiplied by 20 assuming each mouse has a total blood volume of 2 mL. The background fluorescence of organs from untreated samples was subtracted from organs exposed to particles and plotted as adjusted fluorescence.

2.12 Statistical Methods

The data from flow adhesion experiments are plotted as adhesion efficiency, the ratio of particles bound in RBC-in-Plasma over RBC-in-FB. For protein corona characterization, SDS-PAGE gels were analyzed with ImageJ. Each n represents an individual donor. The data on all figures and tables are plotted with standard error bars. The statis-tical analysis was conducted using Prism for each data set and specified in the captions. Both adhesion efficiencies and band intensities were analyzed using one-way ANOVA with Dunnett's multiple comparisons test with

PLGA as control. Statistical significance is displayed as (*) = $p<0.05$, (**) = $p<0.01$, (***) = $p<0.001$, (****) = $p<0.0001$ and ns = not significant.

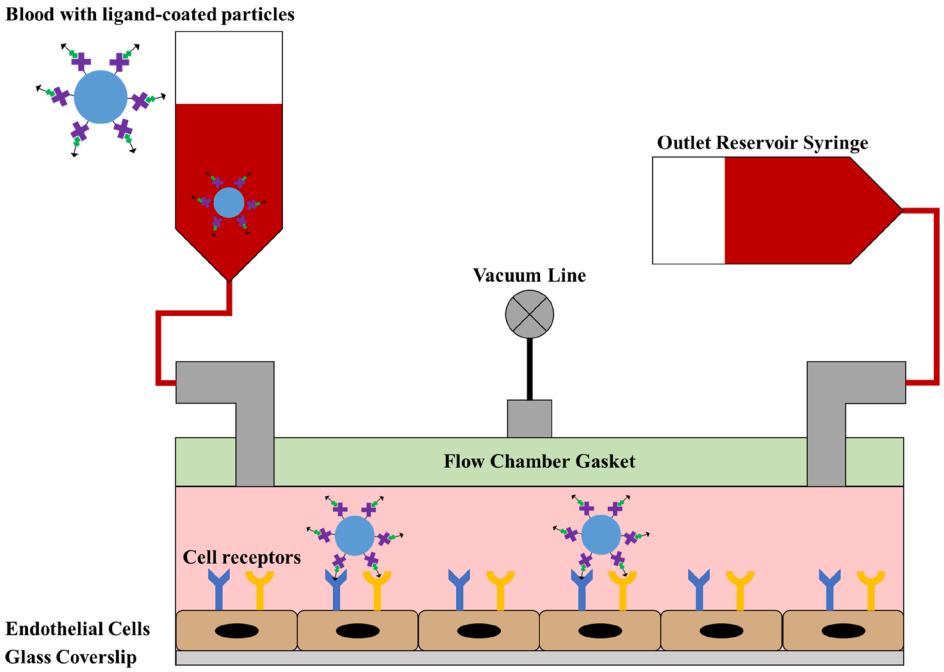

Figure 2.3 Parallel plate flow chamber assay.

Chapter 3 : Glycol Chitosan Coating on PLGA Increases Adhesion to Inflamed Endothelial Cells Even in the Presence of Plasma Proteins

3.1 Abstract

Polylactic-co-glycolic acid (PLGA), a negatively charged copolymer, is the most appealing material because of its tunable biodegradability, biocompatibility, and FDA approval. Unfortunately, the ability of PLGA to adhere to an inflamed endothelium is reduced in the presence of plasma proteins, which creates a significant obstacle for vascular targeting. The surface modification of PLGA with chitosan (CS) and glycol chitosan (GC), a positively charged polysaccharide and its derivative, is a potential approach in improving its adhesion by altering the surface hydrophobicity and charge, which impact protein adsorption. Here, we aimed to characterize the *in vitro* adhesion and plasma protein coronas of PLGA, CSPLGA, and GCPLGA particles conjugated with a targeting ligand at physiological conditions to an inflamed endothelium in the presence of red blood cells in buffer or plasma. The surface charge of PLGA shifted to neutral or positive after coating with CS or GC, respectively. Interestingly, GCPLGA saw the highest level of retention in particle binding after exposure to plasma relative to flow buffer. The enhanced adhesion of GCPLGA is linked to increased cellular association to the endothelium over other particle types. The extent of adhesion recovery of GCPLGA was dependent on targeting ligand type, ligand density, and shear rate. Ultimately, this contributes information to drug carrier design, specifically in terms of favorable surface hydrophobicity, charge, and protein coronas obtained.

3.2 Introduction

Vascular targeted carriers encounter several barriers as they enter the bloodstream, such as opsonization, that prevent their successful margination, localization, and adhesion to damaged vasculature. Designing VTCs that have increased circulation and an affinity for the endothelium could improve their targeting capability. The formation of the protein corona after adsorption of plasma proteins onto the surface of VTCs has a significant impact on circulation time and ability to reach the target site. An increase in the number of opsonins present in the protein corona can determine the rate of phagocytic clearance of VTCs. Poly (lactic-co-glycolic acid) (PLGA) particles are of great interest for the delivery of therapeutics due their biodegradability, biocompatibility, and FDA approval. Unfortunately, PLGA particles suffer from high adsorption of opsonins, i.e., immunoglobulins, which affect their ability to circulate and adhere to the vasculature. The most common method used to increase circulation time is through the addition of poly (ethylene glycol) (PEG) to the surface, which has shown to reduce protein adsorption and reduce phagocytosis. Unfortunately, recent studies have found that repeated administration of PEGylated drug carriers can lead to the production of PEG antibodies in the host. Additionally, PEG is commonly found in household and consumer products, which has increased the number of people with pre-existing PEG antibodies.[67] The presence of PEG antibodies in the bloodstream can potentially compromise the activity and safety of prescribed PEG therapeutics. For this reason, there is a need to find alternative polymers for the modification of drug carriers to improve their biological fate, such as increased circulation time and cellular association.

Mucoadhesive polymers, such as chitosan (CS) and its derivative glycol chitosan (GC), are alternative coatings used to change surface charge and hydrophobicity of various drug carriers.[44] Drug carriers with a neutral charge and hydrophilic surface have been shown to reduce the total

amount of protein, as well as alter the composition of protein corona. Chitosan is a positively charged, polysaccharide with high solubility in acidic conditions that is degraded by enzymatic catalysis.[45] Glycol chitosan contains hydrophilic ethylene branches improving its solubility in neutral and acidic environments.[68] These coatings have demonstrated their ability to improve physiochemical stability, controlled release, drug bioavailability, and various other advantages for a wide range of carrier types and drug delivery applications.[44,46] Amoozgar et al. directly compared the addition of low molecular weight chitosan to PEG onto PLGA particles as a stealth coating. The chitosan coating reduced opsonization and phagocytic uptake compare to PLGA, which as dependent on the molecular weight of CS.[69] Other studies have used chitosan and PEG in combination with PLGA for designing long circulating drug vehicles.[70,71] These studies showed reduced protein binding, decreased macrophage uptake, increased blood circulation, and lower accumulation of CS/PEG modified particles in the liver. Glycol chitosan has an ethylene glycol branch that could provide a similar benefit to the combination of CS/PEG coating. The addition of glycol chitosan (GC) onto the surface of PLGA increased the amount of particles present in the blood and lymph nodes over CS-coated PLGA and bare PLGA due to the better mucoadhesive ability of GC.[72] Since modifying the surface of PLGA with CS and GC has shown to improve circulation time, we wanted to understand whether these coatings could ameliorate the reduced adhesion seen for PLGA in the presence of plasma proteins. Here, we fabricated CS and GC coated PLGA using the physical adsorption method to reserve functional groups for ligand conjugation and characterized the surface charge.[47] Next, we evaluated the adhesion of uncoated and coated PLGA microparticles to an inflamed endothelium in various physiological mediums. We also investigated how CS and GC coatings affect the adsorption of plasma proteins. Ultimately, this

will provide information on the utility of CS and GC coated PLGA microparticles as carriers for vascular-targeted drug delivery.

3.3 Results

3.3.1 Size and surface properties of PLGA and coated PLGA microparticles

Microparticles were fabricated using the emulsion solvent evaporation method and different coatings were achieved by varying the surfactant in the water phase. The coatings are physically adsorbed onto the surface of PLGA droplets during fabrication through electrostatic interactions between carboxylic acid and amine groups present on PLGA and mucoadhesive coatings, respectively. Rhodamine was encapsulated in all particle types to visualize them during particle binding assays. Fabrication conditions were adjusted to obtain spheres of about 2 μm diameter, which have shown optimal targeting to blood vessel wall over nanosized carriers.[73] The surface morphology of all particle types was characterized by SEM and images are found in Figure 3.1. All microparticles had a spherical shape and a smooth surface, except for GCPLGA that showed some surface roughness. The particle size measured from SEM images and zeta potential of PLGA, CSPLGA, and GCPLGA are displayed in Table 3.1. The resulting diameters for PLGA and CSPLGA microparticles were around 1.6 μm, while the diameter for GCPLGA was 1.9 μm. The zeta potential for PLGA coated with CS and GC saw shifts in charge from standard PLGA confirming the presence of surface coatings listed in Table 3.1. Standard PLGA had a strong negative charge at -30.3 mV. CSPLGA demonstrated a neutral charge of about +10.7 mV. A strong positive charge was seen for GCPLGA at +32.7 mV. This shift in zeta potential from net negative towards the positive direction confirms that CS and GC are on the surface of PLGA, given the known cationic nature of chitosan polymers.[74] To explore another positively charged surface, PLGA was also coated with polyethylenimine (PEI), which resulted in a size of 1.4 μm and surface

charge of +49.5 mV. The encapsulation of rhodamine did not significantly impact the size or zeta potential at these fabrication conditions.

Table 3.1 Size and zeta potential of PLGA and coated PLGA microparticles. [U] = unloaded, [R] = rhodamine loaded.

Particle Type	Size (µm)	Zeta Potential (mV)
[U] PLGA	1.6 +/- 0.6	-30.3 +/- 7.3
[U] CSPLGA	1.7 +/- 0.5	+10.7 +/- 2.7
[U] GCPLGA	1.9 +/- 0.6	+32.7 +/- 2.3
[U] PEIPLGA	1.4 +/- 0.5	+49.5 +/- 2.4
[R] PLGA	1.6 +/- 0.5	-26.2 +/- 3.7
[R] CSPGLA	1.6 +/- 0.5	+7.18 +/- 2.7
[R] GCPLGA	2.0 +/- 0.7	+30.9 +/- 2.8
[R] PEIPLGA	1.4 +/- 0.4	+46.3 +/- 6.5

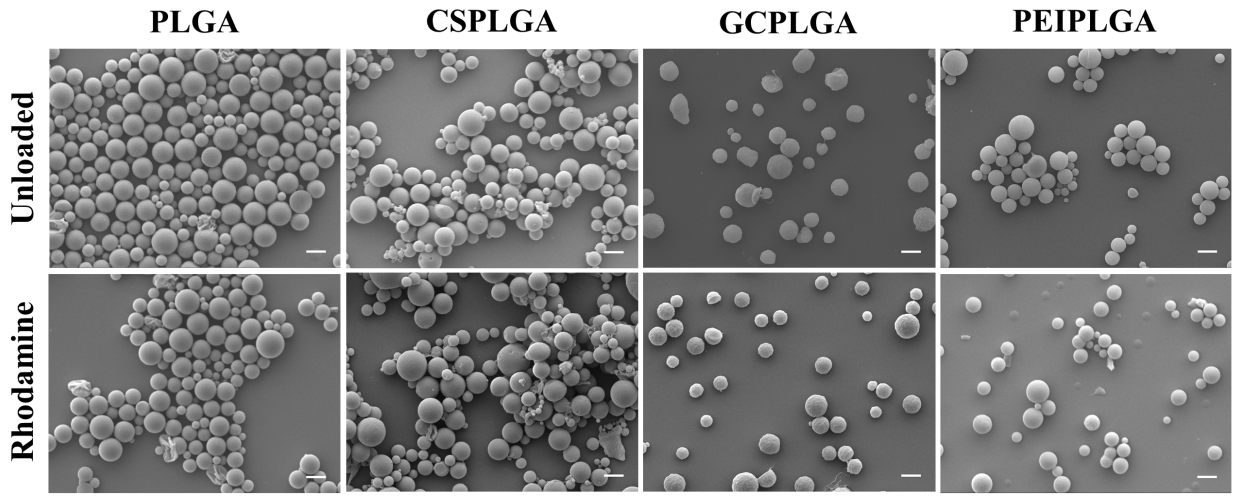

Figure 3.1 SEM images of unloaded and rhodamine loaded PLGA, CSPLGA, GCPLGA, and PEIPLGA microparticles. CS = chitosan, GC = glycol chitosan, PEI = polyethylenimine. Scale bar = 2 µm.

Additionally, elemental analysis of the particle surface with x-ray photoelectron spectroscopy (XPS) was used to identify nitrogen atoms present on the coatings utilized, which are absent on PLGA. The full spectra and the nitrogen N1s spectrum regions for both unloaded

and rhodamine-loaded particles obtained from XPS are shown in Figure 3.2. The nitrogen peak is apparent for unloaded CSPLGA confirming the presence of chitosan on the PLGA surface. Rhodamine-loaded CSPLGA did not show a prominent nitrogen peak. The shift in surface charge from -26.2 mV to +7.18 mV (Table 3.1) and the fact that chitosan is the only surfactant in the water phase of CSPLGA suggests the presence of chitosan on the particle surface. The nitrogen peak was prominent for both unloaded and rhodamine loaded GCPLGA and PEIPLGA confirming the successful coating on the PLGA surface. The elemental composition obtained from XPS show a slight decreased in the percent of nitrogen atoms present after encapsulation of rhodamine for CSPLGA, GCPLGA, and PEIPLGA as displayed in Table 3.2.

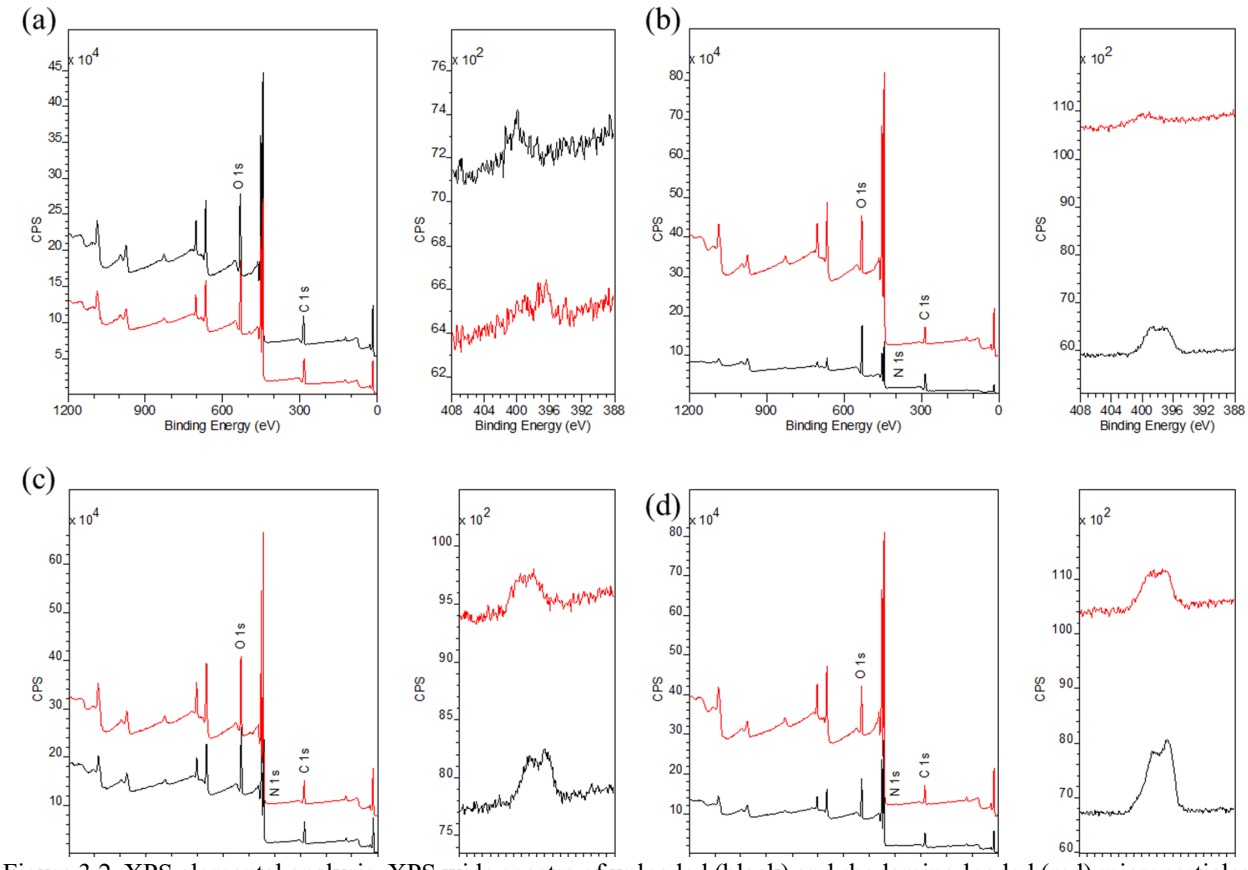

Figure 3.2 XPS elemental analysis. XPS wide spectra of unloaded (black) and rhodamine-loaded (red) microparticles on the left and N1s spectrum region on the right. (a) PLGA, (b) CSPLGA, (c) GCPLGA, and (d) PEIPLGA. CasaXPS was used to plot spectra.

Table 3.2 Elemental composition from XPS.

Particle Type /Composition (%)	Carbon	Nitrogen	Oxygen
[U] PLGA	57.28	0.00	42.72
[U] CSPLGA	62.77	0.94	36.29
[U] GCPLGA	55.25	0.74	44.01
[U] PEIPLGA	57.61	2.86	39.54
[R] PLGA	62.98	0.00	37.02
[R] CSPGLA	49.23	0.00	50.77
[R] GCPLGA	51.29	0.52	48.19
[R] PEIPLGA	55.89	1.54	42.57

Table 3.3 Avidin and targeting ligand site densities measured via flow cytometry.

Particle Type/ (#/μm^2)	Avidin	aICAM [High site density]	sLe^A
PLGA	25,000 +/- 10,000	6,600 +/- 1,400 [15,000 +/- 3,000]	4,600 +/- 1,600
CSPLGA	14,000 +/- 4,000	6,600 +/- 1,300 [16,000 +/- 4,000]	6,400 +/- 2,000
GCPLGA	35,000 +/- 29,000	6,500 +/- 2,000 [16,000 +/- 4,000]	5,500 +/- 1,900
PEIPLGA	17,000 +/- 900	-	6,500 +/- 700

3.3.2 Evaluation of Targeted PLGA, CSPLGA, and GCPLGA Adhesion in ACD Plasma

Next, we evaluated whether the addition of surface coatings onto PLGA can improve particle binding to an inflamed HUVEC monolayer using a parallel plate flow chamber to model a human blood vessel. First, all particle types were conjugated with avidin followed by the attachment of biotinylated targeting moieties and the approximate site densities are listed in Table 3.3. Biotinylated anti-ICAM and sLe^A were used to target ICAM-1 and E-selectin because of their presence on endothelial cells in inflammatory environments with maximum surface expression at

24 and 4 hours, respectively. To determine the impact of plasma proteins on particle adhesion, targeted particles were added to a mixture of RBC-in-Buffer or RBC-in-Plasma at a concentration of $5x10^5$ particles/mL with a fixed hematocrit of 40%. For plasma conditions, particles were incubated for 5 minutes in RBC-in-Plasma prior to being added into the flow chamber to allow protein corona to form. First, we evaluated the adhesion of PLGA, CSPLGA and GCPLGA conjugated with anti-ICAM1. The representative fluorescent images of bound particles at 200 s^{-1} are shown in Figure 3.3. Both aICAM targeted PLGA and CSPLGA show a drastic reduction in the number of particles bound in plasma, while GCPLGA retained most of its binding.

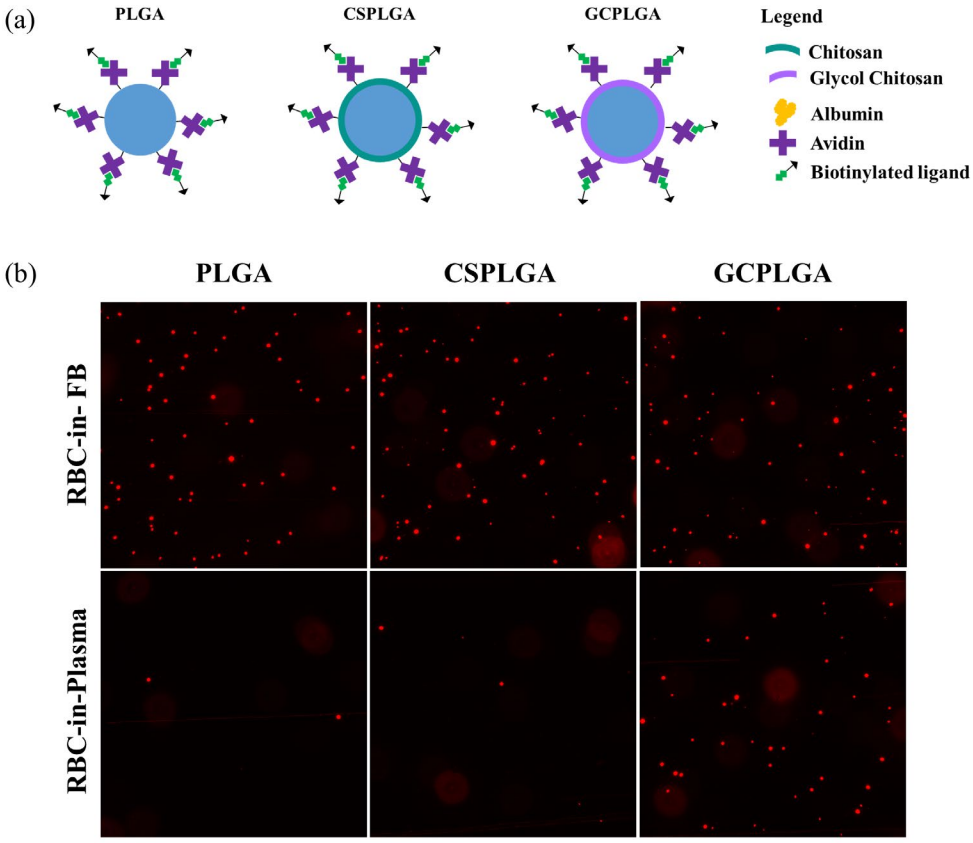

Figure 3.3 (a) Schematic of coated and targeted PLGA. (b) Fluorescent images of anti-ICAM PLGA, CSPLGA, and GCPLGA particles bound to an inflamed endothelium exposed to RBC-in-FB and RBC-in-Plasma at 200 s^{-1}.

The binding of each particle type in plasma is plotted relative to its binding in flow buffer, depicted as adhesion efficiency in Figure 3.4. At 200 s^{-1}, both aICAM targeted PLGA and CSPLGA had an adhesion efficiency of 4.8% and 2.8%, respectively. aICAM targeted GCPLGA kept 52% of its adhesion in plasma relative to flow buffer, which is significant improvement over aICAM PLGA ($p<0.0001$). As the shear rate is increased, aICAM GCPLGA showed a decrease in adhesion efficiency to 35% at 500 s^{-1}. It was further decreased to 14% at 1000 s^{-1}. Next, we increased the aICAM site density to more than double to determine its effect on adhesion efficiency. There was a slight increase in adhesion efficiency for "High" aICAM targeted PLGA and CSPLGA to 11% and 21%, respectively. The adhesion efficiency of GCPLGA with a "High" aICAM site density showed a significant increase at 200 s^{-1} (84%, $p=0.0024$) and 500 s^{-1} (63%, $p=0.0004$) over the starting aICAM site density on GCPLGA. At a high shear rate of 1000 s^{-1}, "High" aICAM GCPLGA saw a significant decrease in adhesion efficiency (24%) compared its binding to 200 s^{-1} ($p<0.0001$). Next, we exchange the targeting ligand from anti-ICAM to sLe^A, which has different binding kinetics that result in faster capture. The binding of sLe^A targeted PLGA and CSPLGA was minimal at all shear rates tested with an adhesion efficiency below 21%. sLe^A targeted GCPLGA had the highest adhesion efficiency (84% to 63%)), which did not decrease as the shear rate was increased. At 500 s^{-1}, we also evaluated the adhesion of PLGA coated with PEI and targeted with sLe^A to examine the adhesion of another positively charged particle. The adhesion efficiency of sLe^A PEIPLGA was 46% ($p<0.0001$) compared to 72% for sLe^A GCPLGA ($p<0.0001$) at the intermediate shear rate, which are both significantly higher than sLe^A PLGA.

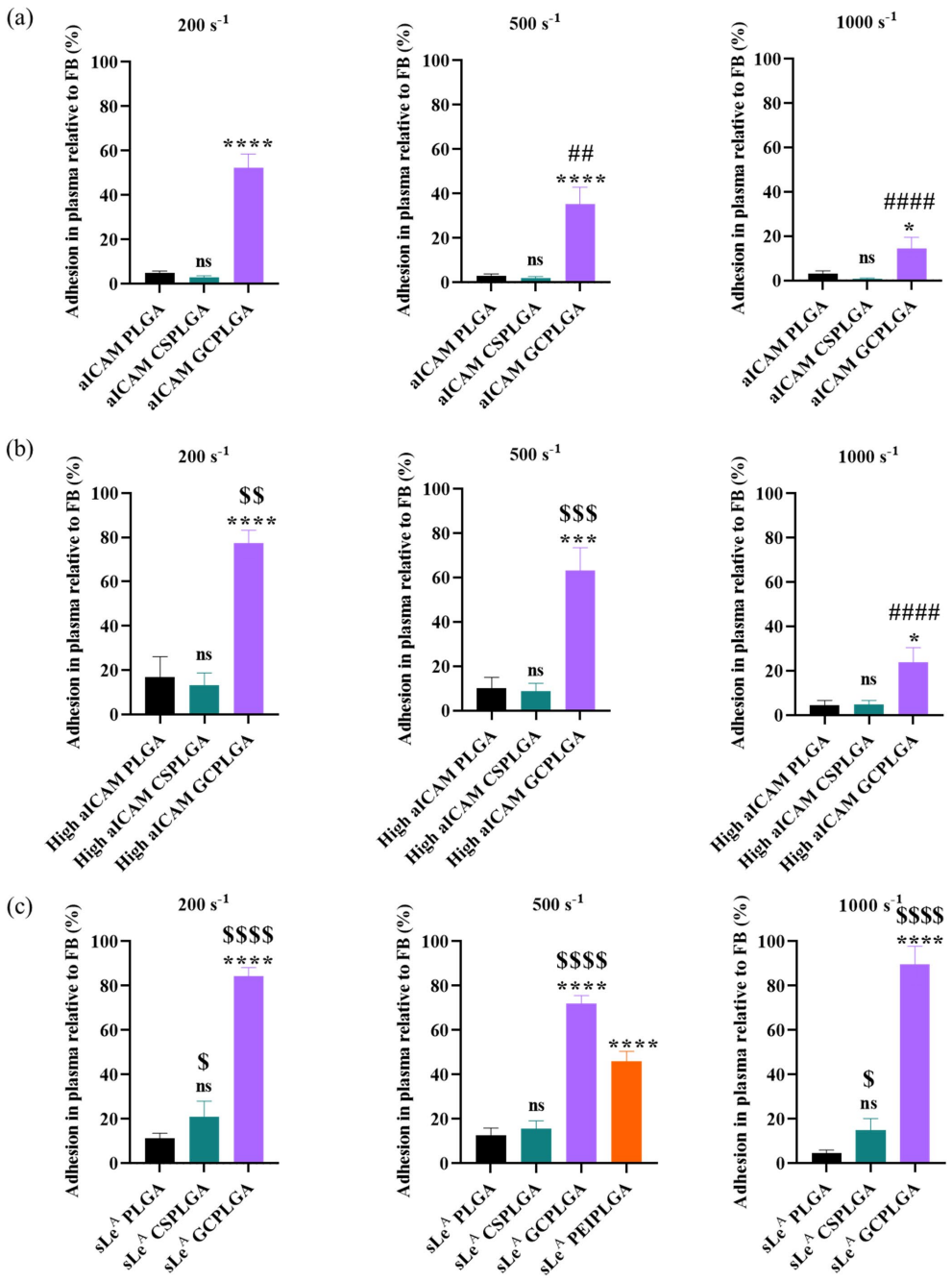

Figure 3.4 Adhesion of targeted PLGA, CSPLGA and GCPLGA to an inflamed endothelium. Particles were added to RBC-in-FB or RBC-in-ACD plasma at a $5x10^5$ particles/mL concentration and perfused over HUVEC activated for 24 or 4 hours. Particles in plasma were incubated for 5 minutes prior to experiment. Quantified adhesion of particles in RBC-in-Plasma relative to RBC-in-FB at 200, 500, and 1000 s^{-1} using three different targeting schemes: anti-ICAM1 (a), High aICAM (b), and sLe^A (c). Statistical analysis was completed using one-way ANOVA with Dunnett's multiple comparison test with PLGA as control. (*) = $p<0.05$, (**) = $p<0.01$, (***) = $p<0.001$, (****) = $p<0.0001$ and ns = not significant. (#) represents significance to their binding in 200 s^{-1} and ($) represents significance to their aICAM binding. n=10 distinct donors. Error bars represent standard error. sLe^A = sialyl Lewis A, CS = chitosan, GC = glycol chitosan, PEI = polyethylenimine, ACD = acid-citrate-dextrose, RBC = red blood cell, FB = flow buffer.

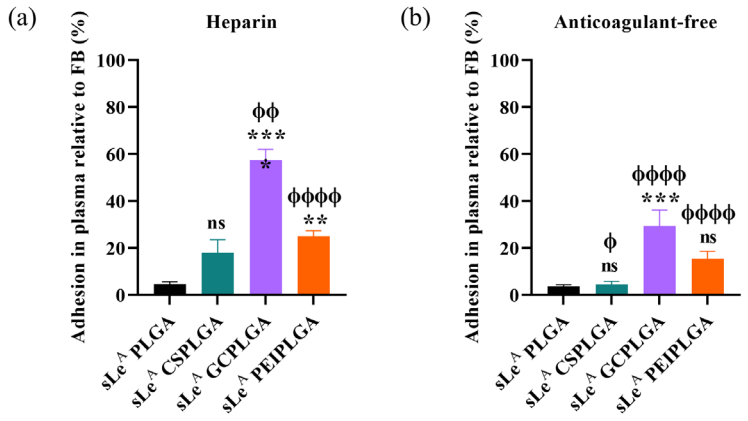

Figure 3.5 Adhesion of sLe^A targeted PLGA, CSPLGA, GCPLGA and PEIPLGA in heparin plasma (a) and anticoagulant-free (ACF) plasma (b). Particles were added to RBC-in-FB, RBC-in-HEP Plasma and RBC-in-ACF Plasma at a $5x10^5$ particles/mL. Particles in RBC-in-HEP Plasma were incubated for 5 minutes prior to being added to the parallel plate flow chamber. The endothelial cell monolayers were activated for 4 hours. Statistical analysis was completed using one-way ANOVA with Dunnett's multiple comparison test with PLGA as control. (*) = $p<0.05$, (**) = $p<0.01$, (***) = $p<0.001$, (****) = $p<0.0001$ and ns = not significant. (Φ) represents significance to their binding in ACD Plasma. n=10 distinct donors. Error bars represent standard error. sLe^A = sialyl Lewis A, CS = chitosan, GC = glycol chitosan, PEI = polyethylenimine, ACD = acid-citrate-dextrose, HEP = heparin, ACF = anticoagulant-free, RBC = red blood cell, FB = flow buffer.

3.3.3 Evaluation of Targeted PLGA, CSPLGA, GCPLGA, and PEIPLGA in Various Plasma Conditions

Previous work has shown that it is important to examine the adhesion of PLGA particles in various physiological mediums, such as other anticoagulants and serum. Here, the adhesion of sLe^A targeted particles was examined in various physiological mediums because they resulted in the highest recovery for GCPLGA across shear rate in ACD plasma. Heparin prevents clotting by binding to antithrombin and other types of proteins, which can alter protein interactions with particles. We evaluated the adhesion of particles in heparin (HEP) plasma and anticoagulant-free plasma (ACF) at a constant shear rate of 500 s^{-1} shown in Figure 3.5. There was no significant difference for sLe^A targeted PLGA and CSPLGA particle binding in the mediums tested. Both sLe^A targeted GCPLGA and PEIPLGA were both significantly higher than sLe^A PLGA, $p<0.0001$ and $p=0.0019$ respectively. For sLe^A GCPLGA microparticles, the adhesion efficiency was reduced to 57% when the ACD is exchanged for heparin ($p=0.0063$). sLe^A PEIPLGA adhesion

efficiency was also reduced to 25% in heparin plasma compared to ACD plasma($p<0.0001$). The adhesion efficiencies for sLe^A GCPLGA and PEIPLGA were 29% and 15%, respectively.

3.3.4 Plasma Protein Corona of Coated PLGA Particles in ACD Plasma

The adsorption of plasma proteins onto the particle surface has demonstrated to affect their efficacy as drug carries. As previously presented, the ability of PLGA to bind to an inflamed endothelial cell monolayer has been negatively impacted by the adsorption of large molecular weight proteins, such as immunoglobulins. To understand whether the recovery in adhesion for GCPLGA particles can be attributed to a reduction in protein adsorption or difference in the makeup of the protein corona, SDS-PAGE gels were conducted. Representative gels of aICAM and sLe^A targeted particles incubated in FB or ACD plasma are shown in Figure 3.6. Each gel was analyzed using ImageJ and the intensities of bands were grouped based on molecular weight range to understand any changes in in protein corona composition. Proteins with a molecular weight between 75-51 kDa composed 47-55% of the protein corona on all aICAM and sLe^A targeted particles. Regardless of targeting ligand, GCPLGA showed an increase in proteins with a molecular weight range of 37-20 kDa and 19-10 kDa. These two molecular weight ranges also appear on GCPLGA incubated in flow buffer, which contains 1% BSA. More specifically, there is a slight decrease in the composition of proteins with molecular weight ranges of 250-151 kDa and 150-76 kDa for aICAM GCPLGA compared to aICAM PLGA. sLe^A GCPLGA had a slight decrease in composition of proteins with a molecular weight of 75-51 kDa. Next, we compared bands at 66 kDa and 150 kDa to assess any changes in adsorption of albumin or immunoglobulins, which is shown in Figure 3.6d-e. Overall, GCPLGA saw an increase in intensity at the 66 kDa band and a slight decrease at the 150 kDa band intensity compared to PLGA for both aICAM and sLe^A targeted particles.

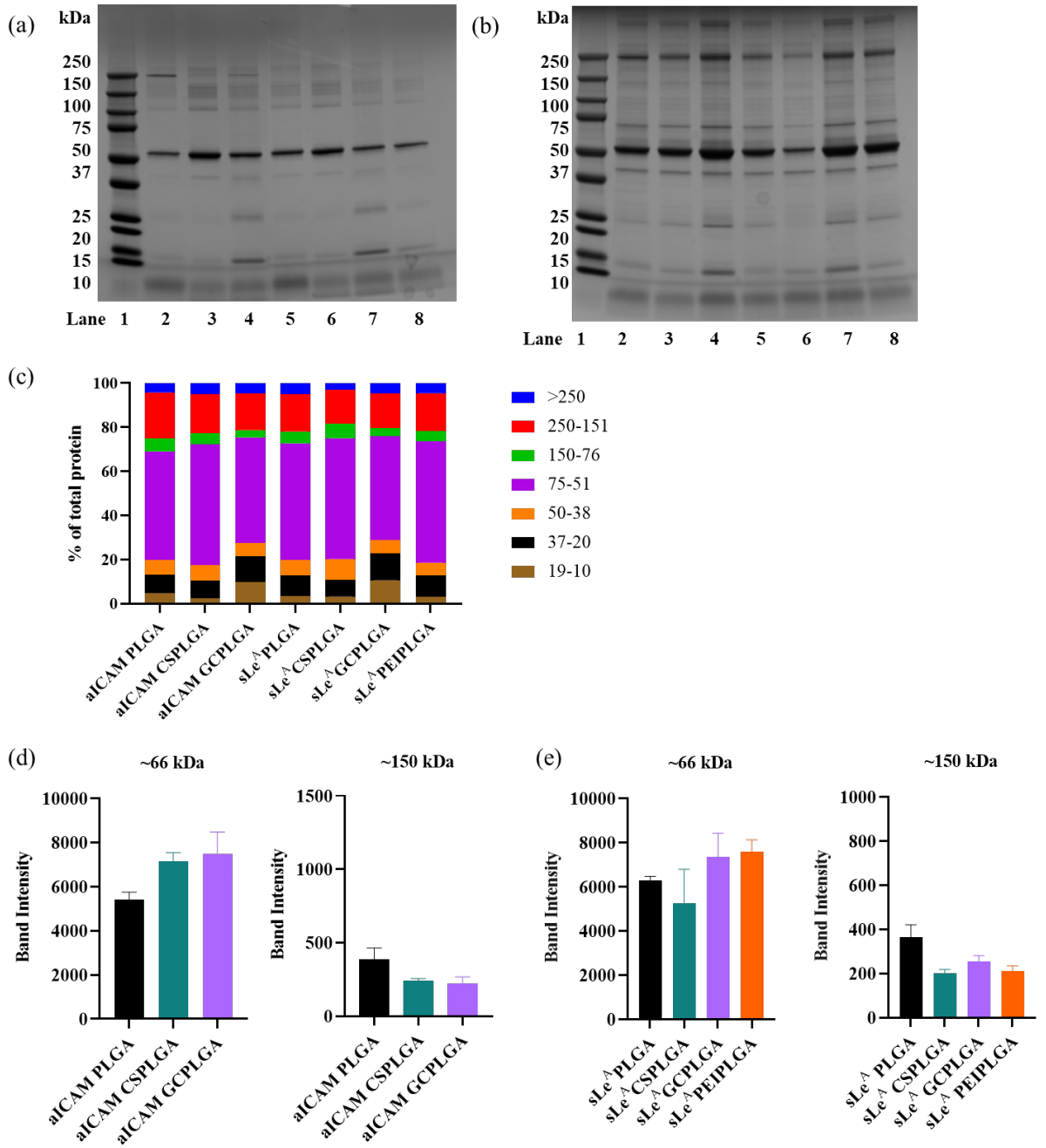

Figure 3.6 SDS-PAGE plasma protein corona characterization of targeted PLGA, CSPLGA, GCPLGA and PEIPLGA. Gels of particles incubated in FB (a) and ACD plasma (b) for 5 minutes at 37 C. Lane 1: Molecular weight standard, Lane 2: aICAM-PLGA, Lane 3: aICAM-CSPLGA, Lane 4: aICAM-GCPLGA, Lane 5: sLe^A-PLGA, Lane 6: sLe^A-CSPLGA, Lane 7: sLe^A-GCPLGA, and Lane 8: sLe^A-PEIPLGA. (c) Semiquantitative analysis of protein corona composition in ACD plasma. Band intensities at 66 and 150 kDa for aICAM (d) and sLe^A (e) targeted particles. n=2 distinct donors. Error bars represent standard error. sLe^A = sialyl Lewis A, CS = chitosan, GC = glycol chitosan, PEI = polyethylenimine, ACD = acid-citrate-dextrose, FB = flow buffer.

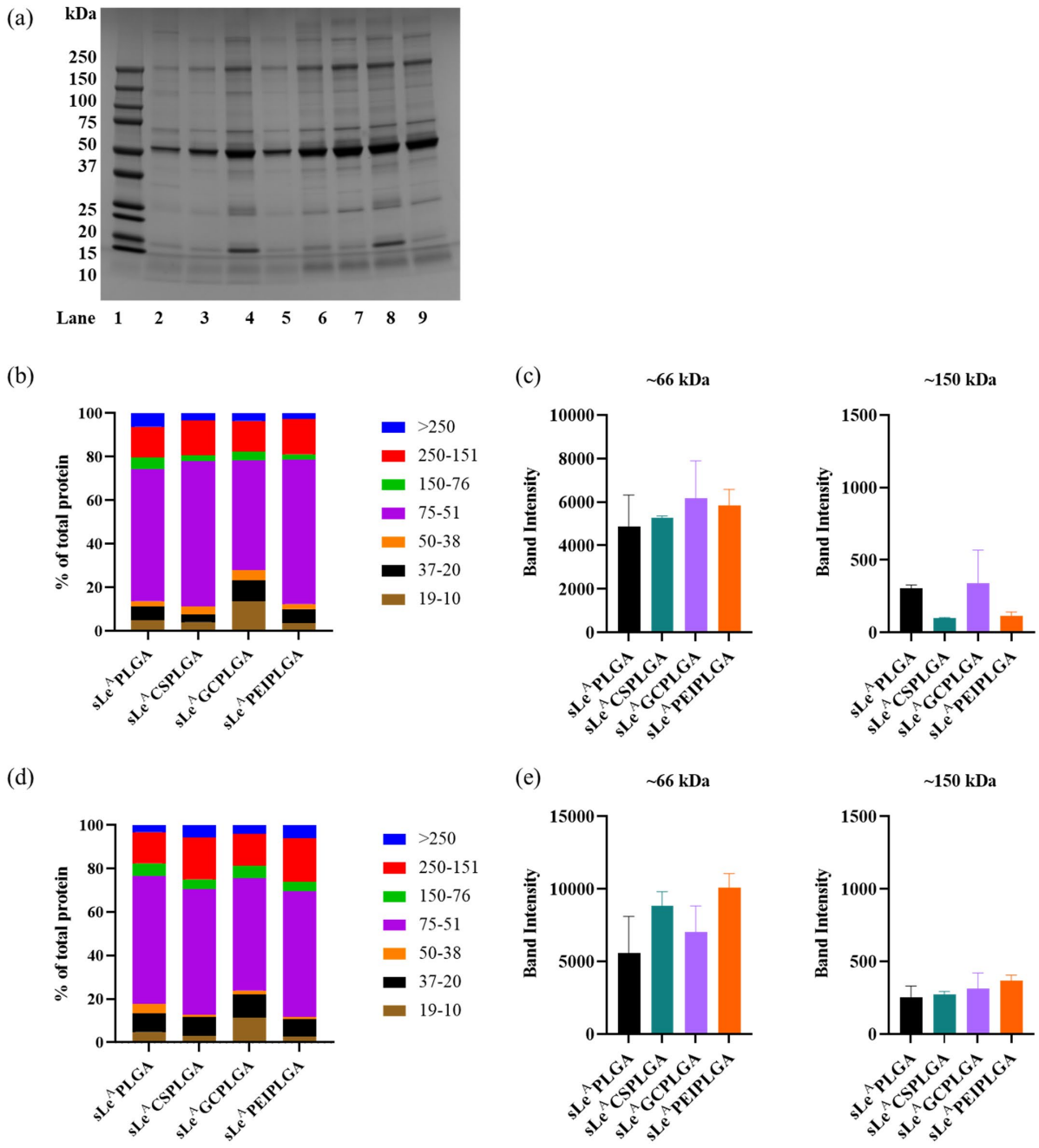

Figure 3.7 Plasma protein corona characterization of sLe^A PLGA, CSPLGA, GCPLGA and PEIPLGA in heparin and anticoagulant-free plasma. (a) SDS-PAGE of sLe^A targeted particles incubated HEP and ACF plasma for 5 minutes at 37 C. Lane 1: Molecular weight standard, Lane 2: PLGA in HEP, Lane 3: CSPLGA in HEP, Lane 4: GCPLGA in HEP, Lane 5: PEIPLGA in HEP, Lane 6: PLGA in ACF, Lane 7: CSPLGA in ACF, Lane 8: GCPLGA in HEP and Lane 9: PEIPLGA in ACF. (c) Semiquantitative analysis of protein corona composition in ACD plasma. Band intensities at 66 and 150 kDa in aICAM (d) and sLe^A (e) targeted particles. n=2 distinct donors. Error bars represent standard error. sLe^A = sialyl Lewis A, CS = chitosan, GC = glycol chitosan, PEI = polyethylenimine, ACD = acid-citrate-dextrose, HEP = heparin, ACF = anticoagulant-free, FB = flow buffer.

3.3.5 Protein Corona of Coated PLGA in Heparin and Anticoagulant-free Plasma

We also characterized the protein corona composition of different molecular weights on coated PLGA particles exposed to heparin and anticoagulant-free plasma. A representative gel of sLe^A targeted particles in these two plasma conditions is displayed in Figure 4.6. In heparin plasma, all coated PLGA particles showed a decrease in the presence of proteins with a molecular weight >250 kDa in the corona compared to bare PLGA. A slight increase in the extent of proteins with a molecular weight range between 75-51 kDa for CSPLGA and PEIPLGA present in the corona, while there was a decrease for GCPLGA. Alike the adsorption in ACD plasma, there was an increase in lower molecular weight ranges between 37-20 kDa and 19-10 kDa for GCPLGA. Comparing the 66 and 150 kDa show a slight increase in intensity for GCPLGA compared to PLGA. Next, we analyzed the protein corona composition of particles exposed to anticoagulant-free plasma. All coated PLGA particles saw a decrease in the amount of proteins with molecular weights between 50-38 kDa over bare PLGA. The composition of GCPLGA saw a decrease at 75-51 kDa and increases at 37-20 kDa and 19-10 kDa. Directly comparing the 66 and 150 kDa bands of particles exposed to ACF did not show any differences between PLGA and coated PLGA.

3.4 Discussion

Drug carriers formulated from PLA and PLGA synthetic polymers are characterized as having a relatively hydrophobic surface and strong negative charge, which has been shown to significantly increase protein adsorption. The addition of hydrophilic polymers is onto the surface of drug carriers has been widely used to reduce protein adsorption to prolong circulation time. Poly (ethylene glycol) (PEG) has been considered as the gold standard for surface modification with many PEGylated formulations successfully entering the market. Unfortunately, recent studies have shown development of antibodies specific for PEG after repeated administration of PEGylated

therapeutics, which is worsened by widespread use of daily household products incorporating PEG.[67] For this reason, there is a need to find alternative surface coatings that change surface hydrophobicity and charge.

Surface modification of drug carriers via chitosan and glycol chitosan has been shown to prolong blood circulation times, improve encapsulation of drugs with low solubility, enhance antimicrobial activity, and increase cellular association.[72,75,76] Both chitosan and glycol chitosan are hydrophilic polymers that can alter surface charge, which leads us to hypothesize that these coatings onto PLGA particles could influence protein adsorption and increase affinity to the endothelium to improve vascular adhesion. Here, we fabricated PLGA microparticles coated with chitosan (CS) and glycol chitosan (GC) using physical adsorption, which relies on electrostatic interactions between carboxylic and amine functional groups. PVA was not included in the water phase of coating polymers since we did not want residual PVA to influence any particle interactions, which has been detected on CSPLGA and GCPLGA in other studies.[72]

We characterized the surface of CSPLGA and GCPLGA microparticles using zeta potential measurements and XPS to confirm the presence of nitrogen atoms. The surface charge of CSPLGA and GCPLGA shifted PLGA's negative charge to a neutral and positive charge, respectively. The difference in charge between coatings could be due to differences in molecular weight reported by manufacturers as approximately 83 and 575 kDa for CS and GC respectively. The percentage of nitrogen atoms decreased from CS to GC, which could be explained by the addition of the ethylene glycol branch on GC increasing the number of carbon and oxygen atoms. We also included PLGA coated with PEI to compare another positively charged surface.

Since cationic particles tend to have enhanced cellular association due an affinity for the negatively, charged cell membrane, we evaluated the adhesion of PLGA, CSPLGA, GCPLGA,

and PEIPLGA to an inflamed endothelial cell monolayer in the presence of buffer and plasma.[77,78] Plasma protein adsorption can impact the cellular association and uptake of cationic particles. The addition of chitosan did not improve the adhesion of PLGA regardless of targeting ligand used. Interestingly, GCPLGA showed a significant increase in the amount of particle binding retained after exposure to plasma compared to PLGA in all conditions tested. The ratio of GCPLGA particles bound in plasma relative to flow buffer was dependent on the ligand type, ligand density, and shear rate applied. The adhesion efficiency increased as the targeting schemes changed from anti-ICAM, "High" anti-ICAM, and sLe^A. The impact of shear rate was more apparent for GCPLGA particles targeted with anti-ICAM. Conversely, the influence of shear rate was eliminated when using sLe^A as the targeting ligand. The enhance adhesion for sLe^A GCPLGA particles can be explained by the ability of sLe^A to interact with multiple receptors and decrease the carrier velocity allowing for firm adhesion to the endothelium.[79,80] PEIPLGA particles targeted with sLe^A also observed significant increase in adhesion efficiency over PLGA but not as much as GCPLGA particles. We also explored the impact of anticoagulant on the adhesion of coated PLGA particles, which showed a decrease in adhesion efficiency for GCPLGA and PEIPLGA from ACD to heparin to the anticoagulant-free plasma condition.

We also characterized the composition of the protein corona formed on PLGA, CSPLGA, GCPLGA and PEIPLGA microparticles to understand whether any changes were driving the differences seen in particle binding. In ACD plasma, sLe^A targeted GCPLGA and PEIPLGA observed a slight increase in the band above the 50 kDa standard band that most likely corresponds to albumin. The preferential adsorption of albumin onto cationic particles has previously been reported.[23] The presence of albumin in the protein corona has shown to have favorable biological interactions.[25] Additionally, we saw a decrease in the 150 kDa band intensity, which corresponds

to either immunoglobulins G or A based on their molecular weight. These protein adsorption patterns did not persist when the particles were exposed to heparin or anticoagulant-free plasma.

Since the adsorption of plasma proteins does not completely explain the improved adhesion seen with the GC and PEI coatings, we also looked at the ability of modified PLGA to adhere to endothelial cells. The appendix contains the results from experiments using unconjugated or avidin-conjugated particles to inactivated endothelial cells (Figure 7.4). These control experiments show that CS, GC, and PEI coated PLGA experience some level of unspecific binding. The CS coating only led to binding in buffer conditions, which was eliminated in the presence of plasma. The GC and PEI coating increased the level of unspecific binding in both buffer and plasma conditions, suggesting higher cellular association to the endothelium. The unspecific binding for PLGA coated with GC and PEI decreased in the presence of plasma and almost eliminated at higher shear rates. The increased cellular association of GCPLGA and PEIPLGA over PLGA and CSPLGA with endothelial cells may contribute to the enhanced particle binding in plasma conditions.

3.5 Conclusions

In this work, we evaluated the effect of surface modification of PLGA microparticles with mucoadhesive polymers on their ability to bind to the vasculature in the present of plasma proteins. We utilized chitosan and glycol chitosan to alter surface hydrophilicity and charge to influence cellular association and protein adsorption to ameliorate the adhesion of PLGA in plasma conditions. Here, PLGA particles were successfully coated with CS, GC, and PEI, which produced a range of positively charged surfaces. Interestingly, GCPLGA and PEIPLGA particles had the highest level of adhesion in plasma relative to their binding in flow buffer conditions. The adhesion efficiency for GCPLGA was dependent on the ligand type, ligand site density, and shear rate. In

general, there were some changes in the composition of the protein corona. The improved adhesion of GCPLGA is most likely due to an increase in bio-adhesive forces keeping particles at the endothelium. Further studies need to be conducted to identify specific protein present in bands of interest to understand any potential benefits. Overall, this work contributes information to the utility of positively charged PLGA particles as vascular targeted carriers for targeting the endothelium.

3.6 Supplemental Data

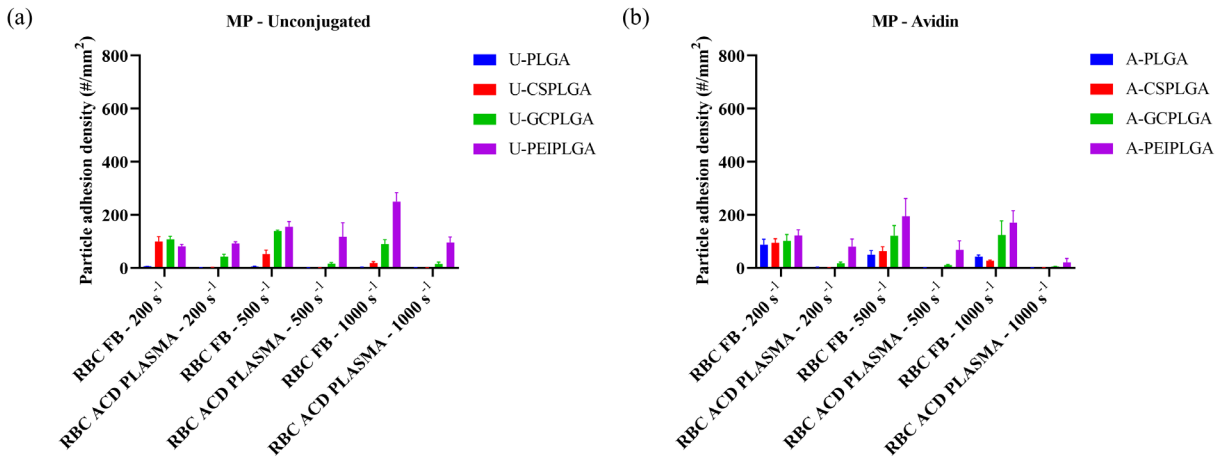

Figure 3.8 Particle binding of unconjugated (a) and avidin conjugated (b) PLGA, CSPLGA, GCPLGA, and PEIPLGA.

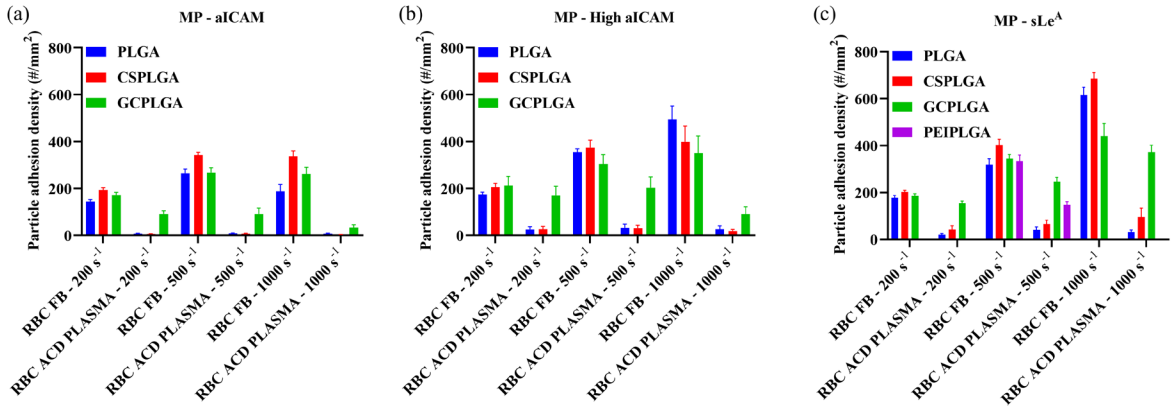

Figure 3.9 Raw particle adhesion density of targeted microparticles. (a) aICAM, (b) High aICAM, and (c) sLe^A.

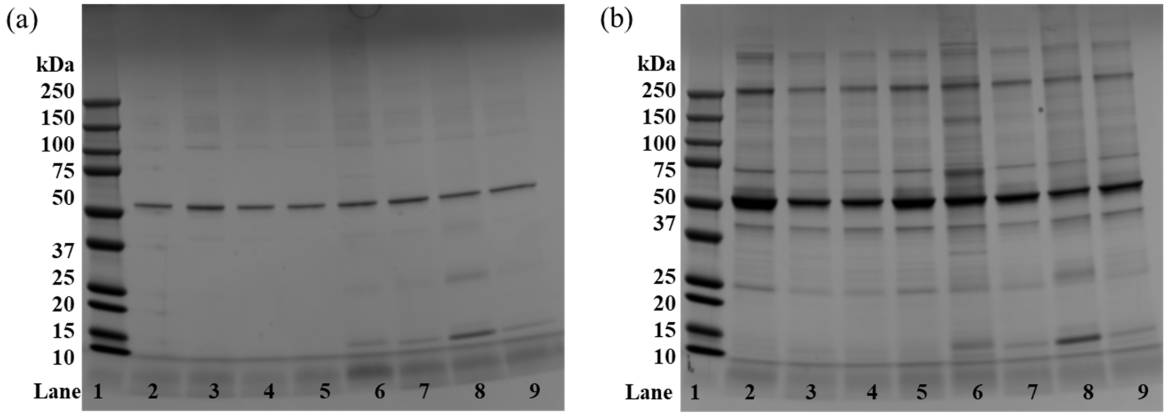

Figure 3.10 SDS-PAGE characterization plasma protein corona of unconjugated (UNC) and avidin (AVI) conjugated PLGA, CSPLGA, GCPLGA and PEIPLGA microparticles in FB (a) and ACD plasma (b) incubated to 5 min at 37 C. Lane 1: Molecular weight standard, Lane 2: UNC-PLGA, Lane 3: UNC-CSPLGA, Lane 4: UNC-GCPLGA, Lane 5: UNC-PEIPLGA, Lane 6: AVI-PLGA, Lane 7: AVI-CSPLGA, Lane 8: AVI-GCPLGA and Lane 9: AVI-PEIPLGA.

Chapter 4 : Surface Modification of PLGA with Albumin and Chitosan Enhances Adhesion to Inflamed Endothelium for Improved Vascular Targeting

Most of this work has been submitted for publication as: Lopez-Cazares, Genesis and Eniola-Adefeso, Omolola. "Surface Modification of PLGA with albumin and chitosan enhances adhesion to inflamed endothelium for improved vascular targeting." Pharmaceutics (2022)

4.1 Abstract

Vascular-targeted carriers have the potential to localize therapeutics and imaging agents to inflamed, diseased sites. Poly (lactic-co-glycolic acid) (PLGA) is a negatively charged copolymer commonly studied due to its biodegradability and FDA approval. Unfortunately, PLGA particles experienced reduced adhesion to inflamed endothelium in the presence of plasma proteins. In our study, PLGA microparticles were coated with chitosan (CS), human serum albumin (HSA), or both to improve adhesion. We evaluated the binding of sLe^A targeted PLGA, HSA-PLGA, CSPLGA, and HSA-CSPLGA to activated endothelial cells in the presence of red blood cells in flow buffer or plasma. sLe^A CSPLGA adhesion was also reduced in plasma. In comparison, sLe^A HSA-PLGA kept 35-52% of its adhesion in plasma compared to flow buffer conditions across shear rates. At low and intermediate shear, sLe^A HSA-CSPLGA maintained 80% of its adhesion after exposure to plasma and reduced to about 50% at high shear. Interestingly, the protein corona characterization showed increases at the 75 and 150 kDa band intensities for HSA-PLGA and

HSA-CSPLGA, which could correlate to histidine-rich glycoprotein and immunoglobulin G. The changes in protein corona on HSA-coated particles seem to positively influence particle binding, emphasizing the importance of understanding plasma protein-particle interactions.

4.2 Introduction

Vascular targeted carriers (VTCs) have the potential to transport therapeutics and imaging agents involved in the treatment of several diseases, including cancer and cardiovascular disease (CVD).[2] Intravenous administration of VTCs could be extremely useful in reaching vascular disease sites that typically require invasive surgery, such as atherosclerotic plaques. Once injected, VTCs can increase tissue specificity and localize drug concentration via disease biomarkers present on the vasculature and surrounding target tissues, leading to reduced off-target toxicity. Particulate carriers (e.g., micelles, liposomes, and polymeric particles) are of great interest due to their ability to encapsulate drugs while preserving drug structure and protecting the drug from degradation. Micelles and liposomes are highly biocompatible carriers con-structed from lipids and amphiphilic molecules but are restricted to encapsulating only hydrophobic or hydrophilic drugs, respectively.[81] Liposomes are the most widely studied VTCs and have been successfully translated into the clinic mainly for the treatment of cancer.[14] However, their instability in physiological mediums, lack of controlled release, and fast oxidation of some phospholipids that can affect their storage are of current concern.[82,83] Polymeric particles are a potential alternative with an array of tunable properties that demonstrate improved drug stability, effective controlled release, and enhanced resistance to degradation over other carrier types.[10,84,85] However, the number of polymeric VTCs available in the clinic is minimal, creating a need to design and optimize polymeric particles as successful drug delivery systems.

Synthetic polymers, such as poly (lactic acid) (PLA) and poly (lactic-co-glycolic acid) (PLGA), are primarily employed in current injectable pharmaceutical products due to their timely biodegradability and biocompatibility.[12] Both PLA and PLGA are negatively charged polymers easily degraded via hydrolysis into their monomeric forms that are subsequently digested by the human body.[16] PLGA is the most widely studied material because of its tunable biodegradability and capability to encapsulate various drugs ranging from small molecules to proteins.[17] Despite the benefits of PLGA, only 19 injectable long-acting formulations have been authorized for clinical use since its FDA approval in 1989, where most are designed for intramuscular administration.[86] One main obstacle facing the clinical translation of intravenously administered PLGA carriers is the insufficient understanding of interactions between PLGA and biological environments in the vasculature. Recent publications evaluating the ability of PLGA particles to act as a VTC have demonstrated that high protein adsorption, specifically immunoglobulins A and M, onto its surface drastically reduces binding to an inflamed endothelial monolayer in whole blood or plasma conditions.[19,22,42,87] The addition of polyethylene glycol (PEG) onto the surface of drug carriers is commonly used to reduce protein adsorption that leads to increased circulation.[36] Unfortunately, PEGylation of the PLGA surface did not improve its adhesion to inflamed endothelial cells in the presence of plasma proteins.[19,42] Incorporating PEG onto drug delivery systems has also been shown to develop antibodies in the host after repeated administration leading to rapid clearance.[8,88] Additionally, PEGylation of polystyrene and PLGA particle surfaces has exhibited increased uptake by neutrophils in whole blood, which could prevent carriers from reaching diseased target sites.[89]

Natural biodegradable polymers, such as chitosan and albumin, have been used to develop drug carriers due to their abundance, biocompatibility, and low toxicity.[90] The attachment of

chitosan and albumin to the surface of drug carriers has been employed to improve biological interactions serving as potential alternatives to PEG.[44,91] Chitosan is a positively charged polysaccharide with high solubility in acidic conditions degraded by enzymatic catalysis.[45] Albumin is the most abundant protein found in the blood and has dysopsonin properties.[51] The addition of chitosan or albumin onto the surface of particle carriers has demonstrated many advantages, including improved physicochemical stability, extended circulation time, and controlled drug release for a wide range of drug delivery applications.[44,46,90,91] Here, we prepared PLGA particles coated with chitosan, human serum albumin, or both to mitigate PLGA's low adhesivity and high protein adsorption. Chitosan (CS) was physically adsorbed during particle fabrication, and human serum albumin (HSA) was covalently attached to the surface of PLGA or CS coated PLGA. After coating PLGA, we coupled sialyl Lewis A (sLe^A) or human anti-ICAM1 onto the particles to target E-selectin and ICAM. We evaluated the adhesion of targeted PLGA, HSA-PLGA, CSPLGA, and HSA-CSPLGA to an inflamed endothelial monolayer in the presence of plasma proteins. We observed a significant improvement in particle binding for sLe^A targeted HSA-PLGA and HSA-CSPLGA over PLGA. We also investigated how CS and HSA coatings influence the adsorption of plasma proteins and identified differences at the 75 and 150 kDa molecular weights. Ultimately, this will contribute information on the utility of CS and HSA coated PLGA particles as carriers for vascular-targeted drug delivery.

4.3 Results

4.3.1 Characterization of albumin and chitosan coated PLGA microparticles

We fabricated PLGA and CSPLGA microparticles using the emulsion solvent evaporation method and covalently attached human serum albumin. The SEM images of both unloaded and

rhodamine-loaded particles fabricated are shown in Figure 3.1. The particle size and zeta potential of PLGA and CSPGLA are displayed in Table 3.1.

Additionally, the full spectra and the nitrogen N1s spectrum regions for both unloaded and rhodamine loaded PLGA and CSPLGA obtained from XPS are shown in Figure 3.1. The nitrogen peak is apparent for unloaded CSPLGA confirming the presence of chitosan on the PLGA surface. Rhodamine-loaded CSPLGA did not show a prominent nitrogen peak, but the shift in surface charge from -26.2 mV to +7.18 mV (Table 3.1) suggests the presence of chitosan on the particle surface. Table 3.2 is the elemental composition determined from XPS.

Table 4.1 Particle size and zeta potential.

Particle Type	Size (µm)	Zeta Potential (mV)
[U] PLGA	1.6 +/- 0.6	-30.3 +/- 7.3
[U] CSPLGA	1.7 +/- 0.5	+10.7 +/- 2.7
[R] PLGA	1.6 +/- 0.5	-26.2 +/- 3.7
[R] CSPGLA	1.6 +/- 0.5	+7.18 +/- 2.7

Table 4.2 XPS elemental composition

Particle Type /Composition (%)	Carbon	Nitrogen	Oxygen
[U] PLGA	57.28	0.00	42.72
[U] CSPLGA	62.77	0.94	36.29
[R] PLGA	62.98	0.00	37.02
[R] CSPGLA	49.23	0.00	50.77

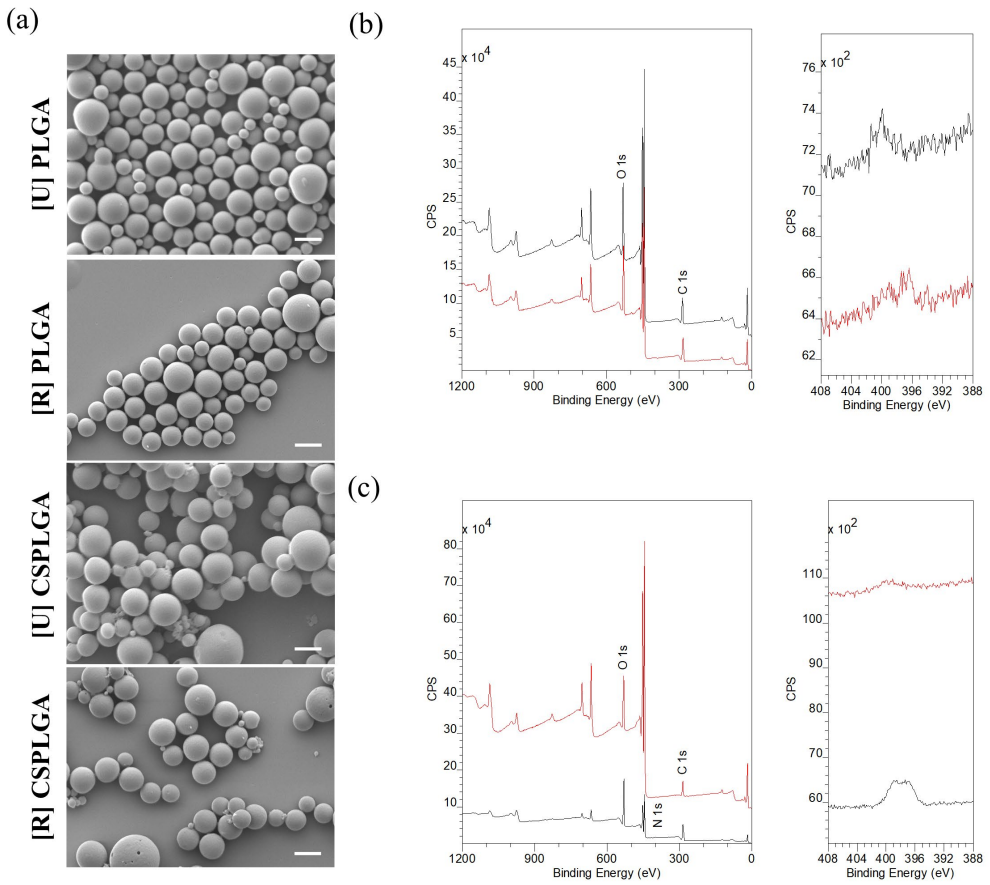

Figure 4.1 Particle surface characterization. (a) SEM images of unloaded [U] and rhodamine [R] loaded PLGA and CSPLGA. (b) XPS wide spectra of [U] PLGA (black) and [R] PLGA (red) on the left and N1s spectrum region on the right. (c) XPS wide spectra of [U] CSPLGA (black) and [R] CSPLGA (red) on the left and N1s spectrum region on the right. Scale bar = 2 μm.

After fabrication, human serum albumin was conjugated to the surface of microparticles. The albumin measured was approximately 21,000 and 122,000 sites/μm^2 on PLGA and CSPLGA, respectively (Table 3.3). Next, particles were conjugated with the protein avidin, allowing the attachment of any biotinylated ligands or antibodies for targeting cell adhesion molecules expressed on the vascular wall. The amount of albumin was also measured after the avidin reaction (Table 3.3). After avidin reaction, the number of albumin sites detected was approximately 14,000 and 44,000 sites/μm^2 on PLGA and CSPLGA, respectively. A schematic of the final targeted particles to clearly show various coating schemes is depicted in Figure 3.2.

Table 4.3 Protein surface site density determined via flow cytometry. Based on the particle size (1.6 μm) and albumin (32-64 nm^2), the max estimated surface coverage is 16,000 – 30,000 albumin molecules per μm^2.

Particle Type/ (#/μm^2)	Albumin [sites after avidin]	Avidin
PLGA	-	8,000 +/- 3,000
HSA-PLGA	21,000 +/- 8,000 [14,000 +/- 10,000]	14,000 +/- 12,000
CSPLGA	-	18,000 +/- 8,000
HSA-CSPGLA	122,000 +/- 32,000 [44,000 +/- 11,000]	32,000 +/- 11,000

Table 4.4 Targeting ligand surface density.

Particle Type/(#/μm^2)	sLe^A [Med. Site density] (aE-selectin) {Med. aE-selectin}	aICAM [High site density]	Dual sLe^A+aICAM sLe^A [aICAM]
PLGA	1,200 +/- 300	5,300 +/- 1,300	-
HSA-PLGA	1,000 +/- 300	-	-
CSPLGA	1,200 +/- 300	5,800 +/- 1,100	-
HSA-CSPGLA	1,300 +/- 300 [4,800 +/- 200] (1,400 +/- 100) {6,000 +/- 300}	6,000 +/- 1,300 [10,000 +/- 1,500]	4,000 +/- 1,200 [6,300 +/- 1,400]

4.3.2 Adhesion of albumin and chitosan coated PLGA microparticles targeted with sLe^A

We evaluated the binding of PLGA, HSA-PLGA, CSPLGA, and HSA-CSPLGA to an inflamed monolayer using a parallel plate flow chamber (PPFC) assay. We conjugated particles with biotinylated sialyl Lewis A (sLe^A), a ligand that binds to E-selectin expressed by endothelial cells during inflammation. All particles were conjugated with 1,000 sites/μm^2 of sLe^A, as reported in Table 3.4. We compared the binding of sLe^A targeted particles in RBC-in-Flow Buffer (FB) to RBC-in-Plasma since earlier work showed reduced adhesion of PLGA in the presence of plasma proteins. Representative images of sLe^A targeted particles bound to inflamed endothelial cells at a shear rate of 200 s^{-1} are shown in Figure 3.2. All particle types were able to bind in the RBC-in-FB condition. There was a significant reduction in particle binding for sLeA PLGA and CSPLGA in RBC-in-Plasma conditions. In contrast, sLe^A HSA-PLGA and HSA-CSPLGA showed significant particle binding even in plasma. The quantified raw particle adhesion density of sLe^A

particles is displayed in Supplemental Figure 1 in the Appendix. The number of particles bound in RBC-in-Plasma was normalized to their binding in RBC-in-FB, defined here as adhesion efficiency plotted in Figure 3.2. At 200 s^{-1}, the adhesion efficiencies of sLe^A targeted PLGA and CSPLGA particles were 23% and 13%, respectively. Both showed a drastic reduction in binding, suggesting that the addition of chitosan onto PLGA does not mitigate the previously reported negative impact of plasma proteins on PLGA particle adhesion. Conversely, both sLe^A targeted HSA-PLGA and HSA-CSPLGA particles retained a significantly higher level of binding in the presence of plasma. HSA-PLGA particles experienced double the adhesion efficiency (46%) compared to PLGA ($p=0.0459$). HSA-CSPLGA particles saw the highest amount of binding in plasma with 78% adhesion efficiency, a 3-fold increase compared to PLGA ($p<0.0001$).

We next evaluated particle binding at 500 and 1000 s^{-1} to assess whether increasing the shear rate would affect particle adhesion efficiency in the same conditions for the 200 s^{-1} low shear assay. The adhesion efficiencies of all sLe^A targeted particle types did not change significantly with the increase in the wall shear rate from 200 to 500 s^{-1}. When the shear rate increases to 1000 s^{-1}, all sLe^A targeted particles, except for HSA-CSPLGA, showed no significant change in adhesion efficiencies. For sLe^A HSA-CSPLGA, the adhesion efficiency was reduced to 46%, significantly different from its binding at 200 s^{-1} ($p=0.0003$). Both sLe^A targeted HSA-PLGA and HSA-CSPLGA observed a 4-fold increase in adhesion efficiency at the highest shear rate tested compared to PLGA with $p<0.0001$ and $p=0.0001$, respectively. Overall, the HSA-CS coating on PLGA recovered the most targeted particle adhesion in plasma relative to bare PLGA across all shear rates evaluated. Lastly, we evaluated the adhesion of untargeted particles to an inactivated endothelium to learn whether the particle binding recovery of HSA-PLGA and HSA-CSPLGA is due to specific ligand-receptor interactions. As shown in Supplemental Figure 2d, the particle

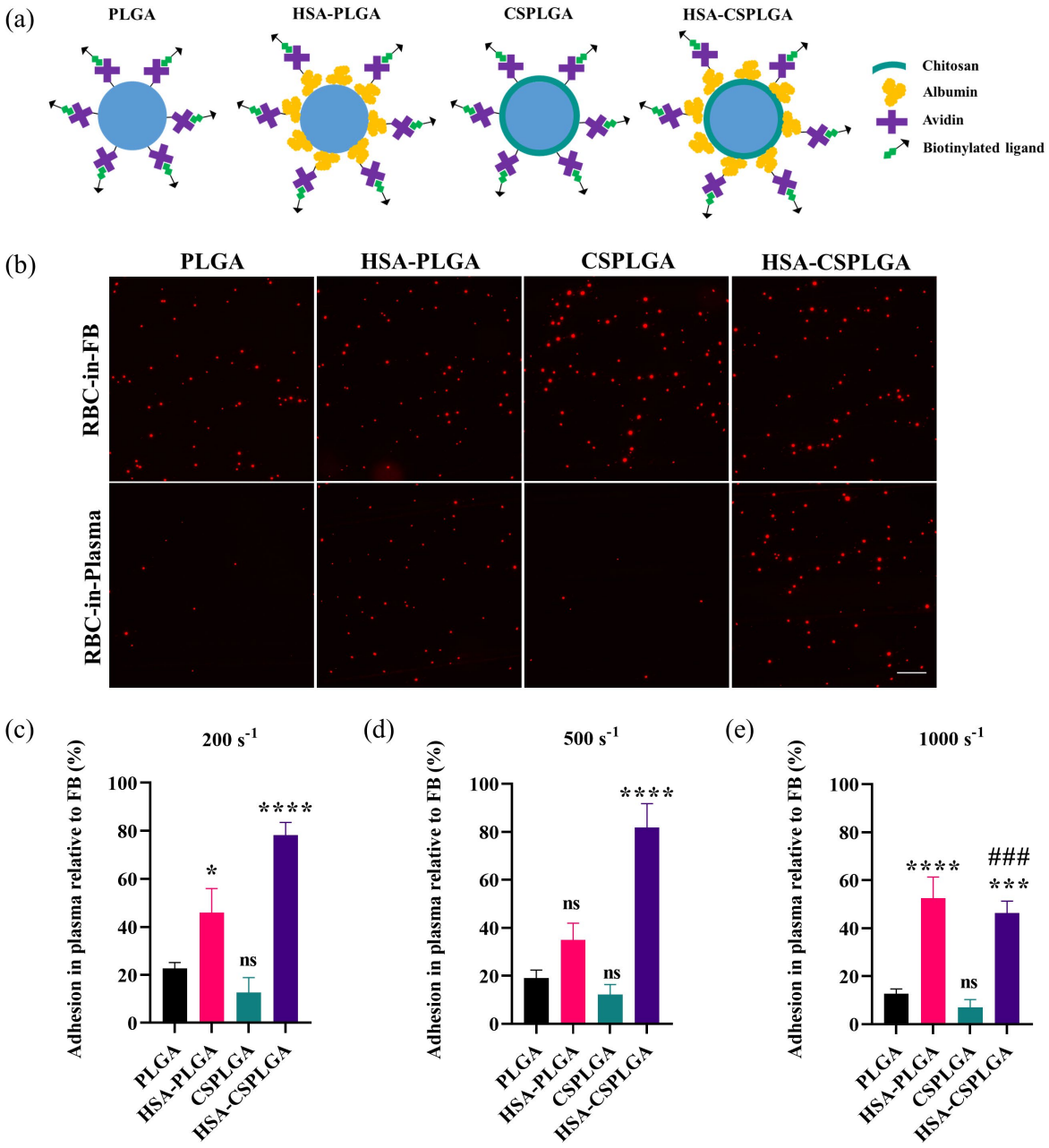

Figure 4.2 Adhesion of sLe^A targeted PLGA, HSA-PLGA, CSPLGA, and HSA-CSPLGA to inflamed endothelium. (a) Schematic of ligand targeted uncoated and coated PLGA. (b) Representative fluorescent images of rhodamine loaded sLe^A targeted particles bound to inflamed endothelial cells in RBC-in-FB and RBC-in-Plasma conditions at 200 s^{-1}. Particles with 1000 sites/μm^2 of sLe^A were added to RBC-in-FB or RBC-in-ACD plasma at a $5x10^5$ particles/mL concentration and perfused over HUVEC activated for 4 hours. Particles in plasma were incubated for 5 minutes prior to experiment. Quantified adhesion of particles in RBC in Plasma relative to RBC FB at 200, 500, and 1000 s^{-1} are shown in (c)-(e). Statistical analysis was completed using one-way ANOVA with Dunnett's multiple comparison test with PLGA as control. (*) = $p<0.05$, (**) = $p<0.01$, (***) = $p<0.001$, (****) = $p<0.0001$ and ns = not significant. n=10 distinct donors. Error bars represent standard error. The scale bar is 100 µm. sLe^A = sialyl Lewis A, HSA = human serum albumin, CS = chitosan, ACD = acid-citrate-dextrose, RBC = red blood cell, FB = flow buffer

adhesion density of untargeted particles in RBC-in-Plasma at 200 s^{-1} was minimal for all avidin conjugated particles, except for HSA-CSPLGA. HSA-CSPLGA with no avidin showed similar binding to avidin conjugated HSA-CSPLGA in RBC-in-Plasma, suggesting some unspecific interactions due to the addition of albumin at low shear. When the shear rate increases to 1000 s^{-1}, the adhesion of avidin conjugated HSA-CSPLGA is slightly reduced, whereas all other untargeted particles had almost no binding in RBC-in-Plasma.

4.3.3 Alternative ligand schemes on HSA-CSPLGA to improve binding at high shear

sLe^A targeted HSA-CSPLGA particles demonstrated the most improvement in adhesion efficiency over PLGA at low and intermediate shear rates but reduced at 1000 s^{-1} leading us to explore alternative targeting schemes to withstand the increase in shear. During inflammation, endothelial cells also overexpress intercellular cell adhesion molecule 1 (ICAM-1), which is involved in the firm attachment of leukocytes to the endothelium. Here, a biotinylated anti-ICAM1 (aICAM) antibody was conjugated to HSA-CSPLGA particles at a density of 5,700 sites/μm^2 on average. The quantified adhesion of aICAM targeted particles at 1000 s^{-1} is shown in Figure 3.3. The adhesion efficiencies of aICAM targeted PLGA, CSPLGA, and HSA-CSPLGA were 37%, 23%, and 41%, respectively. There was no significant difference for aICAM HSA-CSPLGA over bare PLGA ($p=0.8015$). Next, the amount of aICAM sites was increased to about 10,000 sites/μm^2 to understand whether that would promote firm adhesion of HSA-CSPLGA when exposed to plasma. The increase in aICAM sites shifted adhesion efficiency to 52% but is not statistically significant ($p=0.1381$) compared to 5,300 sites of aICAM on PLGA (Figure 3.3b). Given that dual targeting is another approach to improve particle binding affinity by using two ligands in synergy to target multiple receptors, we conjugated HSA-CSPLGA with 4,000 sites/μm^2 of sLe^A plus 6,300 sites/μm^2 of aICAM to target both E-selectin and ICAM-1 on the activated endothelium. The

adhesion efficiency of sLe^A+aICAM targeted HSA-CSPLGA particles was 72%, representing a significant increase over aICAM only PLGA (p=0.0007). Overall, only the dual-targeted HSA-CSPLGA served to improve the adhesion efficiency of the HSA-CSPLGA at high shear blood flow.

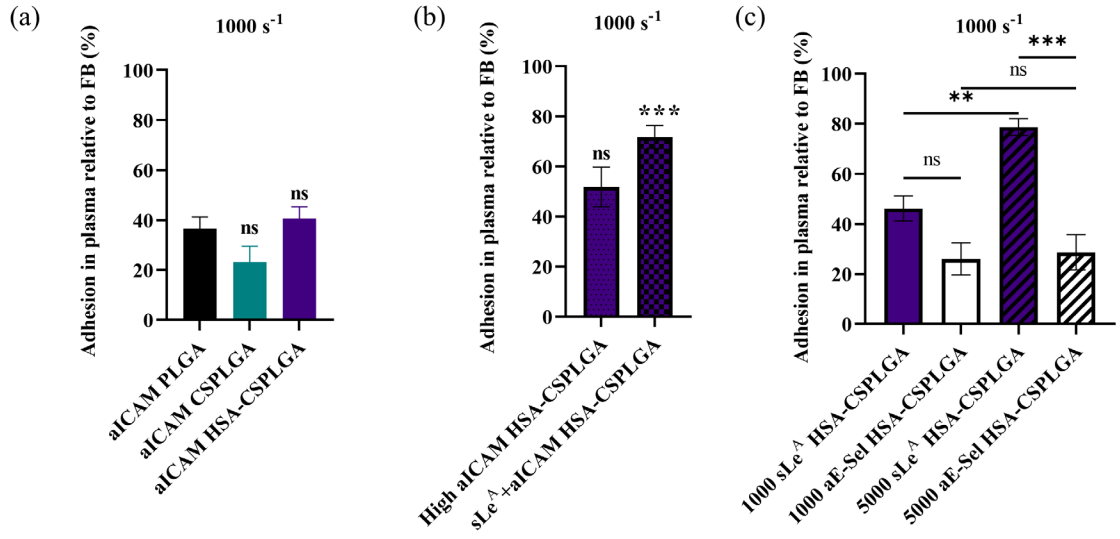

Figure 4.3 Alternative targeting schemes to improve binding of HSA-CSPLGA in ACD plasma at a high shear rate. (a) Binding of aICAM-1 targeted particles over endothelial cells activated for 24 hrs. Particles with ~5,700 sites aICAM-1/μm^2 were added in RBC FB and RBC ACD plasma at a $5x10^5$ particles/mL concentration and perfused over HUVEC activated for 24 hours. Particles in plasma were incubated for 5 minutes before the experiment. (b) Binding of particles with higher aICAM-1 site density (~10,000) and dual-targeted HSA-CSPLGA (~6,000 aICAM-1 plus ~5,000 sLe^A) after 24 hrs. of HUVEC activation. (c) Comparing binding between sLe^A and anti-E-selectin on HSA-CSPLGA after 4 hrs. of HUVEC activation. Statistical analysis was completed using one-way ANOVA with Dunnett's multiple comparison test with aICAM PLGA as control for A. (*) = $p<0.05$, (**) = $p<0.01$, (***) = $p<0.001$, (****) = $p<0.0001$ and ns = not significant. n≥ 9 distinct donors for A and B, n=5 for C. Error bars represent standard error.

To discern whether using other antibodies as the targeting ligand would produce similar results as anti-ICAM1, the adhesion of anti-E-selectin targeted particles was also evaluated and compared to sLe^A. For these experiments, HSA-CSPLGA was conjugated with 1000 sites/μm^2 of sLe^A or aE-selectin (Figure 3.3c). For this set of experiments, the raw particle adhesion density of HSA-CSPLGA with aE-selectin or sLe^A is shown in Supplemental Figure 3A. The binding in RBC-in-FB for 1000 sites/μm^2 of aE-selectin is slightly lower compared to 1000 sites/μm^2 of sLe^A on HSA-CSPLGA. When either ligand is increased to 5000 sites/μm^2 the raw particle adhesion in

RBC-in-FB condition is identical. These results in FB prove that both targeting ligands can bind in the absence of plasma proteins. First, the adhesion efficiency of HSA-CSPLGA with 1000 sites/μm^2 of aE-selectin was found to be 26%. This result is lower than HSA-CSPLGA with the same amount of sLe^A (46%) previously described above but they are not statistically different (p=0.1168). Since it is possible that 1000 sites/μm^2 of these ligands is not adequate to support firm adhesion at higher shear rates, we increased the amount of sLe^A and aE-selectin to about 5000 sites/μm^2. HSA-CSPLGA with an increased sLe^A density resulted in an adhesion efficiency of 79%, which is significantly higher than 1000 sLe^A sites/μm^2 (p=0.0045). Interestingly, there was no improvement in adhesion efficiency for HSA-CSPLGA when the aE-selectin site density was increased. These experiments show the impact of various targeting ligand schemes on the adhesion efficiency of HSA-CSPLGA.

4.3.4 Characterization of plasma proteins on coated PLGA with sLe^A

Prior work suggests that the negative particle binding experienced by PLGA is linked to the protein corona acquired onto the particle surface. To examine whether changes in the adsorption of plasma proteins are driving differences in particle binding, we characterized the protein corona using SDS-PAGE. sLe^A targeted particles were incubated in ACD plasma for 5 minutes at 37 C to mimic flow experiments. Images of representative gels of sLe^A targeted particles incubated in FB and ACD plasma are shown in Figure 3. Visually, there is a decrease in protein adsorption on sLe^A PLGA particles with chitosan surface coating, as indicated by fainter or absent protein bands. The sLe^A PLGA particles coated with albumin (HSA) or chitosan plus albumin showed an increase in protein adsorption, i.e., bolder band intensities across various molecular weights. However, some areas of interest show distinct differences between particle types. sLe^A targeted HSA-PLGA and HSA-CSPLGA showed a significant increase at the 10-25, 50-75, and

76-150 kDa molecular weight ranges compared to PLGA. Given that the 10-25 kDa molecular weight band also appears in gels of HSA-PLGA and HSA-CSPLGA exposed to buffer, the proteins in this region most likely do not influence the differences in particle binding (Figure 3a).

The lanes between 50-75 and 76-150 kDa molecular weight ranges were analyzed semi-quantitatively using ImageJ relating band intensity to the peak area. These results are plotted in Figure 3c-e. The first band above 50 kDa is the albumin band. Figure 3c directly compares the albumin band intensity showing a slight increase for all particles compared to PLGA but are not statistically different. Next, the band intensity at about 75 kDa for HSA-PLGA and HSA-CSPLGA shows a 2-fold ($p=0.0127$) and 3-fold ($p=0.0010$) increase compared to PLGA, respectively (Figure 3d). The band at approximately 150 kDa is of particular interest since earlier work proved that high adsorption of immunoglobulins, specifically IgA and IgM, drive the low adhesion of PLGA in plasma conditions.[22] Figure 4e compares the band intensity at 150 kDa for all particle types. HSA-PLGA showed more than a 3-fold increase in intensity compared to PLGA ($p=0.0288$), while HSA-CSPLGA had a 4-fold increase ($p=0.0038$). The increases in band intensity at the 75 kDa and 150 kDa molecular weight ranges potentially influence the improved adhesion of HSA-conjugated particles in plasma.

We also evaluated the adsorption of proteins onto HSA-CSPLGA conjugated with sLe^A, anti-E-selectin, or anti-ICAM1 to figure out whether that would explain the differences in particle binding. There were no clear distinctions in band intensity for HSA-CSPLGA with various targeting ligands shown in Figure 3.5. This means that the differences in binding of HSA-CSPLGA with different ligand schemes are most likely due to ligand-receptor kinetics and not protein adsorption.

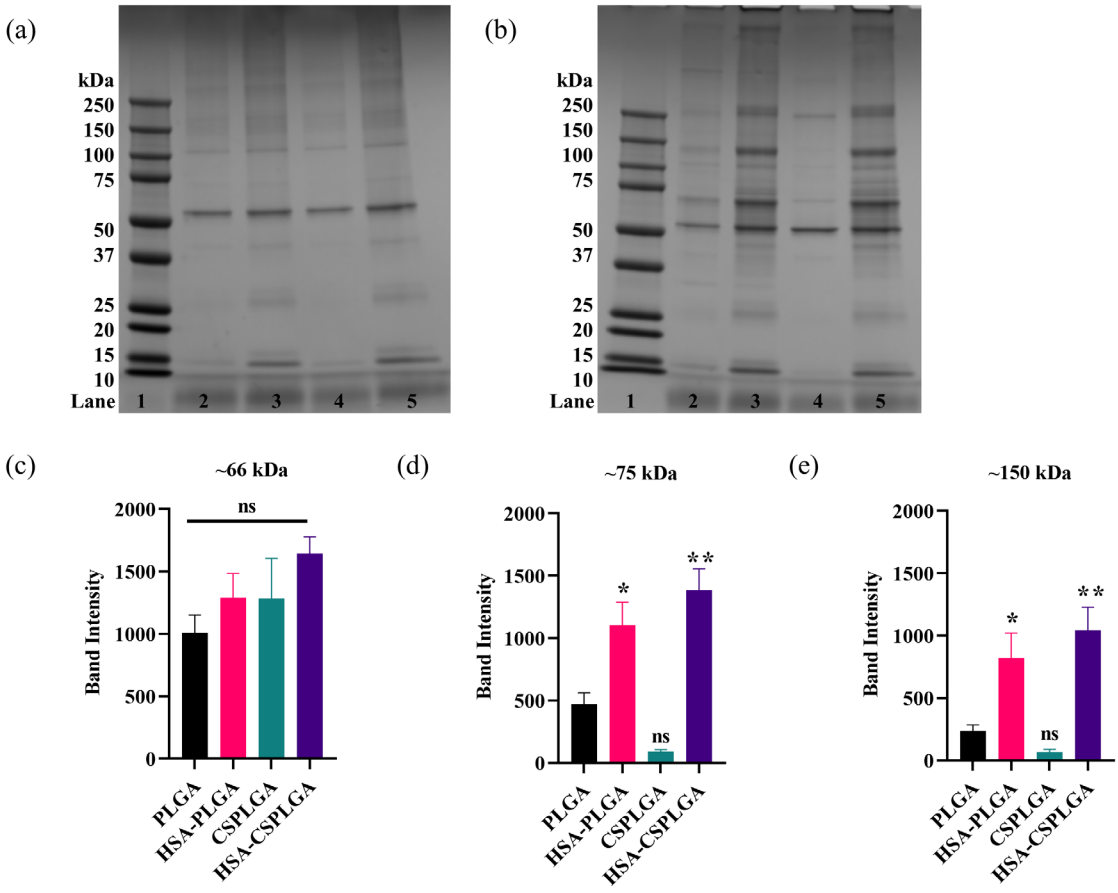

Figure 4.4 Protein corona characterization of sLe^A targeted PLGA, HSA-PLGA, CSPLGA, and HSA-CSPLGA in Flow Buffer (FB) and ACD plasma. $2.5x10^6$ particles conjugated with 1000 sites/μm^2 of sLe^A were incubated in 650 µL of 78% ACD plasma for 5 minutes at 37C. SDS-PAGE of sLe^A targeted particles in FB (a) and ACD plasma (b). Lane 1: molecular weight ladder, Lane 2: PLGA, Lane 3: HSA-PLGA, Lane 4: CSPLGA, and Lane 5: HSA-CSPLGA. Each lane was analyzed with ImageJ. Plotted are isolated band intensities at ~66 kDa (c), ~75 kDa (d), and ~150 kDa (e). Statistical analysis was completed using one-way ANOVA with Dunnett's multiple comparison test with PLGA as control: (*) = $p<0.05$(**) = $p<0.01$, (***) = $p<0.001$, (****) = $p<0.0001$ and ns = not significant. n=4 distinct donors. Error bars represent standard error.

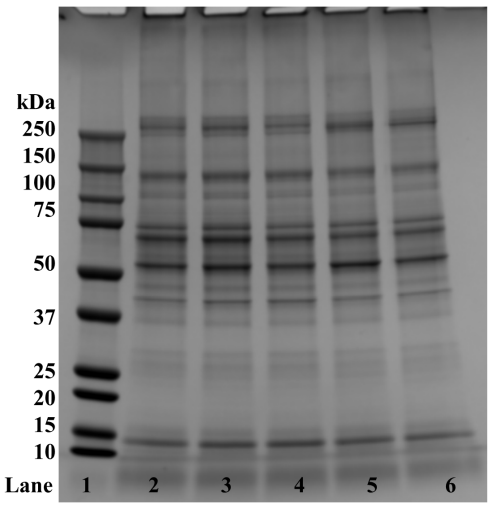

Figure 4.5 SDS-PAGE gel of HSA-CSPLGA with various targeting ligands. Lane 1: molecular weight ladder, Lane 2: 1,000 sites/μm^2 anti-E-selectin, Lane 3: 5,000 sites/μm^2 sLe^A, Lane 4: 1,000 sites/μm^2 anti-E-selectin, and Lane 5: 1,000 sites/μm^2 anti-ICAM1.

4.3.5 Impact of anticoagulant on binding and protein adsorption of coated PLGA

The choice of anticoagulants can impact particle binding and protein adsorption since they inhibit clotting through different mechanisms. Up to this point, ACD was used in the experiments detailed above, which works by chelating calcium. Heparin is another anticoagulant that binds to antithrombin to prevent clotting, affecting protein interactions. The adhesion of albumin, chitosan, or dual coated PLGA with sLe^A was evaluated using heparin as the anticoagulant for these experiments. sLe^A targeted particles were exposed to RBC-in-HEP plasma for 5 minutes and perfused over an activated EC monolayer at 500 s^{-1}. As shown in Figure 4, all sLe^A targeted particles except for HSA-CSPLGA had minimal binding in heparinized plasma. The adhesion efficiency of sLe^A HSA-CSPLGA is ten times higher than PLGA ($p=0.0017$). Since there are some differences in binding for particles exposed to plasma with heparin as the anticoagulant, we also conducted an SDS-PAGE analysis shown in Figure 4b. sLe^A particles incubated in heparin plasma for 5 min at 37 C. Here, there is a slight increase in intensity overall for particles coated with

albumin. The areas of interest are shown in Figure 4c-d. There is about a 1.6-fold (p=0.4213) and 2.3-fold (p=0.0604) increase in band intensity for HSA-PLGA and HSA-CSPLGA over PLGA, but they are not statistically significant, respectively. When the band at 150 kDa is isolated, there is a 3-fold increase in band intensity for HSA-PLGA compared to PLGA in heparin plasma (p=0.0002) and an 8-fold increase for HSA-CSPLGA (p<0.0001).

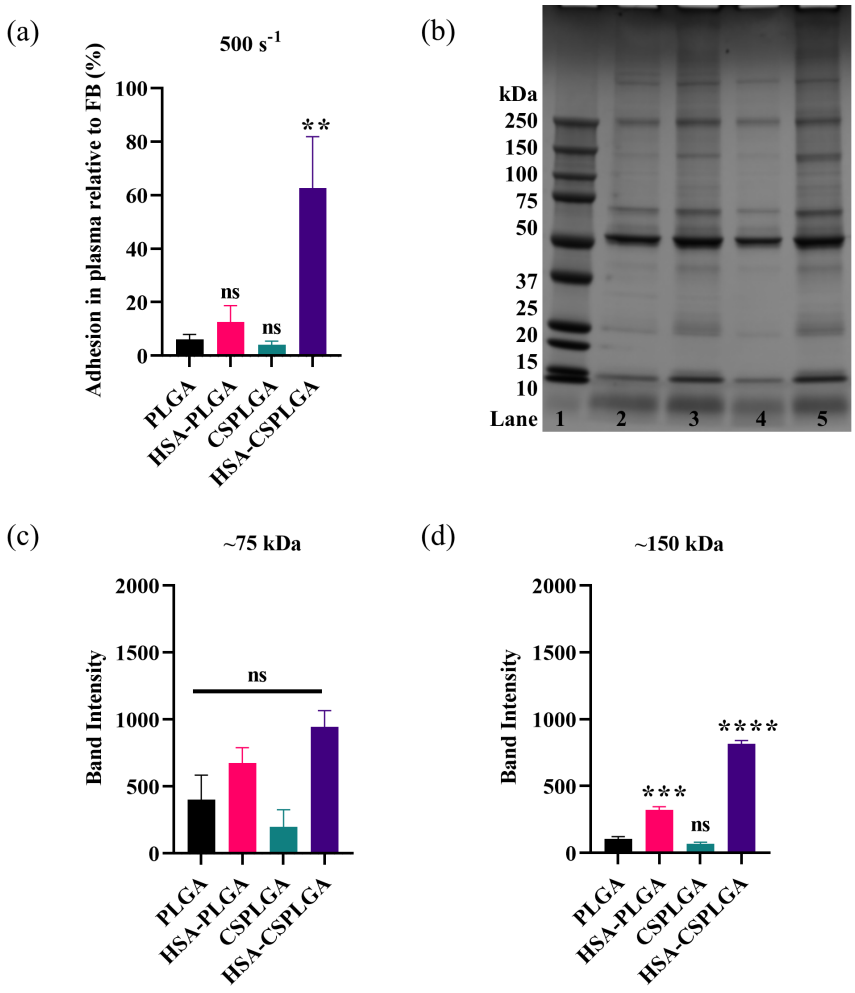

Figure 4.6 Adhesion and protein characterization of sLe^A targeted PLGA, HSA-PLGA, CSPLGA, and HSA-CSPLGA in heparin plasma at 500 s^{-1}. Particles with 1000 sites/μm^2 of sLe^A were incubated in RBC FB and RBC plasma at a $5x10^5$ particles/mL concentration and perfused over HUVEC activated for 4 hours. Particles in plasma were incubated for 5 minutes before the experiment. (a) Particle adhesion efficiency in heparin plasma. (b) SDS PAGE of particles exposed to heparin plasma. Lane 1: molecular weight ladder, Lane 2: PLGA, Lane 3: HSA-PLGA, Lane 4: CSPLGA, and Lane 5: HSA-CSPLGA. Each lane was analyzed with ImageJ. Plotted are isolated band intensities at ~75 kDa (c) and ~150 kDa (d). Statistical analysis was completed using one-way ANOVA with Dunnett's multiple comparison test with PLGA as control: (*) = p<0.05, (**) = p<0.01, (***) = p<0.001, (****) = p<0.0001 and ns = not significant. n=7 for (a) and n=3 for (c)-(d) distinct donors. Error bars represent standard error.

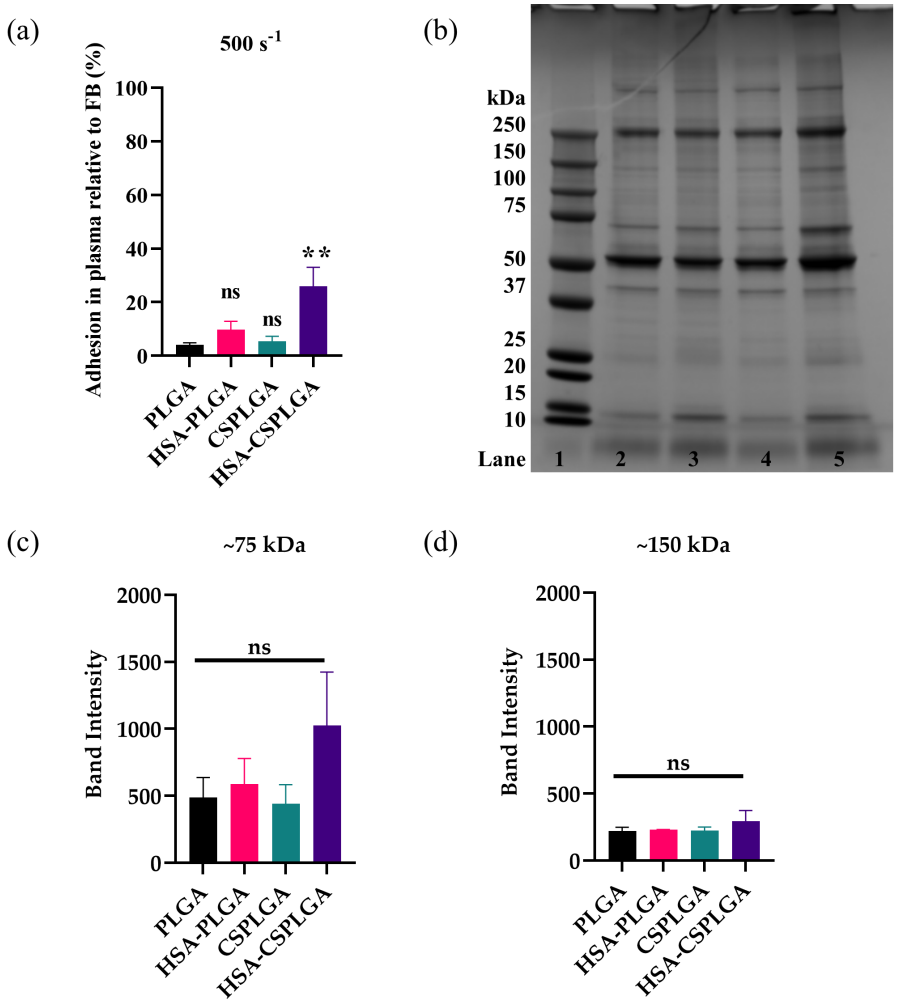

Figure 4.7 Adhesion and protein characterization of sLe^A targeted PLGA, HSA-PLGA, CSPLGA, and HSA-CSPLGA in anticoagulant-free plasma at 500 s^{-1}. Particles with 1000 sites/μm^2 of sLe^A were incubated in RBC FB and RBC plasma at a $5x10^5$ particles/mL concentration and perfused over HUVEC activated for 4 hours. Particles in plasma were added immediately. (a) Particle adhesion efficiency in heparin plasma. (b) SDS-PAGE of particles exposed to anticoagulant-free plasma for 5 min at 37 C. Lane 1: molecular weight ladder, Lane 2: PLGA, Lane 3: HSA-PLGA, Lane 4: CSPLGA, and Lane 5: HSA-CSPLGA. Each lane was analyzed with ImageJ. Plotted are isolated band intensities at ~75 kDa (c) and ~150 kDa (d). Statistical analysis was completed using one-way ANOVA with Dunnett's multiple comparison test with PLGA as control: (*) = $p<0.05$, (**) = $p<0.01$, (***) = $p<0.001$, (****) = $p<0.0001$ and ns = not significant. n = 7 for A and n = 3 for B-D distinct donors. Error bars represent standard error.

We explored incubating sLe^A targeted particles in anticoagulant-free (ACF) plasma to model an environment closer to physiological conditions. ACF plasma is defined here as plasma isolated after drawing and immediately used before any significant clotting is observed. The adhesion efficiency of sLe^A particles exposed to RBC-in-ACF plasma is shown in Supplemental

Figure 4a. All particles had a significant reduction in binding in ACF plasma compared to ACD plasma. The adhesion efficiency of sLe^A HSA-CSPLGA was more than six times higher than PLGA, demonstrating some improvement ($p=0.0017$) in these conditions. SDS-PAGE was conducted for particles exposed to ACF plasma for 5 min at 37 C (Supplemental Figure 4b). The differences in protein bands are less clear when sLe^A targeted particles are exposed to ACF plasma. There is no significant difference at the 75 and 150 kDa bands as plotted in Supple-mental Figure 4c-d. HSA-CSPLGA show about a 2-fold increase at the 75 kDa band compared to PLGA ($p=0.3382$). Interestingly, the adhesion efficiency of HSA-CSPLGA decreases when the anticoagulant changes from ACD to ACF. The differences in band intensity also decrease at 75 and 150 kDa in those plasma conditions.

4.3.6 *In vivo* biodistribution of untargeted HSA-PLGA and HSA-CSPLGA

Thus far, we have shown that the addition of albumin onto the surface of PLGA and CSPLGA microparticles can improve particle binding to endothelial cells *in vitro* even in the presence of plasma proteins. We also wanted to evaluate how the albumin coating would affect the biodistribution of the particles *in vivo* in a healthy mouse model. A representative image of whole organ scans and their fluorescence intensity after 30 minutes post-administration of particles is plotted in Figure 3.8. The data plotted is adjusted fluorescence intensity, where the background intensity of organs from untreated mice is subtracted from organ intensity of samples from mice treated with particles. Bare PLGA particles were mostly found in the liver and in the spleen. HSA-PLGA and HSA-CSPLGA particles were found in the lungs, liver, and spleen. Particles were not detected in the blood after 30 minutes.

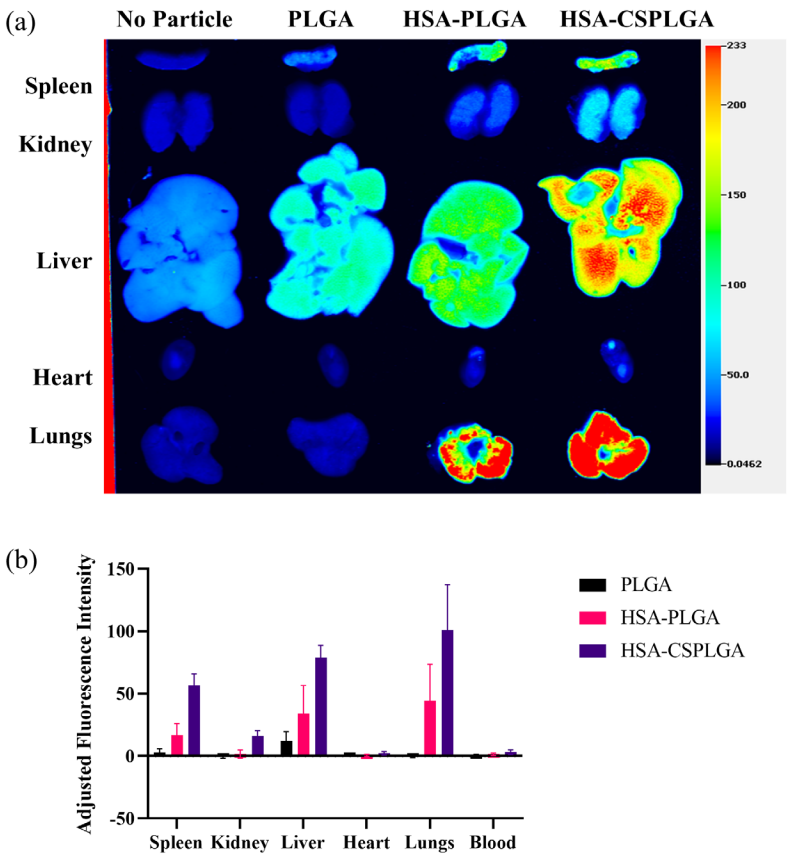

Figure 4.8 *In vivo* biodistribution of HSA-PLGA and HSA-CSPLGA after 30 minutes. (a) Whole organ scans. (b) Adjusted Fluorescence Intensity (Sample organ minus Untreated organ background). N=3.

4.4 Discussion

To date, a limited number of polymeric particle systems have been successfully translated into the market for clinical use due to a lack of understanding of biological interactions.[12,92] For example, when drug carriers enter the bloodstream, the rapid adsorption of plasma proteins onto their surface has been shown to impact significantly their biological fate, such as clearance rate, biodistribution, and targeting efficacy.[24,31,32,93] Physicochemical properties of drug carriers can affect the formation and composition of the protein corona, such as surface charge and hydrophilicity.[23] PLGA continues to be an appealing material in the design of drug carriers, but studies in our lab have demonstrated reduced binding in the presence of plasma proteins. The high

adsorption of unfavorable proteins (i.e., immunoglobulins) onto PLGA is a critical issue that needs to be addressed before its successful application as a targeted drug carrier. Surface modification of drug carriers can influence the amount and types of proteins that adsorb onto the surface leading to favorable biological interactions, such as reduced cellular uptake or increased circulation time for various particle types.[43,94,95] PEGylation is the gold standard for reducing protein adsorption, but this did not improve the targeting efficacy of PLGA to an inflamed endothelial, creating a need for alternative coatings.

Several studies have shown that coating PLGA with chitosan or albumin has increased circulation times, improved delivery of drugs to tumor sites, and reduced protein adsorption.[53,69,71] We hypothesized that changing the surface of PLGA using chitosan, albumin, or both could reduce or alter protein adsorption, improving binding to an inflamed endothelium for vascular targeting. In this work, PLGA was successfully coated with chitosan and albumin via physical adsorption and covalent attachment. Fabrication conditions were adjusted to obtain spheres of about 2 μm diameter, which have shown optimal targeting to blood vessel wall over nanosized carriers.[64] The addition of chitosan onto the surface of PLGA has been reported to shift the zeta potential towards a positive charge.[47] Here, CSPLGA displayed a slightly positive charge close to neutral. Both PLGA and CSPLGA were successfully coated with albumin. Interestingly, CSPLGA had a higher amount of albumin, most likely due to the primary amines present at every chitosan monomer allowing conjugation to carboxylic groups on albumin. Conversely, PLGA only has two carboxylic acid groups at each polymer end, thus limiting the number of albumin molecules that can be conjugated despite many amine sites available on the protein.

Drug carriers must marginate and localize to the vascular wall to actively target the vasculature, followed by specific binding to cellular markers on the endothelium. For this study,

we chose to target E-selectin and ICAM-1 because these receptors are overexpressed by endothelial cells during inflammation. Interestingly, CSPLGA showed a drastic reduction in binding in the presence of plasma proteins, suggesting that the addition of chitosan onto PLGA does not mitigate the previously reported negative impact of plasma proteins on PLGA particle adhesion. While albumin-coated particles targeted with sLe^A experienced a significant improvement in binding to an inflamed endothelium even in the presence of plasma proteins. sLe^A targeted HSA-PLGA maintained the same ratio of particles bound in plasma to flow buffer across all shear rates tested. The particle with the highest percentage of particles bound in plasma to flow buffer was sLe^A HSA-CSPLGA. At the low and intermediate shear rates, sLe^A HSA-CSPLGA outperformed HSA-PLGA by keeping 80% of its particle adhesion even after exposure to plasma proteins but was reduced to about 50% at high shear. In our study, we have demonstrated that the addition of albumin can enhance the adhesion of PLGA and CSPLGA. Also, the amount of albumin could play a role since HSA-CSPLGA had more albumin sites and performed the best.

To increase the adhesion of HSA-CSPLGA at 1000 s^{-1}, we exchanged sLe^A for anti-ICAM1 to target ICAM-1 on the endothelium, which is involved in the firm arrest of leukocytes during inflammation. The aICAM targeted HSA-CSPLGA only kept about 40% of its binding in plasma relative to flow buffer condition and showed no improvement over aICAM targeted PLGA. An alternative approach to improving drug carriers' binding is employing two ligands in synergy to enhance targeting by mimicking leukocytes' rolling and firm adhesion. One study showed increased binding and uptake by endothelial cells when liposomes were decorated with antibodies for E-selectin and ICAM.[96] For our work, HSA-CSPLGA with a 2:3 ratio of sLe^A to aICAM resulted in 70% adhesion efficiency at high shear. The dual targeting approach resulted in the most significant increase in particle binding in plasma conditions at high shear, possibly because sLe^A

can interact with multiple endothelial cell receptors. Specifically, sLe^A has been shown to bind to both E-selectin and P-selectin expressed on endothelial cells.[97] In one study, the binding of sLe^X and aICAM targeted polystyrene was enhanced by the initial rolling initiated by sLe^X interactions with P-selectin.[80] Additionally, the enhanced binding of particles coated with albumin could be due to interactions with albumin-specific receptors on the endothelium, such as gp60.[59] These results suggest that having multiple interactions with the endothelium is beneficial for supporting the firm adhesion of particles.

We were also interested in seeing whether changes in the protein corona of modified PLGA could be driving the differences in particle adhesion. Several other studies have focused on manipulating the protein corona by pre-coating particles with favorable proteins, such as albumin.[54,98] We covalently attached the albumin to the surface to prevent desorption after exposure to plasma proteins. When we characterized the protein corona, two bands stood out. There was a significant increase in intensity at the 75 and 150 kDa bands for particles coated with albumin. HSA-CSPLGA had the highest intensity at these two bands, likely influencing its enhanced binding in plasma. The first band of interest potentially consists of histidine-rich glycoprotein (HRG), with a molecular weight of about 75 kDa. HRG is present at relatively high concentrations in human plasma and has been shown to interact with several ligands.[99] Previously HRG has been shown to act as a dysopsonin when it adsorbs onto the surface of silica nanoparticles leading to a reduction in uptake by macrophages.[100] The presence of dysopsonin proteins can aid particulate carriers in evading phagocytes. The second band of interest is most likely composed of immunoglobulins (Ig), specifically IgA or IgG, with molecular weights around 150 kDa. The increase in the immunoglobulin band was interesting since earlier work has shown that the adsorption of these large molecules reduces the binding of PLGA particles. When individual Igs

were depleted from plasma, Ig A and IgM were the main culprits in reducing particle binding. The depletion and re-addition of IgG to plasma did not significantly reduce particle binding, which suggests that IgG may be present on the surface of our HSA-CSPLGA particles. Interestingly, IgG has also been shown to interact with HRG. The interaction between IgG and HRG could be adsorbing in tandem onto HSA-CSPLGA particles. Interestingly when heparin was used as the anticoagulant, the adhesion of sLe^A targeted HSA-CSPLGA was slightly reduced compared to its binding in ACD plasma but was still significantly better than bare PLGA. The change in particle binding could be explained by the HRG interacting with heparin instead of the particle surface, supported by a decrease in the 75 kDa band intensity for heparin plasma. Mass spectrometry and depletion assays could further confirm the identity of these proteins since they seem to play a role in improving particle adhesion. Lastly, HRG has been shown to interact with the CLEC-1A, C-type lectin domain family 1 member A, receptor on endothelial cells.[101] The increase in HRG in the protein corona of HSA-coated particles creates another opportunity to interact with CLEC-1A on the endothelium.

4.5 Conclusions

In our study, we evaluated the effect of surface modification on PLGA particle adhesion in the presence of plasma proteins. Specifically, we focused on coating PLGA with chitosan, albumin, or both to improve biological interactions. Our results indicate that the addition of albumin to the surface of particles enhances the binding of PLGA to an inflamed endothelium even in the presence of plasma proteins. The amount of albumin on the particle surface could play a role in the level of particle adhesion since HSA-CSPLGA outperformed HSA-PLGA. Interestingly, the addition of chitosan alone onto PLGA showed no improvement even though there was a reduction in protein adsorption. The dual coating of chitosan and albumin onto PLGA experienced the

highest level of improved particle binding. The improvement in adhesion efficiency depended on ligand type and targeting schemes, especially at higher shear. Increasing the number of interactions between drug carriers and the endothelium by conjugating multiple ligands or ligands with an affinity for multiple receptors could be necessary for enhanced particle binding. We infer that HRG and IgG, based on molecular weight, have a higher presence on the surface of albumin-conjugated particles relative to bare PLGA, which could benefit particle adhesion. Ultimately, our work suggests that the adhesion of PLGA particles is possible when the protein corona is altered after surface modification with albumin, leading to favorable protein adsorption.

4.6 Supplemental Data

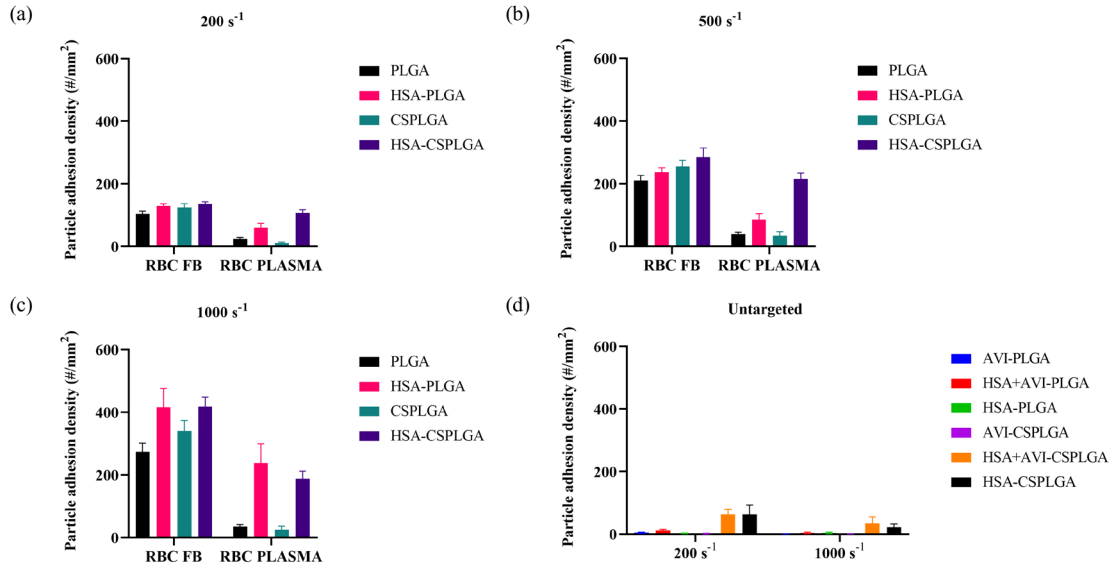

Figure 4.9 Raw particle adhesion density of sLe^A or untargeted PLGA, HSA-PLGA, CSPLGA and HSA-CSPLGA. sLe^A targeted particle binding in RBC in FB and RBC in ACD plasma at 200 s^{-1} (a), 500 s^{-1} (b) and 1000 s^{-1} (c) over endothelium activated for 4 hours. (d) Binding of untargeted particles exposed for RBC in ACD plasma for 5 minutes. n = 10 distinct donors for (a)-(c) and n = 3 for (d).

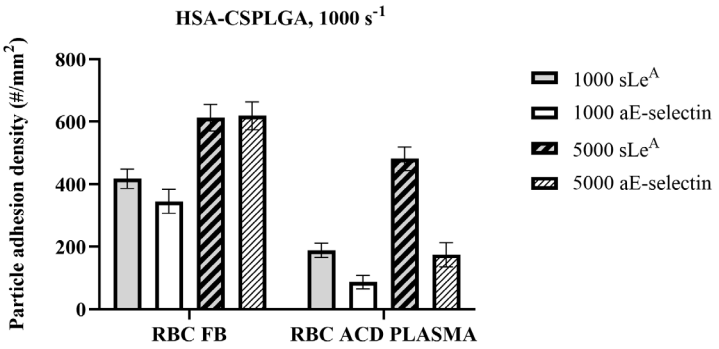

Figure 4.10 Raw particle adhesion density of sLe^A or anti-E-selectin targeted HSA-CSPLGA. Targeted particle binding in RBC-in-FB and RBC-in-ACD Plasma at 1000 s^{-1} over endothelium activated for 4 hours. N=5.

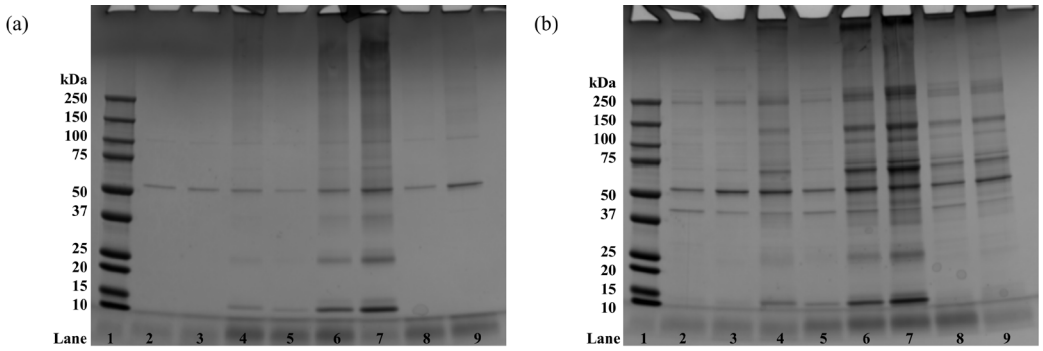

Figure 4.11 Protein adsorption characterization of control and sLe^A PLGA or coated PLGA particles. SDS-PAGE on untargeted particles incubated in FB (a) and ACD plasma (b) for 5 min at 37 C. Lane 1: molecular weight ladder, Lane 2: U-PLGA, Lane 3: U-CSPLGA, Lane 4: AVI-PLGA, Lane 5: AVI-CSPLGA, Lane 6: HSA+AVI-PLGA, Lane 7: HSA-+AVI-CSPLGA, Lane 8: HSA-PLGA and Lane 9: HSA-CSPLGA. Lane 1: molecular weight ladder, Lane 2: PLGA, Lane 3: HSA-PLGA, Lane 4: CSPLGA, and Lane 5: HSA-CSPLGA. U = unconjugated, HSA = human serum albumin, AVI = avidin conjugated.

Chapter 5 : Adhesion of PLGA Nanoparticles with Optimized Surface Coatings to an Inflamed Endothelium

5.1 Abstract

Nanoparticles (NPs) are attractive drug carriers for their ability to penetrate tissues and enhanced uptake by a variety of cells creating alternative avenues to deliver therapeutics. Unfortunately, PLGA NPs experienced reduced adhesion to inflamed endothelium in the presence of plasma proteins. In our study, PLGA and CSPLGA nanoparticles were coated with human serum albumin (HSA) since they positively impacted the adhesion of PLGA microparticles (MPs). We evaluated the binding of sLe^A targeted PLGA, HSA-PLGA, and HSA-CSPLGA NPs to activated endothelial cells in the presence of red blood cells in flow buffer or plasma. sLe^A HSA-PLGA NPs kept about 40% of its adhesion in plasma compared to flow buffer conditions at both shear rate tested, which produced similar results to sLe^A HSA-PLGA MPs. Conversely, sLe^A HSA-CSPLGA NPs maintained only about 30% of its adhesion after exposure to plasma, which was drastically different compared to sLe^A HSA-CSPLGA MPs that had a max adhesion efficiency of 80% at low shear. Interestingly, the protein corona characterization showed increases at the 75 and 150 kDa band intensities for HSA-PLGA and HSA-CSPLGA NPs, which could correlate to histidine-rich glycoprotein and immunoglobulin G. Overall, this study suggests that surface coatings that optimize adhesion of PLGA MPs may not directly translate to NPs due to other factors the affect particle binding and protein adsorption on NPs.

5.2 Introduction

Nanoparticles (NPs) are promising vehicles for the delivery of therapeutics and imaging agents in the treatment of many diseases. NPs are typically in the size range between 10 – 1000 nm allowing them to navigate through capillaries, unlike microparticles that can be trapped and cleared by capillary beds after intravenous injection.[102] Additionally, there are several other advantages of NPs, which include prolonged circulation, capability to penetrate tissues, and being easily taken up by a variety of cells.[103] Even though there has been an abundance of research in the application of nanoparticles, successful translation continues to be hampered by a lack in understanding the differences between animal models and humans.[104] Additionally, the heterogeneity of many diseases between patients and other biological barriers encountered by NPs has slowed down any progress, illustrated by the limited number of FDA approved NP delivery systems.[12,104] Designing NP delivery systems that are able to overcome biological barriers, such as complex blood flow and phagocytosis, is necessary to advance the field of nanotherapeutics. The protein corona plays a critical role in the ability of nanoparticles to overcome these barriers by creating a biological fingerprint on the surface that decides its fate within the body.

Biodegradable NPs fabricated from synthetic polymers, specifically PLGA and PLA, have long been the material of choice in the development of drug delivery systems because of their biocompatibility and tunable controlled drug release properties. Unfortunately, these types of NPs suffer from high levels of protein adsorption due to their hydrophobicity, which leads to short circulation times resulting after recognition and clearance by the MPS.[105] Surface modification of polymeric NPs is an approach used to manage the adsorption of unfavorable proteins that lead to faster clearance rates keeping them from reach the target tissue. The adsorption of proteins can either be reduced or the composition can be altered, which depends on the coating and core

material used. From the experiments discussed above, the addition of albumin onto PLGA and CSPLGA microparticles showed a significant improvement in adhesion to an inflamed endothelium potentially influenced by changes in the protein corona. Here, we fabricated PLGA and chitosan coated PLGA nanoparticles followed by covalent attachment of albumin the surface. We wanted to determine whether these coatings could benefit the ability of PLGA nanoparticles in a similar fashion. We evaluated the adhesion of modified PLGA NPs to an inflamed endothelium using sialyl Lewis A, sLe^A, as the targeting ligand and a parallel plate flow chamber set up. Interestingly, surface modification of PLGA and CSPLGA nanoparticles only saw a slight increase in adhesion over unmodified PLGA. The protein corona present on modified PLGA nanoparticles was characterized using SDS-PAGE and resulted in similar protein patterns as the microparticles with the same coatings. This suggests that further optimization studies may be necessary to aid the adhesion of PLGA nanoparticles, such alternative coatings or other design parameters (i.e., size, targeting ligand).

5.3 Results

5.3.1 Surface Characterization of PLGA and CSPLGA NPs Coated with Albumin

PLGA and CSPLGA nanoparticles were fabricated using the emulsion solvent evaporation method followed by covalent attached human serum albumin. SEM images of both unloaded and rhodamine loaded particles are shown in Figure 5.1. The particle size and zeta potential of PLGA and CSPGLA are displayed in Table 5.1. The resulting diameters for PLGA and CSPLGA nanoparticles were all approximately 320 nm, except for unloaded CSPLGA that had a diameter of 360 nm. All nanoparticles had a spherical shape and a smooth surface. In our study, PLGA NPs had a negative charge of about -25 mV, while CSPLGA demonstrated a shift to approximately +11 mV. This shift in zeta potential from net negative to positive confirms that chitosan is on the

surface of PLGA, given the known cationic nature of chitosan. Additionally, the full spectra and the nitrogen N1s spectrum regions for both unloaded and rhodamine loaded PLGA and CSPLGA obtained from XPS are shown in Figure 5.1. The nitrogen peak is apparent for unloaded CSPLGA confirming the presence of chitosan on the PLGA surface. Rhodamine-loaded CSPLGA did not show a prominent nitrogen peak, but the shift in surface charge from -24 mV to +11 mV (Table 5.1) suggests the presence of chitosan on the particle surface. Table 3.2 is the elemental composition determined from XPS.

Table 6.1 Size and zeta potential of PLGA and CSPLGA.

Particle Type	Size (nm)	Zeta Potential (mV)
[U] PLGA	320 +/- 120	-25.2 +/- 5.8
[U] CSPLGA	360 +/- 120	+11.4 +/- 1.6
[R] PLGA	310 +/- 80	-24.0 +/- 5.4
[R] CSPLGA	320 +/- 100	+11.1 +/- 4.2

Table 6.2 Zeta potential of protein and ligand conjugated NPs.

Particle Type	Zeta Potential (mV)
[R] HSA-PLGA	+12.9
[R] HSA-CSPLGA	+24.5
[R] AVI-PLGA	+7.98
[R] AVI-HSA-PLGA	+14.9
[R] AVI-HSA-CSPLGA	+18.9
[R] sLe^A-PLGA	+9.21
[R] sLe^A HSA-PLGA	+13.6
[R] sLe^A HSA-CSPLGA	+26.4

Table 6.3 Elemental composition of PLGA and CSPLGA NPs.

Particle Type /Composition (%)	Carbon	Nitrogen	Oxygen
[U] PLGA	58.52	0.00	41.48
[U] CSPLGA	63.17	0.47	36.36
[R] PLGA	61.28	0.00	38.72
[R] CSPGLA	67.99	0.00	32.01

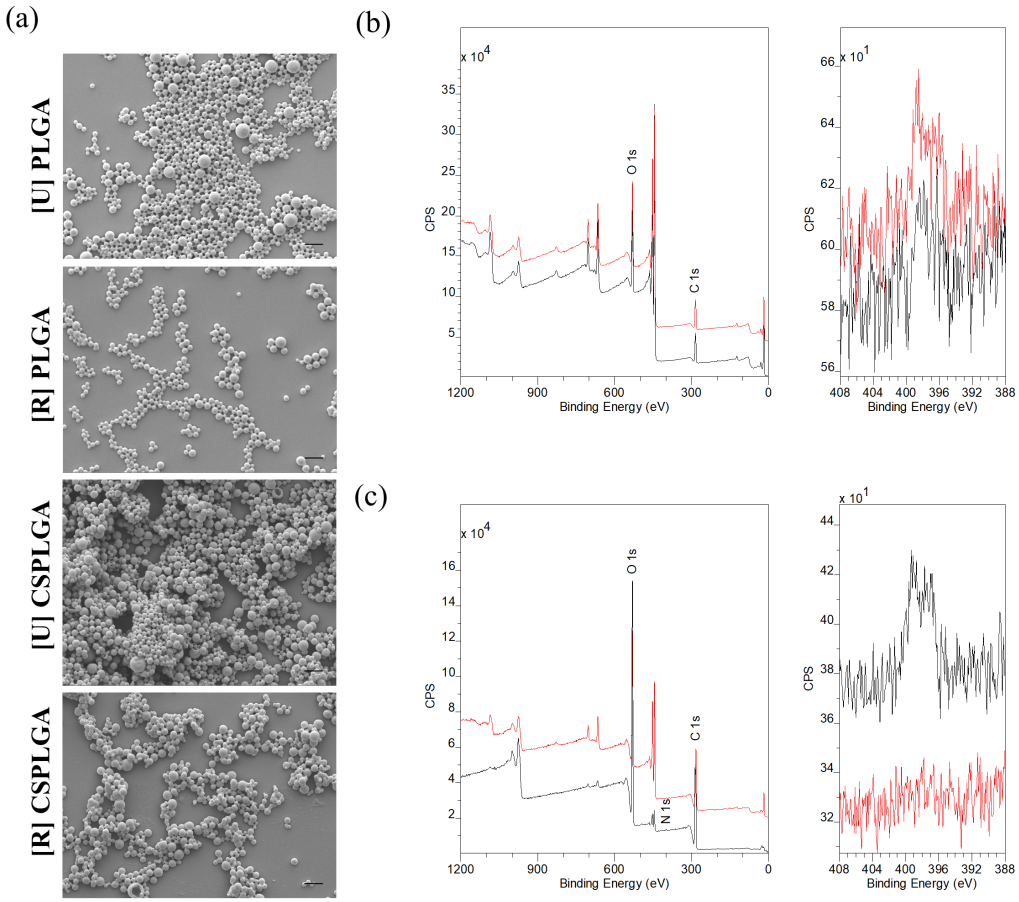

Figure 6.1 Particle surface characterization of nanoparticles. (a) SEM images of unloaded [U] and rhodamine [R] loaded PLGA and CSPLGA. (b) XPS wide spectra of [U] PLGA (black) and [R] PLGA (red) on the left and N1s spectrum region on the right. (c) XPS wide spectra of [U] CSPLGA (black) and [R] CSPLGA (red) on the left and N1s spectrum region on the right. Scale bar = 1 μm.

After fabrication, human serum albumin was conjugated to the surface of microparticles. The albumin measured was approximately 640,000 and 1,200,000 sites/μm^2 on PLGA and CSPLGA, respectively (Table 5.4). Next, particles were conjugated with the protein avidin, allowing the attachment of any biotinylated ligands or antibodies for targeting cell adhesion molecules expressed on the vascular wall. The amount of albumin was also measured after the avidin reaction (Table 5.4). After avidin reaction, the number of albumin sites detected was approximately 470,000 and 600,000 sites/μm^2 on PLGA and CSPLGA, respectively.

The zeta potential of nanoparticles was measured after protein and ligand conjugated listed in Table 5.3. The addition of albumin to PLGA and CSPLGA resulted in surface charges of +12.9 and +24.5 mV, which caused a positive shift compared to unconjugated particles. The surface charge of avidin and sLe^A conjugated PLGA was close to neutral (~ +9 mV), while avidin and sLe^A conjugated HSA-PLGA saw a slight positive charge (~ +14 mV). Additionally, the surface charge of avidin and sLe^A conjugated HSA-CSPLGA was positive around +23 mV.

Table 6.4 Protein and ligand site density. Based on albumin (32-64 nm^2), the max estimated surface coverage is 16,000 – 30,000 albumin molecules per μm^2

Particle Type/ (#/μm^2)	**Albumin [sites after avidin]**	**Avidin**	**sLe^A**
PLGA	-	160,000 +/- 95,000	11,000 +/- 900
HSA-PLGA	640,000 +/- 360,000 [470,000 +/- 180,000]	610,000 +/- 12,000	12,000 +/- 1,000
HSA-CSPGLA	1,200,000 +/- 270,000 [600,000 +/- 150,000]	1,300,000 +/- 370,000	12,000 +/- 1,300

5.3.2 Adhesion of sLe^A targeted PLGA, HSA-PLGA, and HSA-CSPLGA NPs

We evaluated the binding of PLGA, HSA-PLGA, and HSA-CSPLGA to an inflamed monolayer using a parallel plate flow chamber (PPFC) assay. We conjugated particles with biotinylated sialyl Lewis A (sLe^A), a ligand that binds to E-selectin expressed by endothelial cells during inflammation. All particles were conjugated with at least 10,000 sites/μm^2 of sLe^A, as reported in Table 5.4. Here, we evaluated the binding of HSA-PLGA and HSA-CSPLGA nanoparticles since there was a significant improvement in adhesion for albumin coated microparticles over unmodified PLGA as presented in Chapter 3. Representative images of sLe^A targeted nanoparticles bound to inflamed endothelial cells at a shear rate of 200 s^{-1} are shown in Figure 5.2. All particle types were able to bind in the RBC-in-FB condition and binding increased for albumin coated nanoparticles (Figure 7.7). There was a significant reduction in particle binding

for sLe^A PLGA in RBC-in-Plasma conditions. sLe^A targeted HSA-PLGA and HSA-CSPLGA nanoparticles also observed a reduction in particle binding after exposure to plasma. The quantified raw particle adhesion density of sLe^A particles is displayed in Figure 7.7 in Supplemental Data. The number of particles bound in RBC-in-Plasma was normalized to their binding in RBC-in-FB, defined here as adhesion efficiency plotted in Figure 5.2.

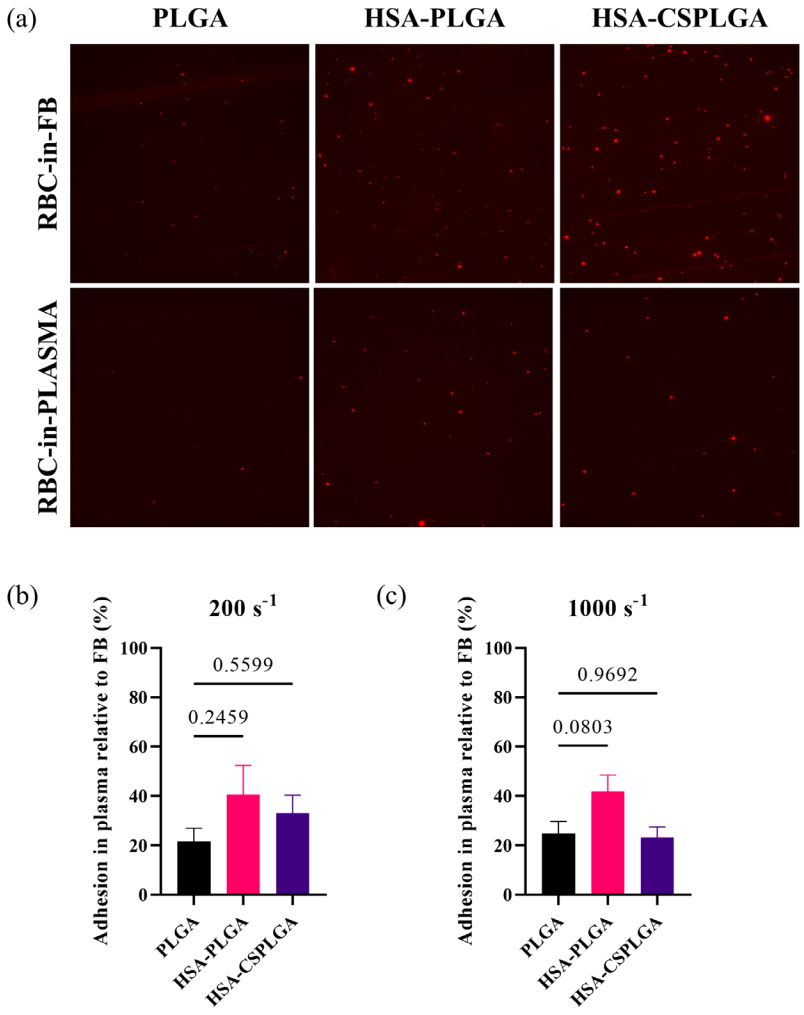

Figure 6.2 Adhesion of albumin coated PLGA and CSPLGA nanoparticles. (a) Representative fluorescent images of sLe^A targeted nanoparticles bound to endothelium activated for 4 hrs. Adhesion efficiency of nanoparticles at 200 and 1000 s^{-1}. N = 5 distinct donors. Errors bars are standard error.

At 200 s^{-1}, the adhesion efficiency of sLe^A targeted PLGA nanoparticles was 22% showing a drastic reduction in binding consistent with previous studies. Conversely, both sLe^A targeted HSA-PLGA and HSA-CSPLGA particles saw the highest level of retained particle binding in the presence of plasma. HSA-PLGA particles experienced double the adhesion efficiency (41%) compared to PLGA (p=0.2459). HSA-CSPLGA particles saw only a slight increase in particle binding in plasma with 33% adhesion efficiency compared to PLGA (p = 0.5599). The adhesion efficiencies of sLe^A targeted PLGA and HSA-PLGA stayed the same at 25% and 42% respectively after increasing the shear rate to 1000 s^{-1}. The adhesion efficiency of sLe^A HSA-CSPLGA was reduced to 23% at the high shear.

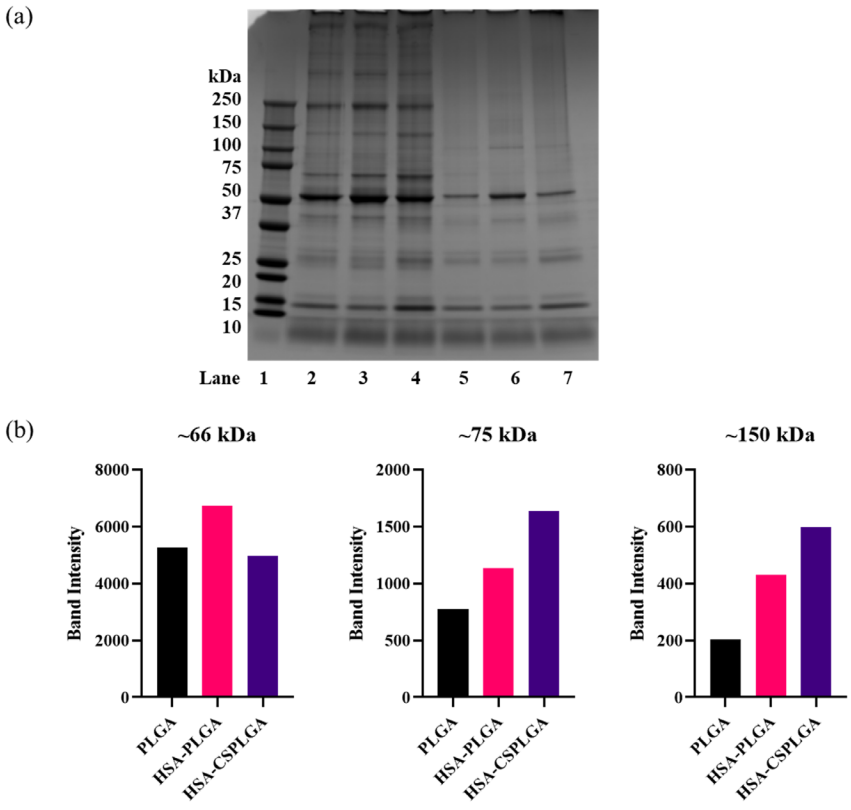

Figure 6.3 (a) SDS-PAGE of sLe^A targeted PLGA, HSA-PLGA and HSA-CSPLGA in ACD plasma and flow buffer (FB). (b) Band intensities at 66, 75 and 150 kDa. Lane 1: Molecular weight standard, Lane 2: PLGA in ACD, Lane 3: HSA-PLGA in ACD, Lane 4: HSA-CSPLGA in ACD, Lane 5: PLGA in FB, Lane 6: HSA-PLGA in FB, and Lane 7: HSA-CSPLGA in FB. N = 1.

5.3.3 Plasma Protein Adsorption onto sLe^A PLGA, HSA-PLGA and HSA-CSPLGA NPs

In the work discussed in Chapter 3, the protein corona of PLGA microparticles coated with albumin saw a significant change in the total amount of proteins adsorbed and distinct trends of specific proteins. We characterized the protein corona using SDS-PAGE. sLe^A targeted particles were incubated in ACD plasma for 5 minutes at 37 C to mimic flow experiments. Image of representative gel of sLe^A targeted nanoparticles incubated in FB and ACD plasma are shown in Figure 5.3. Visually, sLe^A PLGA particles coated with albumin (HSA) or chitosan plus albumin showed an increase in protein adsorption, i.e., bolder band intensities across various molecular weights. However, some areas of interest show distinct differences between particle types. The lanes between 50-75 and 76-150 kDa molecular weight ranges were analyzed semi-quantitatively using ImageJ relating band intensity to the peak area. These results are plotted in Figure 5.3b. The first band above 50 kDa is the albumin band. sLe^A HSA-PLGA NPs had a slight increase in intensity at the 66 kDa band. The 66 kDa band also shows a slight increased for HSA-PLGA or PLGA when exposed to flow buffer containing bovine serum albumin. Next, the band intensity at about 75 kDa and 150 kDa increased for both HSA-PLGA and HSA-CSPLGA NPs.

5.4 Discussion

In general, the adhesion of microparticles and nanoparticles is affected by their interactions with the biological environment. For instance, margination of drug carriers is influenced by size, where micron sized particles benefit from collisions with red blood cells while nanosized particles are trapped within the RBC-rich core.[73,106] Since NPs have additional obstacles to overcome to be able to successfully target the vasculature, we wanted to determine whether optimized surface coatings that enhance the binding of PLGA microparticles would also benefit nanoparticles. Here, we fabricated PLGA and CSPLGA nanoparticles with a diameter close to 300 nm. The surface

charge of PLGA and CSPLGA NPs observed similar zeta potentials to their MP counterparts. Interestingly, the percentage of nitrogen atoms on CSPLGA NPs was slightly reduced to 0.47% compared to CSPLGA MPs with 0.94%. After fabrication, PLGA and CSPLGA NPs were coated with albumin through covalent attachment. The number of albumin sites per surface area measured on NPs compared to MPs was an order of magnitude higher, which could be due to higher adsorption of proteins as the size decreases influenced by increase in surface curvature.[107] Additionally, preliminary zeta potential measurements in deionized water of PLGA and CSPLGA conjugated with albumin, avidin and sLe^A showed a shift in charge towards the positive direction.

Nanoparticle adhesion is drastically impacted by their ability to marginate and localize to the vascular blood vessel was. Our flow adhesion experiments of sLe^A targeted HSA-PLGA and HSA-CSPLGA in RBC-in-flow buffer showed an increase in base particle adhesion density over PLGA at both shear rates tested (Figure 7.7). The addition of albumin onto the PLGA and CSPLGA seems to enhance particle binding in flow buffer probably due to interactions with endothelial cell receptors that bind albumin. Interestingly, adhesion of sLe^A targeted HSA-PLGA and HSA-CSPLGA NPs in RBC-in-Plasma showed differing amounts of particle binding. The adhesion of sLe^A HSA-PLGA NPs kept 40% of its adhesion in plasma relative to flow buffer conditions, which was similar to that of sLe^A HSA-PLGA MPs. Unfortunately, sLe^A HSA-CSPLGA NPs only observed about 30% of its adhesion in plasma relative to flow buffer condition at low shear, which was drastically lower compared to sLe^A HSA-CSPLGA MPs that kept 80% of its adhesion. There are several factors influencing the differences in adhesion between HSA-CSPLGA NPs and MPs. The shear forces could potentially explain the decrease in adhesion for NPs compared to MPs since the contact area is decreased leading to detachment, which might be strong enough in the presence of plasma proteins.[108] Additionally, there seems to be an increase in

protein adsorption for all nanoparticles compared to microparticles keeping the total surface area constant, which is indicated by bolder band intensities. Further studies need to be conducted to fully explain these differences in adhesion. It is possible that the amount of albumin on the surface of nanoparticles needs to be optimized by varying reaction conditions.

5.5 Conclusions

Here, we evaluated the adhesion of sLe^A targeted PLGA, HSA-PLGA and HSA-CSPLGA to endothelial cells and characterized the protein corona. The chemical characterization of the nanoparticle surface saw a shift in surface charge in the positive direction after coating with chitosan and attachment of albumin. We saw an increase in adhesion efficiency for sLe^A HSA-PLGA compared to PLGA, which was kept even with increasing shear rate. Interestingly, sLe^A HSA-CSPLGA only saw a slight increase in adhesion efficiency over PLGA. Again, the protein corona characterization suggested an increase in band intensity at 75 and 150 kDa, like microparticles with the same coatings. This work suggests that surface modification techniques that improve the adhesion of microparticles may not be enough for nanoparticles because of additional obstacles encountered by NPs, such as inefficient margination and decreased contact area.

5.6 Supplemental Data

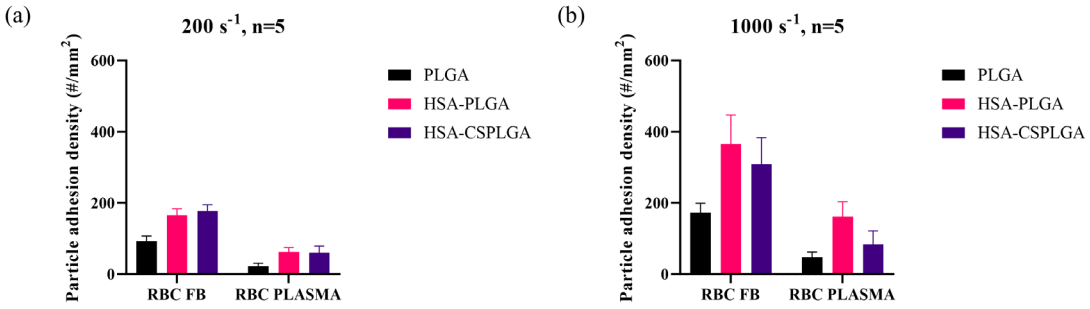

Figure 6.4 Raw nanoparticle adhesion density of sLe^A PLGA, HSA-PLGA, and HSA-CSPLGA at (a) 200 and (b) 1000 s^{-1}.

Chapter 6 : Conclusions and Future Directions

6.1 Overall Summary and Major Conclusions

Vascular targeted carriers have the immense potential to improve the delivery of therapeutics and imaging agents to diseased vasculature by increasing localized drug concentrations and reducing systemic side effects. The adsorption of proteins onto the surface of VTCs continues to be a major obstacle hampering their successful translation into the clinic. VTC design parameters, including size, material, surface properties, etc., can influence their biological interactions affecting overall efficacy. Polymeric particles, such as PLGA, suffer from increased protein adsorption due to its surface hydrophobicity and strong negative charge. Previous work evaluated the adhesion of PLGA to an inflamed endothelium in various physiologically relevant conditions, which demonstrated a significant reduction in particle binding in the presence of plasma proteins. Surface modification of PLGA with PEG did not restore its adhesion in plasma conditions. Recent studies discovered the production of anti-PEG antibodies after re-administration and separately increase uptake by neutrophils, which lead to faster clearance.

This dissertation aims to evaluate the effect of surface modification on PLGA drug carrier adhesion to an inflamed endothelium in plasma environments and the impact on protein corona. There are two main approaches that we can use to address PLGA's protein adsorption problem: (1) Reducing protein adsorption and (2) forming a protein corona composing of favorable proteins. We hypothesized that coating the surface of PLGA with mucoadhesive, hydrophilic polymers would reduce protein adsorption and increase PLGA's affinity to the endothelium. This is shown

in Chapter 3 where PLGA was coated with chitosan and glycol chitosan. Interestingly, the addition of chitosan onto PLGA demonstrated a similar reduction in particle binding in plasma conditions, even though there was a decrease in overall protein adsorption possibly due to its neutrally charged surface. Alternatively, the glycol chitosan coating produced a strong positive charged surface and was able to maintain most of its adhesion even in plasma conditions. The enhanced adhesion of GCPLGA is suggested to be linked to an increase in bio-adhesiveness to the endothelium compared to CSPLGA and bare PLGA. The protein corona of GCPLGA saw slight changes in composition, mainly a decrease in large molecular weight proteins like immunoglobulins. Also, it is possible that chitosan and glycol chitosan are interacting with the CD44 receptor on the endothelium since they have a similar chemical structure to hyaluronic acid.[109] The higher molecular weight of glycol chitosan (~575 kDa) and increased bio-adhesiveness could explain its enhanced adhesion over chitosan (~83 kDa, estimate from TCI). We also tested another positively charged surface coating, PEI, that improved the adhesion of PLGA but not to the same level as GC coating. The fact that PEI is a branched polymer with a different chemical structure and the slightly smaller diameter (1.4 μm) than GCPLGA (2.0 μm) could explain the differences in particle binding. Due to the positively charged surface of GCPLGA, blood biocompatibility studies should be conducted since previously work has shown toxicity for positively charged drug carriers. These studies were not conducted for this thesis since glycol chitosan became unable from company during COVID-19 pandemic due to unavailable raw materials. Luckily, the coating of PLGA with glycol chitosan has shown good hemocompatibility over other chitosan derivatives, especially in the presence of plasma.[110]

Next, we explored the alternative approach of pre-forming a favorable protein corona by coating the surface of PLGA and CSPLGA microparticles with human serum albumin as presented

in Chapter 4. CSPLGA microparticles had six times the number of albumin sites compared to PLGA due to the increase in number of reactive functional groups on chitosan over PLGA polymer. Additionally, CSPLGA microparticles had multiple layers of albumin compared to PLGA with a single layer suggested by the fact that the area of albumin was estimated to be 32-64 nm^2 based on protein orientation. The adhesion of PLGA was improved by the addition of albumin or chitosan plus albumin resulting in higher adhesion efficiencies. The dual coating of chitosan plus albumin on the PLGA surface produced the highest adhesion efficiency. The extent of adhesion for HSA-CSPLGA in plasma was dependent on targeting scheme and shear rate. The enhanced adhesion of albumin coated particles is likely driven by interactions with HSA-specific receptors on endothelial cells. Examples of HSA-specific receptors on ECs include gp60, SPARC, and FcRn that interact with native albumin, while gp18 and gp30 primarily bind modified albumin.[51] Additionally, our *in vivo* biodistribution of untargeted HSA-PLGA and HSA-CSPLGA found that albumin coated particles preferentially accumulated in the lungs, which is supported by literature showing albumin only nanoparticles residing in the lungs.[111,112] Wood et al. suggested that the migration of albumin nanoparticles could be driven by uptake by lung epithelial cells and alveolar macrophages. The lung epithelial cells have also been shown to express the gp60 receptor which binds native albumin.[113]

We also saw differences in adhesion between HSA-PLGA and HSA-CSPLGA due to several reasons. First, HSA-CSPLGA has more albumin and untargeted HSA-CSPLGA demonstrated better cellular association to inactivated endothelium. Secondly, the differences in surface hydrophobicity could lead to variation in the orientation of albumin and native/denatured state on PLGA and CSPLGA. A previous study using PLGA and poloxamer coated PLGA demonstrated that PLGA interacted with bovine serum albumin (BSA) via hydrophobic

interactions, which lead to conformational changes.[95] The poloxamer is a "stealth", hydrophilic polymer, which preferred to interact with BSA via hydrogen-bonding. A separate study looked at the conjugation of chitosan to BSA and found that BSA secondary structure was not altered as long as there were only a few chitosan conjugated.[114] Similar changes could be occurring during our albumin conjugation reactions with PLGA and CSPLGA, which could change interactions with endothelial cell receptors.

Additionally, the characterization of the protein corona on HSA coated particles saw increases in the band intensities at the 75 and 150 kDa band, which we infer to be histidine-rich glycoprotein (HRG) and immunoglobulin G (IgG). The adsorption of IgG could be recruiting HRG since it is one of its ligands. The synergistic adsorption of IgG and HRG was affected when heparin was used as the anticoagulant since it is another HRG-ligand.[115] Aside from interaction with HSA-specific EC receptors, the improved adhesion of albumin conjugated PLGA and CSPLGA could be driven by binding to HRG-specific receptors expressed by endothelial cells.[101] Further work needs to be done to confirm our inference, such as mass spectroscopy to identify specific proteins, depletion assays of proteins that may be driving adhesion, and blocking of receptors on the endothelium.

Chapter 3 and 4 have focused on surface modifications of PLGA microparticles, there are additional barriers that nanoparticles must overcome to efficiently target the vasculature, such as margination. In Chapter 5, we fabricated PLGA and CSPLGA nanoparticles to determine whether their adhesion in plasma could be improved using the same optimized coatings on PLGA microparticles. The addition of albumin onto PLGA nanoparticles increased the adhesion efficiency 2-fold compared to PLGA NPs to a similar level as its microparticle counterpart shown in Chapter 3. Interestingly, the dual coating of chitosan and albumin did not significantly improve

adhesion of PLGA nanoparticles as it did for microparticles with same coating. The nanoparticles with albumin coatings observed similar patterns in protein adsorption to microparticles. This emphasizes the fact that differences in size can alter biological interactions of drug carriers and that the enhanced adhesion of PLGA MPs is not easily translated for NPs with the same coatings. The impact of size and surface curvature has been previously reported demonstrating changes in protein composition and protein structure.[32,43,116] Typically, an increase in surface curvature results in higher protein adsorption. It is possible that changes in curvature are affecting the structure of the albumin coating on NPs presented in this thesis, which alter their interactions with the endothelium affecting their targeting ability. Additionally, NPs suffer from a margination problem causing them to get stuck within the red cell core reducing interactions with the endothelium.[64] Further work could focus on optimizing the adhesion of PLGA nanoparticles specifically looking at the albumin structure and modifying reaction conditions to obtain more effective albumin surface coatings.

6.2 Impact and Future Directions

The work presented in this thesis emphasizes the importance in understanding particle surface to protein interactions and its influence on vascular targeting. Potential directions from this work are discussed below.

(1) Optimization of albumin reaction conditions onto PLGA to improve scale-up. The reaction conditions used in this thesis were conducted in small volumes to achieve maximum amount of protein on the surface. Potential alternatives involve conjugating to different functional groups or precoating the surface with other polymers aside from chitosan to increase the concentration of particles in reaction solution.

(2) The protein structure of albumin could be playing a role in the adhesion of albumin coated particles. Literature has shown that changes protein structure can alter their biological interactions, such as which receptors they bind to or their clearance. Future studies could focus on protein conformational changes and its impact on vascular targeting, which is even more important for nanoparticles formulations. Circular dichroism spectroscopy is commonly used to obtain spectra of drug carriers incorporating proteins, which can be compared to proteins in their native state. Another study evaluated the denaturation of albumin after coating PLGA using enzyme digestion of denatured proteins.

(3) Examining the effect of surface modification on PLGA in *in vivo* vascular targeting. The data collected in this thesis was almost entirely done in *in vitro* experiments, which allowed us to isolate different components in blood. Of course, it would be of great importance to evaluate the adhesion of surface modified PLGA particle in vivo to provide a dynamic environment that could be accomplished using intravital microscopy.

(4) Evaluating the adhesion of PLGA particles with other favorable proteins. In this work, we saw an increase in the adsorption of proteins with a molecular weight of 75 kDa, which we infer to be histidine-rich glycoprotein (HRG). Since particles with higher levels of HRG saw enhanced adhesion, it would be interesting to evaluate the adhesion of PLGA particles conjugated to HRG that has also been considered to act as a dysopsonin.

(5) Investigating the delivery of therapeutics to the lungs using albumin coated PLGA particles for the treatment of lung inflammation or cancer. Preliminary *in vivo* experiments showed that particles modified with albumin accumulated in the lungs compared to bare PLGA. This result was consistent with literature, where particles fabricated from albumin accumulated in the lungs as well. A direct comparison between albumin coated PLGA and albumin particles could

be useful in understanding whether there are advantages to using one drug carrier over the other to provide therapeutic benefit. The drug release profile and degradation of each particle type would also impact their efficacy depending on the application.

6.3 Overall conclusions

In conclusion, we have examined the effect of various surface modifications on the adhesion of PLGA particles. Ultimately, the addition of albumin, chitosan plus, glycol chitosan and polyethylenimine demonstrated enhanced microparticle adhesion in the presence of plasma proteins creating an optimized delivery system for vascular targeting using PLGA. Unfortunately, we did not look at the impact of drug release from surface modified PLGA particles presented here, which is critical when measuring therapeutic efficacy. Additionally, we observed changes in protein corona and endothelial cell association that could be driving the differences in adhesion. Future work should focus on understanding protein conformational changes of albumin when using it as a surface coating and proteins present in the corona. These changes seem to affect the biological interactions of these types of carriers and were not tested in this thesis. This thesis was able to contribute information on the design of biodegradable drug carriers for vascular targeted drug delivery, specifically focusing on surface modification and its impact on particles adhesion and protein adsorption. To develop vascular targeted carriers that can efficiently deliver therapeutics and imaging agents, we need to further study and understand their biological interactions so that they can be translated into the clinic.

References

1. Gooding, H. C. *et al.* Challenges and opportunities for the prevention and treatment of cardiovascular disease among young adults: Report from a national heart, lung, and blood institute working group. *J. Am. Heart Assoc.* **9**, (2020).
2. Hajitou, A., Pasqualini, R. & Arap, W. Vascular targeting: recent advances and therapeutic perspectives. *Trends Cardiovasc. Med.* **16**, 80–8 (2006).
3. Whayne, T. F. Atherosclerosis: current status of prevention and treatment. *Int. J. Angiol.* **20**, 213–22 (2011).
4. Wang, T. *et al.* Atherosclerosis: pathogenesis and pathology. *Diagnostic Histopathol.* **18**, 461–467 (2012).
5. Silvestre-Roig, C. *et al.* Atherosclerotic plaque destabilization: mechanisms, models, and therapeutic strategies. *Circ. Res.* **114**, 214–26 (2014).
6. Shi, J., Kantoff, P. W., Wooster, R. & Farokhzad, O. C. Cancer nanomedicine: progress, challenges and opportunities. (2016). doi:10.1038/nrc.2016.108
7. Simone, E., Ding, B. Sen & Muzykantov, V. Targeted delivery of therapeutics to endothelium. *Cell and Tissue Research* **335**, 283–300 (2009).
8. Howard, M. *et al.* Vascular targeting of nanocarriers: Perplexing aspects of the seemingly straightforward paradigm. *ACS Nano* **8**, 4100–4132 (2014).
9. Kelley, W. J., Safari, H., Lopez-Cazares, G. & Eniola-Adefeso, O. Vascular-targeted nanocarriers: design considerations and strategies for successful treatment of atherosclerosis and other vascular diseases. *Wiley Interdiscip. Rev. Nanomedicine Nanobiotechnology* (2016). doi:10.1002/wnan.1414
10. Koren, E. & Torchilin, V. P. Drug carriers for vascular drug delivery. *IUBMB Life* **63**, 586–595 (2011).
11. Deng, Y. *et al.* Application of the Nano-Drug Delivery System in Treatment of Cardiovascular Diseases. *Front. Bioeng. Biotechnol.* **0**, 489 (2020).
12. Zhong, H., Chan, G., Hu, Y., Hu, H. & Ouyang, D. A Comprehensive Map of FDA-Approved Pharmaceutical Products. *Pharmaceutics* **10**, 263 (2018).
13. Felice, B., Prabhakaran, M. P., Rodríguez, A. P. & Ramakrishna, S. Drug delivery vehicles on a nano-engineering perspective. *Materials Science and Engineering C* **41**, 178–195 (2014).
14. Bulbake, U., Doppalapudi, S., Kommineni, N. & Khan, W. Liposomal Formulations in Clinical Use: An Updated Review. *Pharmaceutics* **9**, (2017).
15. Larson, N. & Ghandehari, H. Polymeric conjugates for drug delivery. *Chemistry of Materials* **24**, 840–853 (2012).
16. Kumari, A., Yadav, S. K. & Yadav, S. C. Biodegradable polymeric nanoparticles based drug delivery systems. *Colloids and Surfaces B: Biointerfaces* **75**, 1–18 (2010).
17. Danhier, F. *et al.* PLGA-based nanoparticles: An overview of biomedical applications. *J. Control. Release* **161**, 505–522 (2012).
18. Nenna, A. *et al.* Polymers and Nanoparticles for Statin Delivery: Current Use and Future

Perspectives in Cardiovascular Disease. *Polym. 2021, Vol. 13, Page 711* **13**, 711 (2021).
19. Sobczynski, D. J. *et al.* Plasma protein corona modulates the vascular wall interaction of drug carriers in a material and donor specific manner. *PLoS One* **9**, e107408 (2014).
20. Mathew, J., Sankar, P. & Varacallo, M. Physiology, Blood Plasma. *StatPearls* (2021).
21. Sempf, K. *et al.* Adsorption of plasma proteins on uncoated PLGA nanoparticles. *Eur. J. Pharm. Biopharm. Off. J. Arbeitsgemeinschaft für Pharm. Verfahrenstechnik e.V* **85**, 53–60 (2013).
22. Sobczynski, D. J. & Eniola-Adefeso, O. IgA and IgM protein primarily drive plasma corona-induced adhesion reduction of PLGA nanoparticles in human blood flow. *Bioeng. Transl. Med.* **2**, 180–190 (2017).
23. Zhao, Z., Ukidve, A., Krishnan, V. & Mitragotri, S. Effect of physicochemical and surface properties on in vivo fate of drug nanocarriers. *Advanced Drug Delivery Reviews* **143**, 3–21 (2019).
24. Gupta, M. N. & Roy, I. How Corona Formation Impacts Nanomaterials as Drug Carriers. *Molecular Pharmaceutics* **17**, 725–737 (2020).
25. Papini, E., Tavano, R. & Mancin, F. Opsonins and Dysopsonins of Nanoparticles: Facts, Concepts, and Methodological Guidelines. *Front. Immunol.* **0**, 2343 (2020).
26. Duan, X. & Li, Y. Physicochemical Characteristics of Nanoparticles Affect Circulation, Biodistribution, Cellular Internalization, and Trafficking. *Small* **9**, 1521–1532 (2013).
27. Gessner, A. *et al.* Nanoparticles with decreasing surface hydrophobicities: influence on plasma protein adsorption. *Int. J. Pharm.* **196**, 245–249 (2000).
28. Lück, M. *et al.* Plasma protein adsorption on biodegradable microspheres consisting of poly(d,l-lactide-co-glycolide), poly(l-lactide) or ABA triblock copolymers containing poly(oxyethylene): Influence of production method and polymer composition. *J. Control. Release* **55**, 107–120 (1998).
29. Ndumiso, M. *et al.* Comparative whole corona fingerprinting and protein adsorption thermodynamics of PLGA and PCL nanoparticles in human serum. *Colloids Surfaces B Biointerfaces* **188**, 110816 (2020).
30. Bertrand, N. & Leroux, J. C. The journey of a drug-carrier in the body: An anatomo-physiological perspective. *Journal of Controlled Release* **161**, 152–163 (2012).
31. Lee, Y. K., Choi, E.-J., Webster, T. J., Kim, S.-H. & Khang, D. Effect of the protein corona on nanoparticles for modulating cytotoxicity and immunotoxicity. *Int. J. Nanomedicine* **10**, 97–113 (2015).
32. Lundqvist, M. *et al.* Nanoparticle size and surface properties determine the protein corona with possible implications for biological impacts. *Proc. Natl. Acad. Sci. U. S. A.* **105**, 14265–70 (2008).
33. Salvador-Morales, C., Zhang, L., Langer, R. & Farokhzad, O. C. Immunocompatibility properties of lipid-polymer hybrid nanoparticles with heterogeneous surface functional groups. doi:10.1016/j.biomaterials.2009.01.005
34. Deng, Z. J., Liang, M., Monteiro, M., Toth, I. & Minchin, R. F. Nanoparticle-induced unfolding of fibrinogen promotes Mac-1 receptor activation and inflammation. *Nat. Nanotechnol. 2011 61* **6**, 39–44 (2010).
35. Walkey, C. D. *et al.* Protein Corona Fingerprinting Predicts the Cellular Interaction of Gold and Silver Nanoparticles. *ACS Nano* **8**, 2439–2455 (2014).
36. Suk, J. S., Xu, Q., Kim, N., Hanes, J. & Ensign, L. M. PEGylation as a strategy for improving nanoparticle-based drug and gene delivery. *Adv. Drug Deliv. Rev.* **99**, 28–51

(2016).
37. Ding, W., Minamikawa, H., Kameta, N., Shimizu, T. & Masuda, M. Effects of PEGylation on the physicochemical properties and in vivo distribution of organic nanotubes. *Int. J. Nanomedicine* **9**, 5811–23 (2014).
38. Li, Y. P. *et al.* PEGylated PLGA nanoparticles as protein carriers: synthesis, preparation and biodistribution in rats. *J. Control. Release* **71**, 203–211 (2001).
39. Samkange, T., D'Souza, S., Obikeze, K. & Dube, A. Influence of PEGylation on PLGA nanoparticle properties, hydrophobic drug release and interactions with human serum albumin. *J. Pharm. Pharmacol.* **71**, 1497–1507 (2019).
40. Partikel, K. *et al.* Effect of nanoparticle size and PEGylation on the protein corona of PLGA nanoparticles. *Eur. J. Pharm. Biopharm.* **141**, 70–80 (2019).
41. Onyskiw, P. J. & Eniola-Adefeso, O. Effect of PEGylation on ligand-based targeting of drug carriers to the vascular wall in blood flow. *Langmuir* **29**, 11127–34 (2013).
42. Namdee, K., Sobczynski, D. J., Onyskiw, P. J. & Eniola-Adefeso, O. Differential Impact of Plasma Proteins on the Adhesion Efficiency of Vascular-Targeted Carriers (VTCs) in Blood of Common Laboratory Animals. *Bioconjug. Chem.* **26**, 2419–2428 (2015).
43. Walkey, C. D., Olsen, J. B., Guo, H., Emili, A. & Chan, W. C. W. Nanoparticle size and surface chemistry determine serum protein adsorption and macrophage uptake. *J. Am. Chem. Soc.* **134**, 2139–47 (2012).
44. Frank, L. A. *et al.* Chitosan as a coating material for nanoparticles intended for biomedical applications. *Reactive and Functional Polymers* **147**, 104459 (2020).
45. Wang, J. J. *et al.* Recent advances of chitosan nanoparticles as drug carriers. *Int. J. Nanomedicine* **6**, 765–74 (2011).
46. Garcia-Fuentes, M. & Alonso, M. J. Chitosan-based drug nanocarriers: where do we stand? *J. Control. Release* **161**, 496–504 (2012).
47. Wang, Y., Li, P. & Kong, L. Chitosan-modified PLGA nanoparticles with versatile surface for improved drug delivery. *AAPS PharmSciTech* **14**, 585–92 (2013).
48. Chen, H. *et al.* Surface modification of mitoxantrone-loaded PLGA nanospheres with chitosan. *Colloids Surf. B. Biointerfaces* **73**, 212–8 (2009).
49. Li, X. *et al.* Platelet compatibility of PLGA, chitosan and PLGA-chitosan nanoparticles. *Nanomedicine (Lond).* **4**, 735–46 (2009).
50. Zhang, Y. *et al.* Preparation and characterization of gadolinium-loaded PLGA particles surface modified with RGDS for the detection of thrombus. *Int. J. Nanomedicine* **8**, 3745–56 (2013).
51. Larsen, M. T., Kuhlmann, M., Hvam, M. L. & Howard, K. A. Albumin-based drug delivery: harnessing nature to cure disease. *Mol. Cell. Ther.* **4**, (2016).
52. Esfandyari-Manesh, M. *et al.* Improved anticancer delivery of paclitaxel by albumin surface modification of PLGA nanoparticles. *DARU J. Pharm. Sci. 2015 231* **23**, 1–8 (2015).
53. Manoochehri, S. *et al.* Surface modification of PLGA nanoparticles via human serum albumin conjugation for controlled delivery of docetaxel. *Daru* **21**, 58 (2013).
54. Peng, Q. *et al.* Preformed albumin corona, a protective coating for nanoparticles based drug delivery system. *Biomaterials* **34**, 8521–8530 (2013).
55. Prashant Kesharwani *et al.* Cationic bovine serum albumin (CBA) conjugated poly lactic-co -glycolic acid (PLGA) nanoparticles for extended delivery of methotrexate into brain tumors. *RSC Adv.* **6**, 89040–89050 (2016).
56. Xu, F. *et al.* Brain delivery and systemic effect of cationic albumin conjugated PLGA

nanoparticles. *http://dx.doi.org/10.1080/10611860902963013* **17**, 423–434 (2009).
57. Muniswamy, V. J. *et al.* 'Dendrimer-Cationized-Albumin' encrusted polymeric nanoparticle improves BBB penetration and anticancer activity of doxorubicin. *Int. J. Pharm.* **555**, 77–99 (2019).
58. Ma, G. J., Ferhan, A. R., Jackman, J. A. & Cho, N.-J. Conformational flexibility of fatty acid-free bovine serum albumin proteins enables superior antifouling coatings. *Commun. Mater.* **1**, 1–11 (2020).
59. Merlot, A. M., Kalinowski, D. S., Richardson, D. R., Vogt, B. & Pharmacology, M. Unraveling the mysteries of serum albumin-more than just a serum protein. (2014). doi:10.3389/fphys.2014.00299
60. Azevedo, C. *et al.* Engineered albumin-functionalized nanoparticles for improved FcRn binding enhance oral delivery of insulin. *J. Control. Release* **327**, 161–173 (2020).
61. O'Donnell, P. B. & McGinity, J. W. Preparation of microspheres by the solvent evaporation technique. *Adv. Drug Deliv. Rev.* **28**, 25–42 (1997).
62. Giri, T. K. *et al.* Prospects of pharmaceuticals and biopharmaceuticals loaded microparticles prepared by double emulsion technique for controlled delivery. *Saudi Pharm. J.* **21**, 125–141 (2013).
63. Lu, L., Duong, V. T., Shalash, A. O., Skwarczynski, M. & Toth, I. Chemical Conjugation Strategies for the Development of Protein-Based Subunit Nanovaccines. *Vaccines* **9**, (2021).
64. Charoenphol, P., Huang, R. B. & Eniola-Adefeso, O. Potential role of size and hemodynamics in the efficacy of vascular-targeted spherical drug carriers. *Biomaterials* **31**, 1392–1402 (2010).
65. Huang, R. B. & Eniola-Adefeso, O. Shear Stress Modulation of IL-1β-Induced E-Selectin Expression in Human Endothelial Cells. *PLoS One* **7**, (2012).
66. Brannon, E. R. *et al.* Polysalicylic Acid Polymer Microparticle Decoys Therapeutically Treat Acute Respiratory Distress Syndrome. *Adv. Healthc. Mater.* 2101534 (2021). doi:10.1002/ADHM.202101534
67. Hoang Thi, T. T. *et al.* The Importance of Poly(ethylene glycol) Alternatives for Overcoming PEG Immunogenicity in Drug Delivery and Bioconjugation. *Polymers (Basel).* **12**, 298 (2020).
68. Lin, F., Jia, H. R. & Wu, F. G. Glycol chitosan: A water-soluble polymer for cell imaging and drug delivery. *Molecules* **24**, (2019).
69. Amoozgar, Z., Park, J., Lin, Q. & Yeo, Y. Low Molecular-Weight Chitosan as a pH-Sensitive Stealth Coating for Tumor-Specific Drug Delivery. *Mol. Pharm.* **9**, 1262–1270 (2012).
70. Mustafa, S., Devi, V. K. & Pai, R. S. Effect of PEG and water-soluble chitosan coating on moxifloxacin-loaded PLGA long-circulating nanoparticles. *Drug Deliv. Transl. Res.* **7**, 27–36 (2017).
71. Parveen, S. & Sahoo, S. K. Long circulating chitosan/PEG blended PLGA nanoparticle for tumor drug delivery. *Eur. J. Pharmacol.* **670**, 372–383 (2011).
72. Pawar, D., Mangal, S., Goswami, R. & Jaganathan, K. S. Development and characterization of surface modified PLGA nanoparticles for nasal vaccine delivery: Effect of mucoadhesive coating on antigen uptake and immune adjuvant activity. *Eur. J. Pharm. Biopharm.* **85**, 550–559 (2013).
73. Charoenphol, P., Huang, R. B. & Eniola-Adefeso, O. Potential role of size and

hemodynamics in the efficacy of vascular-targeted spherical drug carriers. *Biomaterials* **31**, 1392–1402 (2010).
74. Cheung, R. C. F., Ng, T. B., Wong, J. H. & Chan, W. Y. Chitosan: An Update on Potential Biomedical and Pharmaceutical Applications. *Mar. Drugs 2015, Vol. 13, Pages 5156-5186* **13**, 5156–5186 (2015).
75. Lee, E. S., Park, K. H., Park, I. S. & Na, K. Glycol chitosan as a stabilizer for protein encapsulated into poly(lactide-co-glycolide) microparticle. *Int. J. Pharm.* **338**, 310–316 (2007).
76. Chen, M. M. *et al.* Sequential delivery of chlorhexidine acetate and bFGF from PLGA-glycol chitosan core-shell microspheres. *Colloids Surfaces B Biointerfaces* **151**, 189–195 (2017).
77. Yu, D., Zhang, Y., Zhou, X., Mao, Z. & Gao, C. Influence of surface coating of PLGA particles on the internalization and functions of human endothelial cells. *Biomacromolecules* **13**, 3272–3282 (2012).
78. Pillai, G. J., Greeshma, M. M. & Menon, D. Impact of poly(lactic-co-glycolic acid) nanoparticle surface charge on protein, cellular and haematological interactions. *Colloids Surf. B. Biointerfaces* **136**, 1058–66 (2015).
79. Fromen, C. A. *et al.* Evaluation of receptor-ligand mechanisms of dual-targeted particles to an inflamed endothelium. *Bioeng. Transl. Med.* (2016). doi:10.1002/btm2.10008
80. AO, E., PJ, W. & DA, H. Interplay between rolling and firm adhesion elucidated with a cell-free system engineered with two distinct receptor-ligand pairs. *Biophys. J.* **85**, 2720–2731 (2003).
81. Matoba, T., Koga, J. ichiro, Nakano, K., Egashira, K. & Tsutsui, H. Nanoparticle-mediated drug delivery system for atherosclerotic cardiovascular disease. *Journal of Cardiology* **70**, 206–211 (2017).
82. Peer, D. *et al.* Nanocarriers as an emerging platform for cancer therapy. *Nature Nanotechnology* **2**, 751–760 (2007).
83. Allen, T. M. & Cullis, P. R. Liposomal drug delivery systems: From concept to clinical applications. *Advanced Drug Delivery Reviews* **65**, 36–48 (2013).
84. Gupta, A. Sen. Nanomedicine approaches in vascular disease: A review. *Nanomedicine: Nanotechnology, Biology, and Medicine* **7**, 763–779 (2011).
85. Flores, A. M. *et al.* Nanoparticle Therapy for Vascular Diseases. *Arteriosclerosis, thrombosis, and vascular biology* **39**, 635–646 (2019).
86. Park, K. *et al.* Injectable, long-acting PLGA formulations: Analyzing PLGA and understanding microparticle formation. *J. Control. Release* **304**, 125–134 (2019).
87. Sobczynski, D. J. & Eniola-Adefeso, O. Effect of anticoagulants on the protein corona-induced reduced drug carrier adhesion efficiency in human blood flow. *Acta Biomater.* **48**, 186–194 (2017).
88. Knop, K., Hoogenboom, R., Fischer, D. & Schubert, U. S. Poly(ethylene glycol) in Drug Delivery: Pros and Cons as Well as Potential Alternatives. *Angew. Chemie Int. Ed.* **49**, 6288–6308 (2010).
89. Kelley, W. J., Fromen, C. A., Lopez-Cazares, G. & Eniola-Adefeso, O. PEGylation of model drug carriers enhances phagocytosis by primary human neutrophils. *Acta Biomater.* **79**, 283–293 (2018).
90. George, A., Shah, P. A. & Shrivastav, P. S. Natural biodegradable polymers based nano-formulations for drug delivery: A review. *Int. J. Pharm.* **561**, 244–264 (2019).

91. Tao, C., Chuah, Y. J., Xu, C. & Wang, D. A. Albumin conjugates and assemblies as versatile bio-functional additives and carriers for biomedical applications. *Journal of Materials Chemistry B* **7**, 357–367 (2019).
92. Bobo, D., Robinson, K. J., Islam, J., Thurecht, K. J. & Corrie, S. R. Nanoparticle-Based Medicines: A Review of FDA-Approved Materials and Clinical Trials to Date. *Pharmaceutical Research* **33**, 2373–2387 (2016).
93. Bertrand, N. *et al.* Mechanistic understanding of in vivo protein corona formation on polymeric nanoparticles and impact on pharmacokinetics. *Nat. Commun.* **8**, 777 (2017).
94. Schöttler, S. *et al.* Protein adsorption is required for stealth effect of poly(ethylene glycol)- and poly(phosphoester)-coated nanocarriers. *Nat. Nanotechnol.* **11**, 372–377 (2016).
95. Shubhra, Q. T. H., Tóth, J., Gyenis, J. & Feczkó, T. Surface modification of HSA containing magnetic PLGA nanoparticles by poloxamer to decrease plasma protein adsorption. *Colloids Surf. B. Biointerfaces* **122**, 529–36 (2014).
96. RC, G. & DT, A. The role of antibody synergy and membrane fluidity in the vascular targeting of immunoliposomes. *Biomaterials* **31**, 900–907 (2010).
97. Nelson, R. M., Dolich, S., Aruffo, A., Cecconi, O. & Bevilacqua, M. P. Higher-affinity oligosaccharide ligands for E-selectin. *J. Clin. Invest.* **91**, 1157 (1993).
98. Cui, T. *et al.* Protein corona-guided tumor targeting therapy: Via the surface modulation of low molecular weight PEG. *Nanoscale* **13**, 5883–5891 (2021).
99. Poon, I. K. H., Patel, K. K., Davis, D. S., Parish, C. R. & Hulett, M. D. Histidine-rich glycoprotein: the Swiss Army knife of mammalian plasma. (2011). doi:10.1182/blood
100. Fedeli, C. *et al.* The functional dissection of the plasma corona of SiO2-NPs spots histidine rich glycoprotein as a major player able to hamper nanoparticle capture by macrophages. *Nanoscale* **7**, 17710–17728 (2015).
101. Gao, S. *et al.* Histidine-Rich Glycoprotein Inhibits High-Mobility Group Box-1-Mediated Pathways in Vascular Endothelial Cells through CLEC-1A. *iScience* **23**, (2020).
102. Kreuter, J. Nanoparticles and microparticles for drug and vaccine delivery. *J. Anat.* **189**, 503 (1996).
103. Patra, J. K. *et al.* Nano based drug delivery systems: recent developments and future prospects. *J. Nanobiotechnology 2018 161* **16**, 1–33 (2018).
104. Mitchell, M. J. *et al.* Engineering precision nanoparticles for drug delivery. *Nat. Rev. Drug Discov. 2020 202* **20**, 101–124 (2020).
105. Kumari, A., Yadav, S. K. & Yadav, S. C. Biodegradable polymeric nanoparticles based drug delivery systems. *Colloids Surf. B. Biointerfaces* **75**, 1–18 (2010).
106. Carboni, E., Tschudi, K., Nam, J., Lu, X. & Ma, A. W. K. Particle margination and its implications on intravenous anticancer drug delivery. *AAPS PharmSciTech* **15**, 762–771 (2014).
107. Schäffler, M. *et al.* Serum protein identification and quantification of the corona of 5, 15 and 80 nm gold nanoparticles. *Nanotechnology* **24**, 265103 (2013).
108. Kolhar, P. *et al.* Using shape effects to target antibody-coated nanoparticles to lung and brain endothelium. *Proc. Natl. Acad. Sci. U. S. A.* **110**, 10753–8 (2013).
109. Rao, W. *et al.* Chitosan-Decorated Doxorubicin-Encapsulated Nanoparticle Targets and Eliminates Tumor Reinitiating Cancer Stem-like Cells. *ACS Nano* **9**, 5725–5740 (2015).
110. Kaur, N., Mathur, P., Yadav, P., Chakraborty, S. & Shanavas, A. Glycol chitosan in situ coating on PLGA nanoparticle curtails extraneous paclitaxel precipitates and imparts protein corona independent hemocompatibility. *Carbohydr. Polym.* **237**, 116170 (2020).

111. Woods, A. *et al.* In vivo biocompatibility, clearance, and biodistribution of albumin vehicles for pulmonary drug delivery. *J. Control. Release* **210**, 1–9 (2015).
112. Myerson, J. W. *et al.* Supramolecular arrangement of protein in nanoparticle structures predicts nanoparticle tropism for neutrophils in acute lung inflammation. *Nat. Nanotechnol.* (2021). doi:10.1038/S41565-021-00997-Y
113. John, T. A. *et al.* Evidence for the role of alveolar epithelial gp60 in active transalveolar albumin transport in the rat lung. *J. Physiol.* **533**, 547–559 (2001).
114. He, N., Wang, R., He, Y. & Dang, X. Fabrication, structure and surface charges of albumin-chitosan hybrids. *Sci. China Chem. 2012 559* **55**, 1788–1795 (2012).
115. Poon, I. K. H., Patel, K. K., Davis, D. S., Parish, C. R. & Hulett, M. D. Histidine-rich glycoprotein: the Swiss Army knife of mammalian plasma. *Blood* **117**, 2093–2101 (2011).
116. Satzer, P., Svec, F., Sekot, G. & Jungbauer, A. Protein adsorption onto nanoparticles induces conformational changes: Particle size dependency, kinetics, and mechanisms. *Eng. Life Sci.* **16**, 238–246 (2016).